Properties of Time-Dependent Stokes Flow and the Regularization of Velocity Fluctuations in Particle Suspensions

Dissertation

zur Erlangung des Doktorgrades
der Naturwissenschaften
(Dr. rer. nat.)

dem Fachbereich Physik
der Philipps-Universität Marburg
vorgelegt

von

Jürgen Bührle
aus
Blaubeuren
(Alb-Donau-Kreis)

Marburg/Lahn 2007

Vom Fachbereich Physik der Philipps-Universität Marburg
als Dissertation angenommen am: 26.06.2007
Erstgutachter: Prof. Dr. Bruno Eckhardt, Marburg
Zweitgutachter: Prof. Dr. Holger Stark, Berlin
Tag der mündlichen Prüfung: 07.08.2007

Zusammenfassung

Einleitung

Sedimentation bezeichnet die Ablagerung von Teilchen in einer Flüssigkeit unter dem Einfluss einer äußeren Kraft, wie etwa der Schwerkraft oder der Zentrifugalkraft. Sedimentation spielt in einer Vielzahl von natürlichen und industriellen Prozessen eine wesentliche Rolle [20]. Oberflächenstruktur und Teilchengröße sind dabei für die jeweiligen Prozesse sehr verschieden. Wesentliche Eigenschaften der Sedimentation sind jedoch von der Teilchenbeschaffenheit unabhängig. Zur Untersuchung dieser wird in der experimentellen Physik überwiegend die Sedimentation von Glaskugeln in einem Behälter studiert.

Experimentelle Messungen zeigen, dass die Sinkgeschwindigkeit von der Teilchenkonzentration abhängt. Diese Messungen können sehr gut theoretisch beschrieben werden [7, 18, 23, 58]. Im Gegensatz dazu stehen experimentelle Messungen der Geschwindigkeitsfluktuationen im krassen Widerspruch zu theoretischen Vorhersagen und numerischen Simulationen. Basierend auf der zeitunabhängigen Stokesgleichung haben Caflisch und Luke [14] theoretisch gezeigt, dass die Geschwindigkeitsfluktuationen einer Teilchensuspension bei homogener Verteilung der Teilchen proportional zur Größe des Behälters ist: Die Strömung, welche durch ein Teilchen erzeugt wird, fällt antiproportional zum Abstand vom Teilchen ab. Bei einer homogenen Teilchenverteilung befinden sich in einer Kugelschale mit Dicke dr im Abstand r von einem vorgegebenen Punkt $r^2 dr$ Teilchen. Die Geschwindigkeitsfluktuation am vorgegeben Punkt ist proportional zum Quadrat der Strömungsgeschwindigkeit, also proportional zu $1/r^2$. Damit trägt jede Kugelschale unabhängig vom Abstand zur Fluktuation bei. Das Integral über alle Kugelschalen führt dazu, dass die Fluktuation der Geschwindigkeit am vorgegeben Punkt divergiert, beziehungsweise linear von der Größe des Behälters abhängt.

Die Abhängigkeit der Geschwindigkeitsfluktuationen von der Behältergröße wird durch numerische Simulationen bestätigt [17, 25, 26, 27, 28]. Entgegen der theoreti-

schen Vorhersage wird im Experiment keine solche Divergenz beobachtet [21, 48, 60, 61]. Experimente zeigen, dass die Fluktuationen unabhängig von der Behältergröße sind und im Wesentlichen durch den gegenseitigen Abstand der Teilchen bestimmt werden. Umfassende theoretische Untersuchungen haben, um eine Erklärung der Diskrepanz bemüht, den Einfluß der Behälterwand und Inhomogenitäten der Teilchenkonzentration untersucht. Die Diskrepanz ist dennoch nicht geklärt.

Sämtliche theoretische und numerische Untersuchungen beschreiben die Strömung zwischen den Teilchen durch die zeitunabhängige Stokesgleichung. In dieser Arbeit wird untersucht, was sich ändert, wenn man diese Vereinfachung aufgibt und die Strömung zwischen den Teilchen durch die zeitabhängige Stokesgleichung beschreibt, wenn man also die interne zeitliche Entwicklung des Strömungsfeldes mit einbezieht.

Strömung um eine oszillierende Kugel

Der Unterschied zwischen der Strömung, welche man aus der zeitunabhängigen Stokesgleichung und der zeitabhängigen Stokesgleichung erhält, wurde in Kapitel 2 am Beispiel einer Kugel untersucht, welche eine oszillatorische Bewegung entlang einer Achse vollführt. Beide Lösungen wurden 1851 von George G. Stokes in seinem wegweisenden Artikel publiziert [65].

Insbesondere die zeitunabhängige Lösung wird üblicherweise als erste Näherung der Strömung um ein Teilchen verwendet. Sie hängt nur von der instantanen Geschwindigkeit der Kugel relativ zum ruhenden Fluid ab. Die Vortizität nimmt instantan einen Gleichgewichtszustand an. Auch für beliebig hohe Frequenzen wird eine Änderung der Geschwindigkeit der Kugel sofort bis in jede erdenkliche Entfernung auf die Strömung übertragen. Das Geschwindigkeitsfeld des Fluids fällt antiproportional zum Abstand ab.

Im Gegensatz dazu reagiert die Strömung als Lösung der zeitabhängigen Stokesgleichung nur in Entfernungen instantan, welche klein sind gegenüber $\sqrt{\nu/\omega}$, wobei ν und ω die kinematische Viskosität des Fluids und die Frequenz der Oszillation bezeichnen. Für diese Entfernungen fällt die Strömung mit dem Abstand r wie $1/r$ ab. Für Abstände, welche groß gegen $\sqrt{\nu/\omega}$ sind, fällt die Strömung stärker ab. Der Hintergrund für diese beiden Bereiche ist die Diffusion der Vortizität. Während die Vortizität nahe der Kugel beinahe im Gleichgewicht ist, reicht die Periodendauer der Oszillation nicht für eine Diffusion der Vortizität zu Abständen größer als $\sqrt{\nu/\omega}$. Für große Abstände bleibt eine Potenzialströmung übrig, welche von der Verdrängung der Flüssigkeit durch die Verschiebung der Kugel herrührt und wie $1/r^3$ abfällt. Die zeitabhängige und die zeitu-

nabhängige Beschreibung sind gleich, wenn die Vortizität in einem stationären Zustand ist.

Die Unterschiede der beiden Lösungen werden deutlich, wenn man die Menge an Fluid betrachtet, welche durch die Kugel bewegt wird. Zu diesem Zweck legt man einen Querschnitt durch die Kugel und berechnet den Massenstrom, der durch diesen Querschnitt fließt. Bei der zeitunabhängigen Strömung stellt man fest, dass eine unendliche Menge des Fluids durch diesen Querschnitt in Richtung der Kugelbewegung transportiert wird. Bei der zeitabhängigen Betrachtung hingegen wird genau die Menge an Fluid in negativer Bewegungsrichtung der Kugel transportiert, welche von der Kugel verdrängt wird, unabhängig von Frequenz und Viskosität!

Eine ähnliche Argumentation wie für die oszillierende Kugel gilt auch für eine Kugel, die aus der Ruhe heraus instantan eine konstante Geschwindigkeit annimmt. Die Strömung breitet sich ähnlich einer Diffusionsfront aus. Diese von Basset [4] gefundene Lösung wird in Kapitel 3 diskutiert, einhergehend mit einer Lösung der zeitabhängigen Stokesgleichung für beliebige Geschwindigkeiten der Kugel.

Geschwindigkeitsfluktuationen von Teilchensuspensionen

In Kapitel 4 wird schließlich auf das Problem der divergenten Geschwindigkeitsfluktuationen bei der Sedimentation eingegangen. Die Regularisierung der Fluktuationen wird an einem verwandten Problem transparenter. Die Fluktuationen des Konzentrationsfeldes, welches von einer homogenen Verteilung von Quellen erzeugt wird, werden untersucht. Wenn sich der Beitrag einer Quelle zum Konzentrationsfeld instantan der Quelle anpasst, erhält man, ähnlich zur zeitunabhängigen Stokesströmung um eine Kugel, einen Abfall des Konzentrationsfeldes mit dem Abstand r wie $1/r$. Die Fluktuationen des Konzentrationsfeldes fallen ab wie $1/r^2$. Die Integration über die homogene Verteilung führt auf das Ergebnis von Caflisch und Luke [14]. Wenn man hingegen die vollständige Lösung des Konzentrationsfeldes in Betracht zieht, dann sind die Fluktuationen regulär. Dies rührt daher, dass aufgrund der endlichen Reichweite der Diffusion die Fluktuationen des Konzentrationsfeldes ab einem endlichen Abstand wesentlich stärker abfallen als $1/r^2$.

Die Argumentation für Teilchensuspensionen erfolgt analog. Man stellt fest, dass die Fluktuationen in der zeitabhängigen Beschreibung endlich sind. Des Weiteren wird durch eine Abschätzung festgestellt, dass die Geschwindigkeitsfluktuationen vom Quadrat des Abstandes der Teilchen voneinander abhängt, in Übereinstimmung mit experimentellen

Messungen [60].

Diese Arbeit zeigt, dass die zeitabhängige Behandlung der Strömung eine wesentliche Rolle für die Sedimentation von Teilchen spielt, und legt die Grundlagen für nachfolgende Untersuchungen.

Contents

Chapter 1

Introduction

Solid particles, suspended in a fluid and subject to an external force, such as gravity, settle if the density of the particles is higher than the density of the fluid. This process, which separates fluid and particles, is called sedimentation. It is important for a variety of processes in nature and industry [20].

While naturally occuring particles come in a variety of shapes with smooth and rough surfaces, many of the fundamental issues of the sedimentation process can be studied with spherical particles. Experimentally, this situation can be realized, for instance, for glass beads which settle in a vessel. For these systems, theoretical predictions and experiments agree about the average settling rate of the particles, which depends on the concentration of the particles in the fluid, e.g. [7, 18, 23, 58].

In contrast, there is much controversy about the fluctuations of the particle velocities. Available theories assume that the flow past a particle obeys the steady Stokes equation, i.e. the flow is proportional to the instantaneous particle velocity and decays as 1/distance from the particle. Caflisch and Luke [14] pointed out that due to these long-range hydrodynamic interactions, the fluctuations diverge for a homogeneous distribution of particles: At a distance r from a particle, the fluctuations of the flow produced by that particle decay as the velocity squared, i.e. as $1/r^2$. Since a spherical shell at distance r and of width dr contains $r^2 dr$ particles, all shells contribute equally to the fluctuations and the integral over all shells diverges with the volume of the vessel. While numerical simulations confirm the divergence, e.g. [17, 25, 26, 27, 28], it is in marked contrast to experiments [21, 48, 60, 61] which show that the flow is correlated on a finite length and that correlation length and fluctuations are finite and independent of the vessel size. To uncover the discrepancy between simulations and experiments, a number of theoretical studies have looked at effects of the wall [13], vertical stratification of

the sediment [44] or particle concentration fluctuations [32, 45]. However, no conclusive explanation of the discrepancies has emerged.

Such a discrepancy between simulation and experiment is also known from another system: Wu and Libchaber [70] study the flow produced by a flock of self-propelled bacteria in a soap film. They immerse neutrally buoyant particles in the flow and observe that the drift of the particles corresponds to an uncorrelated random walk on large time scales, and to a positively correlated random walk on short time scales. This indicates that there is a correlation of the flow on small length scales, such that the drift of the particle is uniform at short times, whereas the flow is uncorrelated over large distances, such that the particle motion corresponds to an uncorrelated random walk. Again, in contrast to the experiment, simulations [22] show correlations also on large length scales.

All theories and simulations above, for sedimentation and for the bacterial bath, assume that the flow past the particles is steady Stokes flow. This assumption is believed to be fairly robust [13]. In this work, the assumption is dropped and the flow is assumed to be *unsteady* Stokes flow, i.e. the temporal evolution of the velocity field is taken into account. How does unsteady Stokes flow differ from steady Stokes flow? The differences between steady and unsteady flow are known since the equations were formulated. In his seminal 1851 article [65], which is most of all famous for the equations which describe the steady flow around a steadily moving sphere, Stokes also provided the equations for the time-dependent flow past a sphere whose center of mass is in oscillatory motion. However, the consequences of the differences between the two cases and in particular their implications for sediment fluctuations have not been studied. As we will show here, taking the time-dependence into account goes a long way towards resolving many of the puzzles.

The outline of the thesis is as follows. The properties of the time-dependent flow past a sphere in oscillatory motion are reexamined in chapter 2 and compared to steady Stokes flow. The solution for the flow past a sphere, whose center of mass is in arbitrary motion, given by Basset [4], Boussinesq [10, 11] and Oseen [52], is reexamined in chapter 3. Then, in chapter 4, for a suspension of particles and a related diffusion problem the arguments of Caflisch and Luke [14] are reconsidered with time-dependence taken into account for the flow.

Chapter 2

Oscillatory Stokes flow

In 1851, George Gabriel Stokes (see figure 2.1), Professor of Mathematics at the University of Cambridge, published an article entitled "On the Effect of the Internal Friction of Fluids on the Motion of Pendulums" [65]. In it he decribes how in the limit of low velocities, where terms which are linear in the velocity dominate, the viscous flow around a sphere affects the motion of a spherical pendulum. Stokes found the force on a sphere to be proportional to sphere radius and velocity. He was thus able to explain experimentally measured deviations of a pendulum's motion from the inviscid prediction.

In his article, Stokes gives solutions for the flow past a sphere, whose center of mass oscillates unidirectionally, and for the flow past a steadily moving sphere and calculates the friction force in both cases. The latter solution is widely used in science and usually the first approximation for the flow produced by a slowly moving particle in a viscous liquid: The flow around a sphere decays as 1/distance. For the related problem of a cylinder, Stokes found that the linear equations do not provide a steady solution and concluded thus that the assumption of a steady solution at all is not necessarily valid:

> We have evidently a right to conceive a sphere or infinite cylinder to exist at rest in an infinite mass of fluid also at rest, to suppose the sphere or cylinder to be then moved with a uniform velocity V, and to propose for determination the motion of the fluid at the end of the time t. But we have no right to assume that the motion approaches a permanent state as t increases indefinitely. We may follow either of two courses. We may proceed to solve the general problem in which the sphere or cylinder is supposed to move from rest, and then examine what results we obtain by supposing t to increase indefinitely, or else we may assume *for trial* that the motion is

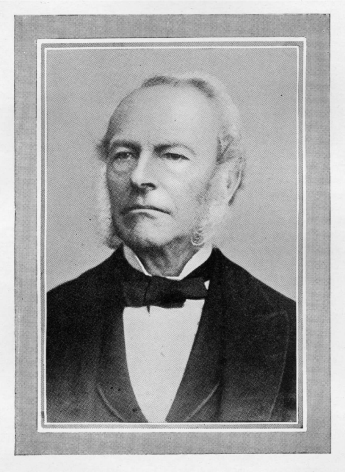

Figure 2.1: Sir George Gabriel Stokes (1819-1903), from [63].

> steady, and proceed to inquire whether we can satisfy all the conditions of the problem on this supposition. The former course would have the disadvantage of requiring a complicated analysis for the sake of obtaining a comparatively simple result, and it is even possible that the solution of the problem might baffle us altogether; but if we adopt the latter course, we must not forget that the equations with which we work are only provisional. p. 54 from [65]

Later in his article, Stokes gives the equations for the time-dependent flow produced by the motion of an infinitely extended plane. The plane is oriented vertically and located at $x = 0$. Starting from rest at $t = 0$, the plane moves vertically at constant velocity $U\mathbf{e}_y$. We are interested in the profile of the vertical velocity in x-direction, i.e. perpendicular to the flow direction. For $x > 0$, the flow is then found to be

$$\mathbf{u}(x,t) = U\mathbf{e}_y \cdot \operatorname{erfc}\left(\frac{x}{\sqrt{4\nu t}}\right), \tag{2.1}$$

where

$$\operatorname{erfc}(\xi) = \frac{2}{\sqrt{\pi}} \int_{\xi}^{\infty} e^{-\zeta^2} d\zeta \tag{2.2}$$

is the complementary error function. For $\xi \to 0$, $\operatorname{erfc}(\xi)$ is $\operatorname{erfc}(0) = 1$. The largest value for the integral kernel is at $\zeta = \xi$. The complementary error function becomes exponentially small as $\xi \gg 1$: The maximum value of the integrand is $\exp(-\xi^2)$. Since the kernel is decaying rapidly with ζ, the kernel contributes over a finite range of ζ to

the integral and erfc(x) becomes exponentially small. For $\xi \to \infty$, the value for erfc(ξ) becomes equal to 0.

Therefore, the solution for all times satisfies the boundary conditions: The velocity of the fluid is equal to the velocity of the wall at $x = 0$ and the velocity of the fluid vanishes at infinity. In the limit $t \to \infty$ or $\nu \to \infty$, the argument $x/\sqrt{4\nu t}$ in the complementary error function becomes equal to unity and one finds that the velocity of the fluid becomes equal to the velocity of the plane, which is the stationary state of the flow, i.e.

$$\mathbf{u}(x,t) = U\mathbf{e}_y \qquad \text{for} \qquad x \ll \sqrt{4\nu t}. \tag{2.3}$$

However physically for any finite ν and t, no matter how large, this is limited to finite distances $x \ll \sqrt{4\nu t}$ since there was no time yet for the flow to diffuse to larger distances.

Thus for a prescribed distance from the wall x, for $t \to \infty$ the flow becomes stationary and the velocity of the fluid equals the velocity prescibed by the wall. Even as $x \to \infty$, for each prescribed value of x, after a sufficiently long time elapsed, the flow is stationary.

However, for a prescribed distance t, the stationary flow is always restricted to $x < \sqrt{4\nu t}$. The flow drops down for larger distances from the wall and in the limit $x \to \infty$ the velocity of the fluid becomes equal to zero, which is the boundary condition at infinity. Thus as $t \to \infty$, for each prescribed value of t, at a sufficiently large distance from the wall the flow drops down to zero.

It is hence important, wether first t diverges for prescribed x and then $x \to \infty$, or wether first x diverges at a fixed time t and then $t \to \infty$. The limits $x \to \infty$ and $t \to \infty$ do not commute!

In the case of the plane, it is obvious that for a prescribed time t a stationary solution is only found at finite distances, since that solution does not satisfy the boundary conditions at infinity. Similar results are found for the time-dependent flow around a cylinder [46]. In contrast, the steady flow around a sphere, derived by Stokes [65], does satisfy the boundary conditions and the limitations are a priori not obvious. The validity of steady Stokes flow past a sphere in oscillatory motion will be investigated in this chapter and compared to time-dependent Stokes flow.

In the remainder of the chapter, for low velocities the magnitudes of the various terms in the more general Navier-Stokes equations are compared. Then, for the flow past a sphere whose center of mass is in oscillatory motion, and for the flow past a steadily moving sphere, Stokes' equations for the flow are reexamined and compared. This is followed by an investigation of the advective term in the Navier-Stokes equation.

A correction to the Stokes equation is found to investigate the restrictions of the time-dependent Stokes equation. Finally, for time-dependent Stokes flow the response of a sphere to a harmonic force is investigated.

2.1 Scaling of Navier-Stokes

For velocities below the speed of sound, the flow of an incompressible Newtonian fluid is described by the Navier-Stokes equation

$$\frac{\partial}{\partial t}\mathbf{u} + (\mathbf{u}\cdot\nabla)\,\mathbf{u} = -\nabla p + \nu\nabla^2\mathbf{u} \tag{2.4}$$

and the incompressibility condition, which is $\nabla\cdot\mathbf{u} = 0$. Here, $\mathbf{u}$ is the velocity of the fluid at a time t, ν is the kinematic viscosity and p the kinematic pressure of the fluid, which is defined as the dynamic pressure P divided by the fluid density ρ, i.e. $p = P/\rho$.

2.1.1 Common scale transformation of the Navier-Stokes equation

The usual estimate of the size of the different terms in (2.4) uses a characteristic length scale L of the boundary's geometry (such as the gap width of a channel or the size of an object in the flow) and the typical velocity scale U, as introduced by the boundary conditions. Then the typical scale of time for changes in the flow field is fixed to be L/U. The term with the partial time-derivative and the advective term both scale like U^2/L, whereas the viscous term scales as $\nu U/L^2$. Based on a scaling which is proportional to the viscosity, the pressure p scales as $\nu U/L$. The Reynolds number Re measures the size of the nonlinear term compared to the viscous term. With this

$$Re = \frac{U^2/L}{\nu U/L^2} = \frac{UL}{\nu}\,, \tag{2.5}$$

the equations of motion in the absence of a volume force become

$$Re\,(\partial_t\mathbf{u} + (\mathbf{u}\cdot\nabla)\mathbf{u}) = -\nabla p + \nabla^2\mathbf{u}. \tag{2.6}$$

If Re becomes small, the nonlinear term can be neglected compared to the viscous term. Since the time-derivative term is also multiplied by Re, the usual conclusion is that for sufficiently small Re the steady Stokes equation can be used, which is

$$0 = -\nabla p + \nabla^2\mathbf{u}. \tag{2.7}$$

One of the consequences is that there is no longer an internal time-scale in the flow. The flow responds instantaneously to a temporal change of the boundaries. If the boundaries are at rest, the flow is at rest as well, whereas a sudden change of the boundaries is transported immediately throughout the whole fluid to any distance. However, for fast changes in time, despite of small Re the factor ∂_t is large enough to make the product of both significant, i.e. one has to keep this time-dependance.

2.1.2 Viscous length scales

The velocity scale U is prescribed by the boundary conditions. For problems where an external frequency ω is prescribed, a diffusional length scale $L_\nu = \sqrt{\nu/\omega}$ may be constructed in terms of the kinematic viscosity and the frequency. It is roughly the distance, up to which viscous flow spreads over one oscillation period. With this internal length scale L_ν as a scaling length, the advective term in equation 2.4 is of the order U^2/L_ν, i.e. $U^2\sqrt{\omega/\nu}$. The viscous term scales as $\nu U/L_\nu^2 = \omega U$ and is thus of the same order as the partial time-derivative term. With this estimate of the magnitudes of the various terms, the ratio between advective and either the viscous or the time-derivative term, defined in the usual way as the Reyolds number, is given as a viscosity based Reynolds number

$$Re_\nu = \frac{UL_\nu}{\nu} = \frac{U}{\sqrt{\omega\nu}}. \tag{2.8}$$

In terms of the amplitude D of the oscillatory motion, such that the typical velocity scale is $U = \omega D$, the Reynolds number may also be written as

$$Re_\nu = \frac{D}{L_\nu} \tag{2.9}$$

i.e. the ratio between the oscillation amplitude and the viscous length. Even if this Reynolds number is small, due to this estimate the partial time-derivative term in the Navier Stokes equation is still of order unity. Then in the limit of $Re_\nu \to 0$, the equation for the flow becomes a time-dependent Stokes equation

$$\frac{\partial}{\partial t}\mathbf{u} = -\nabla p + \nu\nabla^2\mathbf{u}. \tag{2.10}$$

It still contains time dependence on the viscous scale, but no nonlinear advection. Note that for the estimate of the various terms, an external frequency ω, an internal length scale $L_\nu = \sqrt{\nu/\omega}$ and the velocity prescribed at the boundaries U have been used. This gives rise to a time-derivative term and a viscous term that scale alike. It is expected to be valid, if the external scales, like for example D, are small in comparison with the viscous scale L_ν.

2.1.3 Length scale of the body

It is not clear a priori if the advective term really scales as U^2L^{-1}. The introduction of scaling variables does not alter the real magnitudes of the terms and they might get large. An alternative scaling may be introduced in terms of the geometric length L of the object in case, the velocity U and the prescribed frequency ω. The time-derivative term scales as ωU, the advective term scales as U^2/L and the magnitude of the viscous term is given by $\nu U/L^2$. Hence, the ratio of the time-derivative term and the viscous term is given by $\omega L^2/\nu$, whereas the Reynolds number, defined as usual as the ratio of advective and viscous term, is the external Reynolds number

$$Re = \frac{U^2/L}{\nu U/L^2} = \frac{UL}{\nu}. \tag{2.11}$$

Thus, the Reynolds number may be small and ω still large, such that the time-derivative is again nonnegligible, i.e.

$$\frac{\omega L^2}{\nu}\partial_t \mathbf{u} + Re(\mathbf{u}\cdot\nabla)\mathbf{u} = -\nabla p + \nabla^2\mathbf{u}. \tag{2.12}$$

The ratio of time-derivative and viscous term, $\omega L^2/\nu$, measures the time that the flow needs to diffuse a distance L, i.e. L^2/ν, compared to the oscillation period ω^{-1}.

Another comparison of interest which leads to the same result is the ratio of L to the viscous diffusion length $L_\nu = \sqrt{\nu/\omega}$, both squared.

Thus, three different estimates of the magnitudes in the Navier-Stokes equations can be discussed, all scaling differently. But if the Reynolds number is always defined as the ratio of the nonlinear and the viscous term, it is always defined as velocity scale times length scale divided by viscosity ν. Its value then also depends on the respectively chosen U and L. The consequence is that depending on the way the Navier-Stokes equation is nondimensionalized, the limit of the corresponding $Re \to 0$ gives rise to different equations. Thus one has to distinguish carefully between the scaling of the terms, to nondimensionalize them, and the actual size of the terms.

2.2 Reference frames

For the flow around a sphere, the reference frame is chosen most conveniently such that the sphere is at rest in the origin. This requires the transformation from the laboratory frame, where the fluid is at rest at infinity, to the reference frame of the sphere with the

fluid at rest at the surface of the sphere. For a Galilei transformation, the terms of the Navier-Stokes equation

$$\frac{\partial}{\partial t}\mathbf{v} + (\mathbf{v}\cdot\nabla)\,\mathbf{v} = -\nabla p + \nu\nabla^2\mathbf{v} \tag{2.13}$$

are preserved. The flow $\mathbf{v}(\mathbf{y},t)$ describes the velocity of the fluid at position $\mathbf{y}$ and time t. Partial and advective time-derivative on the left-hand side represent the time-derivative along the track of a particle. The Navier-Stokes equation describes the force per unit mass on a fluid parcel in a Newtonian liquid.

To demonstrate the Galilei invariance [35], transform the original coordinates $\mathbf{y}$ to new coordinates $\mathbf{x}$ such that

$$\mathbf{x} = \mathbf{y} - \mathbf{X}(t). \tag{2.14}$$

with a time-dependent translation $\mathbf{X}(t)$. The new velocity is given by

$$\mathbf{u}(\mathbf{x},t) = \mathbf{v}(\mathbf{y},t) - \mathbf{V}(t) \tag{2.15}$$

where $\mathbf{V}(t) = d\mathbf{X}(t)/dt$. Assume $\mathbf{X}(t)$ to describe the center of mass for a spherical particle in the fluid. If the Navier Stokes equation is transformed from the laboratory reference frame to the reference frame of the sphere, $\mathbf{v}$ is the velocity in the laboratory reference frame and $\mathbf{u}$ is the one in the reference frame of the sphere; $\mathbf{y}$ and $\mathbf{x}$ are the spatial coordinates, respectively. In terms of the new velocity $\mathbf{u}(\mathbf{x},t)$, the time-derivative term is given by

$$\begin{aligned}\partial_t\mathbf{v}(\mathbf{y},t) &= \partial_t\mathbf{u}(\mathbf{y}-\mathbf{X}(t),t) + \dot{\mathbf{V}}(t)\\ &= \partial_t\mathbf{u}(\mathbf{x},t) - (\mathbf{V}(t)\cdot\nabla_{\mathbf{x}})\mathbf{u}(\mathbf{x},t) + \dot{\mathbf{V}}(t).\end{aligned} \tag{2.16}$$

The advective term $(\mathbf{v}\cdot\nabla_{\mathbf{y}})\mathbf{v}$ is found to be

$$(\mathbf{v}\cdot\nabla_{\mathbf{y}})\mathbf{v} = (\mathbf{u}\cdot\nabla_{\mathbf{x}})\mathbf{u} + (\mathbf{V}(t)\cdot\nabla_{\mathbf{x}})\mathbf{u}. \tag{2.17}$$

Thus, the term $(\mathbf{V}(t)\cdot\nabla_{\mathbf{x}})\mathbf{u}$ cancels out and in the new coordinates the Navier-Stokes equation reads

$$\frac{\partial}{\partial t}\mathbf{u} + (\mathbf{u}\cdot\nabla)\,\mathbf{u} = -\nabla p + \nu\nabla^2\mathbf{u} - \frac{d}{dt}\mathbf{V}(t). \tag{2.18}$$

where ∇ is the gradient with respect to the coordinates $\mathbf{x}$. The new term on the right hand side is due to the acceleration of the new reference frame relative to the old one. It may be absorbed into the pressure term. When transformed into a new reference frame, velocities and coordinates in the Navier-Stokes equation are substituted by the

new variables. Thus the terms of the Navier-Stokes equation are left invariant with respect to an arbitrary Galilei transformation.

If the unsteady Stokes equation (2.10) is transformed to a reference frame moving with velocity $\mathbf{V}(t)$, e.g. from the laboratory reference frame to the reference frame of the sphere, the new equation is

$$\partial_t \mathbf{u} - (\mathbf{V}(t) \cdot \nabla)\mathbf{u} = -\nabla p + \nu \nabla^2 \mathbf{u} - \frac{d\mathbf{V}}{dt}. \tag{2.19}$$

On the other hand, if the time-dependent Stokes equation is solved in the reference frame of the sphere, one finds for the flow in the laboratory reference frame

$$\partial_t \mathbf{v} + (\mathbf{V}(t) \cdot \nabla)\mathbf{v} = -\nabla p + \nu \nabla^2 \mathbf{v}. \tag{2.20}$$

Thus, the time-dependent Stokes equation is not Galilei invariant. The analytical solution of a specific problem depends therefore on the reference frame chosen for the Stokes equation. The difference of the solutions is small, if the advective term is small, i.e. if the unsteady Stokes equation is valid. Presuming that the linearization of the Navier-Stokes equation is valid, it does therefore not matter, if the unsteady Stokes equation is solved in the reference frame of the sphere or in the laboratory reference frame.

2.3 Stokes' solutions

2.3.1 Stream function and boundary conditions

Consider a sphere moving uniaxially at velocity $V(t)\mathbf{e}_x$ in a fluid which is at rest for $r \to \infty$. The produced flow is then conveniently solved in the reference frame of the sphere in spherical coordinates, see figure 2.2. The flow is azimuthaly invariant (in ϕ-direction) and two-dimensional in the r-θ-plane. This allows to describe the flow in terms of a scalar stream function $\psi(r, \theta, t)$. The advantage of the description of the flow by the stream function is that the solution is automatically divergence free. The meaning of the stream function is the following: constant values of the stream function give rise to contours, which represent the instantaneous streamlines of the flow, i.e. the momentary direction of the fluid velocity.

For spherical coordinates the velocity is given by $\mathbf{u} = \nabla \times [\psi/(r \sin\theta)\mathbf{e}_\phi]$ (see e.g. [6]). The flow can also be described in terms of a vector potential $\mathbf{A} = A_\phi \mathbf{e}_\phi$, such that $\mathbf{u} = \nabla \times \mathbf{A}$. This is then related to the stream function as $A_\phi = \psi/(r \sin\theta)$. The

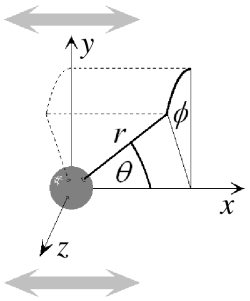

Figure 2.2: Spherical (r, θ, ϕ) and cartesian (x, y, z) coordinates in the reference frame of the sphere. The fluid at infinity is moving with velocity $-V(t)\mathbf{e}_x$, indicated by the grey arrows.

velocity components of the flow are given by

$$u_r = \frac{1}{r^2 \sin\theta}\partial_\theta \psi \qquad \text{and} \qquad u_\theta = -\frac{1}{r\sin\theta}\partial_r \psi. \tag{2.21}$$

At infinity, the boundary conditions for the flow are

$$\left.\begin{array}{rcl} u_r &=& -V(t)\cdot\cos\theta \\ u_\theta &=& V(t)\cdot\sin\theta \end{array}\right\} \quad \text{for} \quad r\to\infty. \tag{2.22}$$

and at $r = R$

$$u_r = 0 \qquad \text{and} \qquad u_\theta = 0. \tag{2.23}$$

The former boundary conditions are satisfied by the free flow in polar coordinates, with stream function

$$\psi_\infty = -\frac{1}{2}V(t)r^2\sin^2\theta. \tag{2.24}$$

The latter boundary conditions yield

$$\psi(r,\theta)|_{r=R} = 0 \qquad \text{and} \qquad \partial_r\psi(r,\theta)|_{r=R} = 0. \tag{2.25}$$

The transformation of the flow from the reference frame of the sphere $\mathbf{u}$ back to the laboratory reference frame $\mathbf{v} = \mathbf{u} + V(t)\mathbf{e}_x$ corresponds to the subtraction of the free flow term (2.24) from the stream function.

2.3.2 Steady flow past a sphere

One of the simplest solutions of the Stokes equation is that for the flow past a steadily moving sphere, see e.g. [6]. For the sphere moving in x-direction at constant velocity

$V(t) = U$, in terms of the stream function $\psi(r, \theta)$, the steady Stokes equation (2.7) becomes

$$E^2 E^2 \psi(r, \theta) = 0 \tag{2.26}$$

where

$$E^2 \psi = \partial_r^2 \psi + \frac{\sin\theta}{r^2} \cdot \partial_\theta \left(\frac{1}{\sin\theta} \partial_\theta \psi \right). \tag{2.27}$$

In the reference frame of the sphere, the solution for ψ is

$$\psi = \left[-\frac{U r^2}{2} + \frac{U R^2}{4} \left(\frac{3r}{R} - \frac{R}{r} \right) \right] \cdot \sin^2\theta. \tag{2.28}$$

Remarkable, and the source of many difficulties, is the slow 1/distance decay of the flow induced by the sphere, viz.

$$u_r = -U\cos\theta + \frac{3}{2}\frac{UR}{r}\left(1 - \frac{R^2}{3r^2}\right)\cos\theta \tag{2.29}$$

$$u_\theta = U\sin\theta - \frac{3}{4}\frac{UR}{r}\left(1 + \frac{R^2}{3r^2}\right)\sin\theta. \tag{2.30}$$

One of the consequences of the slow decay is that the sphere carries an infinite amount of fluid with it, as will be discussed in section 2.4.

2.3.3 Unsteady flow past an oscillating sphere

Unsteady Stokes equation

For the unsteady case, equation (2.10) becomes

$$E^2 \left(E^2 - \frac{1}{\nu}\partial_t \right) \psi = 0. \tag{2.31}$$

Since the operators E^2 and $E^2 - \nu^{-1}\partial_t$ commute, equation (2.31) may be separated into two second-order equations. Hence, the flow is composed of the solutions of

$$\left(E^2 - \frac{1}{\nu}\partial_t \right) \psi = 0 \tag{2.32}$$

and

$$E^2 \psi = 0. \tag{2.33}$$

Equation (2.32) is a diffusion equation with its physical origin in the diffusion of vorticity: taking the curl of equation (2.10), one obtains for the vorticity $\boldsymbol{\omega} = \nabla \times \mathbf{u}$

$$\partial_t \boldsymbol{\omega} = \nu \nabla^2 \boldsymbol{\omega}. \tag{2.34}$$

For the two-dimensional flow the only component for the vorticity is in ϕ-direction and is related to ψ via

$$\omega_\phi = -\frac{E^2\psi}{r\sin\theta}. \tag{2.35}$$

Inserting this into the diffusion equation for the vorticity (2.34) leads to equation (2.32).

The following consideration shows the origin of the flow field associated with (2.33). A velocity potential Φ with $\mathbf{u} = \nabla\Phi$, which due to the incompressibility $\nabla \cdot \mathbf{u} = 0$ satisfies $\nabla^2\Phi = 0$, is related to the components of a potential flow via[1] $u_r = \partial_r\Phi$ and $u_\theta = \partial_\theta\Phi/r$. Substituting these expressions into (2.21), the equations relating the flow to the stream function, one obtains the relationships

$$\partial_r\psi = -\partial_\theta\Phi \cdot \sin\theta \qquad \text{and} \qquad \partial_\theta\psi = r^2 \cdot \partial_r\Phi \cdot \sin\theta. \tag{2.36}$$

Hence equation (2.33) expressed in terms of Φ reads $-\sin\theta \cdot \partial_{r\theta}\Phi + \sin\theta \cdot \partial_{\theta r}\Phi = 0$, which is fullfilled identically. By relating the stream function to a velocity potential, it has been shown that equation (2.33) is fullfilled identically. Therefore, the associated flow is a potential flow.

This represents the character of the unsteady Stokes equation: in addition to the vorticity diffusion flow there is a potential flow and for the Stokes flow past an obstacle, both contribute.

Oscillating sphere

The oscillating sphere moves in x-direction with velocity $V(t) = \mathrm{Re}(U \exp i\omega t)$ where $\mathrm{Re}(x)$ denotes the real part of x. For convenience and since the time-dependent Stokes equation is linear, the flow is solved for a complex valued velocity of the sphere $V(t) = U \exp i\omega t$, but only the real part of the complex valued stream function contributes for the flow. Hence, the time-derivative becomes $\partial_t = i\omega$. For $r \to \infty$, the flow becomes a free flow and the stream function becomes $\psi_\infty = -U \exp i\omega t \cdot r^2 \sin^2\theta/2$, cf. equation (2.24). This suggests an ansatz

$$\psi = F_0(r) \cdot \exp i\omega t \cdot \sin^2\theta. \tag{2.37}$$

$F_0(r)$ is then decomposed as $F_0(r) = f_0(r) + g_0(r)$, where from equations (2.32) and (2.33) respectively

$$\left(\partial_r^2 - \frac{2}{r^2} - \frac{i\omega}{\nu}\right) f_0(r) = 0 \tag{2.38}$$

[1] Note that the potential flow may involve a singularity at $r = 0$. However, for a sphere of finite radius, this singular point is not part of the fluid domain.

and

$$\left(\partial_r^2 - \frac{2}{r^2}\right) g_0(r) = 0. \tag{2.39}$$

The solution for the first equation is obtained as $f_0(r) = \exp(-\kappa r) \cdot (1 + (\kappa r)^{-1})$ with the dispersion relation $i\omega/\nu = \kappa^2$. Two complex solutions exist, which are given by $\kappa = \pm\sqrt{i\omega/\nu}$. Since κ is a complex number, the solutions are oscillating and as a function of r either growing or decaying exponentially. Considering the boundary conditions at infinity, only negative real parts for the exponential function, i.e. positive real parts for κ, have a valid contribution to the stream function. The square roots $\sqrt{i}$ are chosen such that in terms of $k = \sqrt{\omega/\nu}$

$$\kappa = \sqrt{i}k \begin{cases} ke^{i\pi/4} & \text{for} \quad \omega > 0 \\ ke^{-i\pi/4} & \text{for} \quad \omega < 0. \end{cases} \tag{2.40}$$

When positive and negative frequencies are used, it is important to distinguish κ for the two cases. Since only the real part of the solution contributes to the stream function, ω is restricted without loss of generality to positive values. Thus one finds

$$f_0(r) = A \cdot e^{-\sqrt{i}kr} \cdot \left(1 + \frac{1}{\sqrt{i}kr}\right) \tag{2.41}$$

where $\sqrt{i} = \exp(i\pi/4)$ and A is an arbitrary complex constant to be determined from the boundary conditions.

The potential flow contribution may be decomposed into two terms

$$g_0(r) = g_0^d(r) + g_0^f(r) \tag{2.42}$$

where the two independent solutions are found as

$$g_0^d(r) = \frac{C}{r} \tag{2.43}$$

$$g_0^f(r) = D \cdot r^2 \tag{2.44}$$

with the two arbitrary constants C and D. $g_0^d(r)$ is a potential doublet, i.e. the potential flow due to a source and a sink placed at an infinitesimal distance from the origin: The velocity potential for a source of strength $C/4\pi$ is given by $\Phi = -C/r$. A source and a sink aligned at an infinitesimal distance from the origin along $\theta = 0$, which is in x-direction, is obtained by differentiation with respect to x, such that the doublet potential is given by $\Phi^d = -Cx/r^3 = -C\cos\theta/r^2$. Up to a scaling factor, both $g_0^d(r)$ and Φ^d lead to the same flow field for the doublet, which is

$$u_r = \frac{2C\cos\theta}{r^3} \qquad \text{and} \qquad u_\theta = \frac{C\sin\theta}{r^3}. \tag{2.45}$$

From the composition as a source and a sink at an infinitesimal distance, the doublet term is an instantaneous potential flow originating from the fluid that is instantaneously displaced by the sphere.

The second term $g_0^f(r)$ is the free flow resulting from the reference frame transformation. This term vanishes in the laboratory reference frame where the fluid is at rest at infinity.

The stream function which describes the time-dependent Stokes flow past a sphere in oscillatory motion is finally given by

$$\psi(r,\theta,t) = F_0(r)\exp(i\omega t)\sin^2\theta \tag{2.46}$$

and

$$\begin{aligned} F_0(r) &= f_0(r) + g_0^d(r) + g_0^f(r) && (2.47)\\ f_0(r) &= -\frac{3}{2}\frac{UR}{r}\cdot\frac{1+\sqrt{i}kr}{ik^2}\cdot e^{-\sqrt{i}k(r-R)} && (2.48)\\ g_0^d(r) &= \frac{3}{2}\frac{UR}{r}\cdot\frac{1+\sqrt{i}kR+ik^2R^2/3}{ik^2} && (2.49)\\ g_0^f(r) &= -\frac{Ur^2}{2}. && (2.50) \end{aligned}$$

The flow in polar coordinates is obtained as

$$\begin{aligned} u_r(r,\theta,t) &= \frac{1}{r^2\sin\theta}\partial_\theta\psi(r,\theta,t) && (2.51)\\ u_\theta(r,\theta,t) &= -\frac{1}{r\sin\theta}\partial_r\psi(r,\theta,t), && (2.52) \end{aligned}$$

cf. equation (2.21).

The range of the diffusional flow, equation (2.48), is finite and of order k^{-1}, since it is exponentially damped. In addition, due to the complex argument, the exponential function $f_0(r)$ is oscillating with a wave length k^{-1}. To get an impression of the corresponding stream function, figure 2.3(a) shows the stream function $\cos r\sin^2\theta$, which is, apart from a radial modification due to the omitted prefactor, the same as $f_0(r)\cdot\sin^2\theta$. It turns out that the periodic radial part of the stream function is represented as concentrical, equally distanced clockwise and counter clockwise rotating vortex rings.

The doublet term stream function $g_0^d(r)\sin^2\theta$, with $g_0^d(r)$ from equation (2.43) falls of as $1/r^3$ for $r\to\infty$. Figure 2.3(b) shows the streamlines for $\psi = \sin\theta^2/r$. The related stream function is composed of a source and a sink at an infinitesimal distance from $x = 0$. The flow shows a vortex ring, i.e. the section through the axisymmetric flow

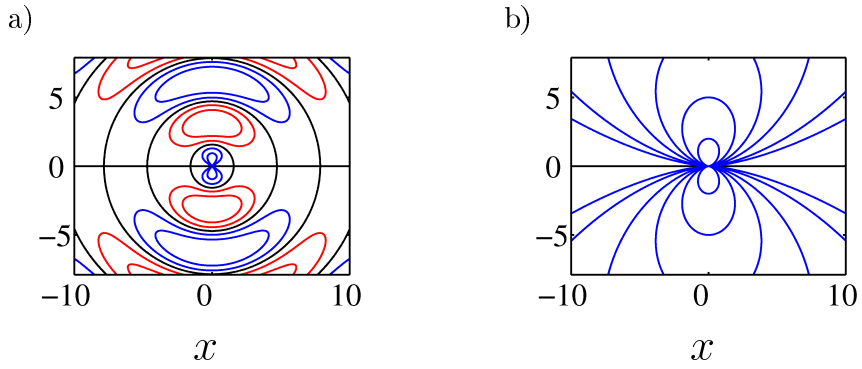

Figure 2.3: Streamlines for functions (a): $\sin\theta^2 \cos r$ and (b): $\sin\theta^2/r$. Blue color for positive values of the stream function, whereas red contours represent negative values. Black color for zero stream function.

in figure 2.3 displays a vortex at $\theta = \pi/2$ and at $\theta = 3\pi/2$, located at an infinitesimal distance from the origin.

The flow of the vorticity diffusion singularity becomes a potential doublet at the center[2]: from equation (2.41) one obtains in the limit $f_0(r) \to A/\sqrt{i}kr$ as $r \to 0$.

For $kr \to \infty$ (i.e. either k large, such that the frequency is large or the viscosity is small, or r much larger than the extension of the vorticity diffusion flow k^{-1}), the length scale of the vorticity flow is small compared to the distance from the sphere. Hence, far away from the sphere, diffusional flow is damped exponentially and the only remaining flow is potential flow. Assuming that k^{-1} is much smaller than the sphere radius, there is a thin layer of vorticity flow around the sphere, followed by the potential flow region, which decays as $1/r^3$. To leading order in this case, from the equations above, the stream function is found to be

$$\psi = Ue^{i\omega t} \cdot \frac{R^3}{2r} \cdot \sin^2\theta + O(k^{-1}). \tag{2.53}$$

This is the flow which results from the instantaneous displacement of fluid by the sphere.

The leading order term is usually reffered to as irrotational flow past a sphere (which corresponds to potential flow) [6].

Assuming kr to be small, i.e. either k small, such that the frequency is small or the viscosity is large, or r much smaller than the extension of vorticity diffusion k^{-1}, $F_0(r)$

[2]Figure 2.3 does not show this behaviour, since the radial dependence of $f_0(r)$ has been omitted.

may be expanded into a Taylor series and one obtains

$$F_0(r) = -\frac{Ur^2}{2} + \frac{UR^2}{4}\left(\frac{3r}{R} - \frac{R}{r}\right) + O(kr), \tag{2.54}$$

which is exactly the solution for the steadily moving sphere, equation (2.28).

At distances small compared to k^{-1}, the vorticity field responds instantaneously and the flow becomes approximately steady Stokes flow. Thus, steady Stokes flow is an appropriate approximation of the flow close to the sphere. The range of the approximation is determined by the diffusion length $\sqrt{\nu/\omega}$ and is large when the viscosity is large. In contrast, vorticity is hardly diffused to distances large compared to $\sqrt{\nu/\omega}$. Vorticity is cut off exponentially and the only flow remaining at large distances is potential flow, decaying as $1/r^3$. For large values for the frequency ω, the steady range may be very small.

The unsteady Stokes equation has similarities to a diffusion equation. If vorticity is diffused to a stationary state, the flow obeys steady Stokes equation. However, the range for the steady Stokes equation to be valid is set by the viscous diffusion length, much similar to the start-up problem for the wall from the beginning of the chapter. For the oscillating sphere, vorticity is diffused up to a finite distance, given by $k^{-1} = \sqrt{\nu/\omega}$. Below this distance, the flow is steady and decaying as $1/r$, whereas no vorticity diffuses to distances large compared to that and the flow is potential flow and decays more rapid, as $1/r^3$.

2.3.4 Flow field

Figure 2.4 shows the sphere oscillating at $X(t) = -D \cdot \sin \omega t$ for different times. The various panels show the steady Stokes solution in the lower half $-2 < y < 0$ and the unsteady solution in the upper half $0 \leq y < 2$. Exceptions are panels (a) and (i), which respectively show the unsteady and the steady solution over the full domain. From these two panels, it is obvious that the flow is symmetrical with respect to the x-axis, which is due to the θ-symmetry of $\sin^2\theta$, i.e. $\psi(\theta) = \psi(-\theta)$.

The time-dependent solution is qualitatively different from the steady solution. First, from figure 2.4, the time-dependent flow shows vortices, which are periodically shed at the sphere surface. Time-dependent flow is the transport of vorticity, such that a change of the sphere velocity is transported at finite speed away from the sphere surface. Therefore, the flow velocity along the x-axis may have alternating sign as one follows the axis. In panels (d) and (h), the flow is non-uniform along the x-axis.

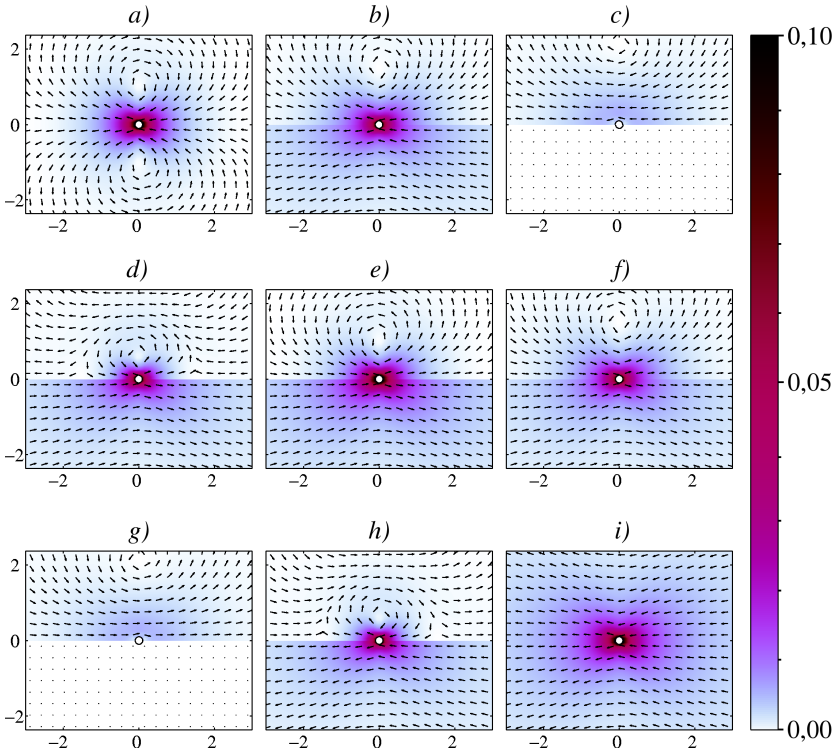

Figure 2.4: For comparison of time-dependent and steady Stokes flow, in panels b to h the lower half of each picture $-2 < y < 0$ shows the steady flow in the laboratory reference frame, whereas the upper half $0 < y < 2$ shows the time-dependent flow around the sphere in oscillatory motion. Panel a shows the unsteady solution over the full range, whereas panel i shows steady Stokes flow. The color represents the absolute value of the fluid velocity. The instantaneous position of the sphere at a time t is given by $X(t) = -D \cdot \sin \omega t$. The panels show the flow over one full period of time at times $t_a = 2\pi\omega^{-1} \cdot 0/8 = 0$, $t_b = 2\pi\omega^{-1} \cdot 1/8$, ..., $t_i = 2\pi\omega^{-1} \cdot 8/8$, such that in c and g, at $t_c = \pi\omega^{-1}/2$ and $t_g = 3\pi\omega^{-1}/2$, the sphere is at rest at its left and right turning point, respectively. Parameters are $R = 0.1$, $D = 0.005$, $\omega = 20$ and $\nu = 10$.

For the steady solution, this is not the case, since this is a Taylor expansion and the fluid velocity changes instantaneously when the sphere velocity is changed. Steady and unsteady solution match at $r = R$ for distances $r - R \ll k^{-1} \approx 0.7$, which clearly displays the valid range of the steady Stokes solution, as was obtained analytically in subsection 2.3.3. This shows that in a finite range vorticity spreads quickly, the fluid responds instantaneously and the flow is steady Stokes flow. Diffusion limits vorticity to distances from the sphere below k^{-1}. For distances larger than that, the fluid does not respond instantaneously. This bound, which separates steady and time-dependent Stokes flow, has been obtained before from the equations.

Unsteady flow drops off more rapid with the distance than the steady flow, which is due to the $1/r^3$ decay from the potential doublet term compared to the $1/r$ decay from the steady flow. Moreover, whereas the steady solution assumes a trivial shape at the turning points of the sphere $X = \pm D$, i.e. when the sphere is instantaneously at rest in panels (c) and (g), the unsteady solution still displays flow, since boundary information is spreading diffusively rather than instantaneously.

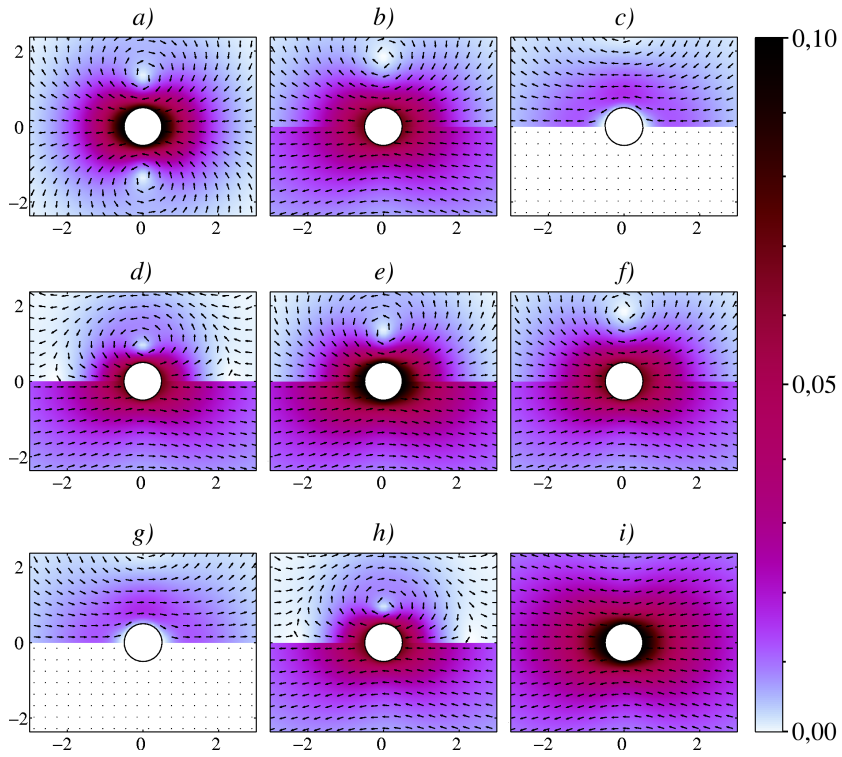

Figure 2.5: Same as figure 2.4, but for $R = 0.5$.

Figure 2.5 shows the flow around an oscillating sphere of radius $R = 0.5$. Qualitatively, the figure is much the same as figure 2.4, but the flow is extended over a wider region. This shows that the flow which is produced by large spheres is stronger than that produced by small spheres, even though the fluid velocities are equal at the sphere surface; note the prefactors of equations (2.48) and (2.49).

From equations (2.19) and (2.20), and figures 2.4 and 2.5, there is an interpretation of the meaning of small Reynolds number, of negligible advective terms: A cross section of the flow in the reference frame of the sphere shows two vortices which are symmetrical about the x-axis, i.e. the flow is a ring vortex. Hence, when transforming back into the laboratory reference frame, the vortices are advected, such that they oscillate back and forth. This is the effect of the advection term in equation (2.20). On the other hand, if the flow is calculated in the laboratory refrence frame and then transformed to the sphere reference frame, then the vortices are oscillating back and forth in the reference frame of the sphere. If the difference between these two velocity fields vanishes, the time-dependent Stokes equation is valid. A condition for that is the restriction to small oscillation amplitudes. If D becomes small compared to k^{-1}, the displacement of the vortices in x-direction becomes small and the time-dependent Stokes limit becomes valid. In figures 2.4 and 2.5, $kD \approx 7 \cdot 10^{-3}$, such that this should be valid.

This shows what has been found with scaling estimates in section 2.1.2: For an oscillation amplitude D the Reynolds number, as defined in equation (2.8), is given by $\omega D L_\nu/\nu = D/L_\nu = kD$. Hence a condition for the advective term to be small is that the oscillation amplitude is small compared to the length scale of the vortices $L_\nu = k^{-1}$, such that $kD \ll 1$. Also, this is a statement about the validity of the time-dependent Stokes equation for large oscillation amplitudes: the amplitude may be arbitrary large, even larger than the sphere radius. Time-dependent Stokes flow will yet be valid if the viscous length scale is even larger, such that $kD \ll 1$. This has been already noted by Stokes [65].

2.4 Flux for steady and unsteady flow

In the laboratory reference frame, the flux produced by the sphere across the plane $x = 0$, which is at $\theta = \pi/2$, is calculated as

$$\begin{aligned} j_x|_{\theta=\pi/2} &= 2\pi \cdot \int_R^\infty v_x|_{\theta=\pi/2}\, r dr \\ &= 2\pi \cdot \int_R^\infty \left[V(t) - u_\theta(r)|_{\theta=\pi/2}\right] r dr \end{aligned} \tag{2.55}$$

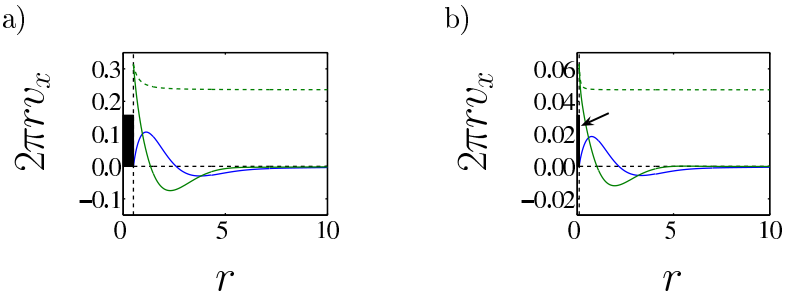

Figure 2.6: Integrand $2\pi r \cdot v_x$ of equation (2.55) for $R = .5$ (a) and $R = .1$ (b). The green line shows the flux for the sphere at maximum velocity, whereas the blue line corresponds to a turning point of the sphere. The area of the black rectangles equal the flux produced by the sphere. Note the arrow pointing to the rectangle for figure (a), where $R = 0.1$. Black dashed lines are for orientation the zero line and $r = R$. Oscillation frequency and amplitude are set to $\omega = 20$ and $D = 0.005$. Viscosity is set to $\nu = 10$.

with v_x the x-component of the flow in the laboratory frame and u_x in the reference frame of the sphere. Note that u_θ at $\pi/2$ is pointing in negative x-direction. For steady Stokes flow, from equation (2.30) we get for the flux of a sphere, which moves at velocity U

$$\begin{aligned} j_x|_{\theta=\pi/2} &= 2\pi \int_R^\infty \frac{3}{4} UR \left(1 + \frac{R^2}{3r^2}\right) dr \\ &= \infty. \end{aligned} \tag{2.56}$$

Hence the flux is diverging for steady Stokes flow.

For the oscillating sphere, $V(t) = U \exp(i\omega t)$ and we get for the flux

$$\begin{aligned} j_x|_{\theta=\pi/2} &= -2\pi \cdot e^{i\omega t} \int_R^\infty \frac{d}{dr}(f_0 + g_0^d) \cdot dr \\ &= -2\pi \cdot e^{i\omega t} \cdot (f_0 + g_0^d)\Big|_R^\infty \\ &= -\pi R^2 \cdot U \exp(i\omega t). \end{aligned} \tag{2.57}$$

Thus, while steady Stokes flow drives an infinite amount of fluid, time-dependent Stokes flow drives exactly the amount of fluid, which is displaced instantaneously by the sphere. The total flux of fluid and particle is equal to zero, independent of frequency and viscosity!

Figure 2.6 shows the integrand of equation (2.55). The area of the black rectangles equal the flux that is produced by the sphere. The vortices, which are presented in

figures 2.4 and 2.5, transport fluid in both directions, corresponding to positive and negative values of the integrand. The total amount of fluid that is moved may be huge, but the net flux has a value, which exactly balances the black rectangle area $\pi R^2 V(t)$ at each point of time and therefore may be small, as is the case in figure 2.6(b).

The dashed green curves show the integrand for the steady Stokes solution: since $v_x \propto r^{-1}$ at large distances, the integrand approaches a constant value, obtained from the first term of equation (2.56). Therefore, the integral given by the area below the dashed green curve is divergent.

The steady Stokes solution is valid up to distances $\sqrt{\nu/\omega}$ from the sphere. For larger distances, the time-dependent equations have to be used for the flow. The steady Stokes range extends to infinity as ν diverges. However, for the flux produced by the sphere it has been shown that the limits $\nu \to \infty$ and $r \to \infty$ do not commute: If ν is extended to infinity, the flow is described by steady Stokes flow at any distance and the flux diverges. Thus, false results may be obtained when steady Stokes flow is used to calculate quantities which require the flow at infinity! In contrast, if first the integral for the flux is evaluated for distances from the sphere up to infinity, one takes into account that the flow does not obey the steady Stokes equation at distances larger then $\sqrt{\nu/\omega}$, which regularizes the flux. Then the flux is finite even for infinite values of ν.

2.5 Correction of the unsteady Stokes flow

N. Riley [59] addressed a correction of the Stokes solution for the flow past a sphere in oscillatory motion by taking into account the advective term in the Navier-Stokes equation. The various terms of the Navier-Stokes equation

$$\partial_t \mathbf{u} + (\mathbf{u} \cdot \nabla)\mathbf{u} = -\nabla p + \nu \nabla^2 \mathbf{u} \tag{2.58}$$

are rescaled as follows: Time is rescaled as $\tilde{t} = \omega t$ (such that $\tilde{t}$ is nondimensional). Velocity is rescaled with the velocity U which is prescribed by the boundaries, i.e. $\tilde{\mathbf{u}} = \mathbf{u}/U$. Length is rescaled with the sphere radius, $\tilde{l} = l/R$. Then in terms of the Reynolds number

$$Re = \frac{UR}{\nu}, \tag{2.59}$$

the Navier-Stokes equation becomes

$$\lambda^2 \partial_{\tilde{t}} \tilde{\mathbf{u}} + Re(\tilde{\mathbf{u}} \cdot \tilde{\nabla})\tilde{\mathbf{u}} = -\tilde{\nabla}\tilde{p} + \tilde{\nabla}^2 \tilde{\mathbf{u}}, \tag{2.60}$$

where $\lambda^2 = \omega R^2/\nu$. This scaling procedure corresponds to the estimate of the various terms in subsection 2.1.3. For convenience, the tilde is droped for $\tilde{\mathbf{u}}$, $\tilde{\nabla}$, $\tilde{p}$ and $\tilde{t}$ in the following part.

One finds different equations depending on how Re and λ^2 scale relative to each other. Following Ockendon [49] or Riley [59], if $Re \ll \lambda^2$, the flow is expanded as $\mathbf{u} = \mathbf{u}_0 + Re\mathbf{u}_1$. The flow related to $\mathbf{u}_0$ is unsteady Stokes flow, such that $\mathbf{u}_0$ satisfies (2.10) and the first order correction to it satisfies

$$\lambda^2 \partial_t \mathbf{u}_1 + (\mathbf{u}_0 \cdot \nabla)\mathbf{u}_0 = -\nabla p + \nabla^2 \mathbf{u}_1, \tag{2.61}$$

together with the incompressibility condition $\nabla \cdot \mathbf{u}_1 = 0$. Apart from the time-derivative term, this is the equation that has been used also by Whitehead [69] in order to improve the steady Stokes solution for the flow past a sphere. He found that the iterated solution is not regular as r approaches infinity. This failure is known as Whitehead's paradox. In contrast, the flow iterated here is not steady Stokes flow, but time-dependent Stokes flow. For that the correction becomes regular again (see Appendix A for the details of the analysis)!

If $\lambda \ll Re$, such that the time-derivative term is much smaller than the advective term, the appropriate expansion for the flow is $\mathbf{u} = \mathbf{u_0} + \lambda^2 \mathbf{u}_1$. Mei [38] finds

$$\begin{aligned} Re(\mathbf{u}_0 \cdot \nabla)\mathbf{u}_0 &= -\nabla p_0 + \nabla^2 \mathbf{u}_0 && (2.62) \\ \partial_t \mathbf{u_1} + Re\,[(\mathbf{u}_0 \cdot \nabla)\mathbf{u}_1 + (\mathbf{u}_1 \cdot \nabla)\mathbf{u}_0] &= -\nabla p_1 + \nabla^2 \mathbf{u}_1. && (2.63) \end{aligned}$$

The first equation is the Oseen equation for the steady flow past the sphere. The second equation is a time-dependent perturbation of the Oseen equation. The meaning of this decomposition of $\mathbf{u}$ is as follows: For finite Reynolds numbers and low frequencies advection becomes important in the range where the fluid responds instantaneously, whereas away from the sphere, the flow is damped diffusively.

The complete solution of equation (2.61) was given by Noriyoshi Dohara [19]. In the remainder of this section, the investigation will be restricted to Reynolds numbers $Re \ll \lambda^2$, such that the advective term is much smaller than the time-derivative term and the decomposition of the flow gives rise to a correction of the unsteady Stokes solution.

2.5.1 Perturbation series

Using equations (2.21) to relate the axialsymmetrical flow $\mathbf{u}$ to the stream function ψ, in physical units the Navier-Stokes equation (2.4) is given by

$$E^2\left(\nu E^2 - \partial_t\right)\psi = \frac{1}{r^2}\left(\frac{\partial(\psi, E^2\psi)}{\partial(r,\mu)} + 2\cdot E^2\psi\cdot L\psi\right). \tag{2.64}$$

where L is defined as

$$L\psi = \frac{\cos\theta}{\sin^2\theta}\partial_r\psi - \frac{1}{r\sin\theta}\partial_\theta\psi. \tag{2.65}$$

As the Navier-Stokes equation, this equation is nonlinear.

For $\psi = \psi_0 + \psi_1$ and $\psi_1/\psi_0 = O(Re)$, one obtains the time-dependent Stokes equation for ψ_0, equation (2.31), and ψ_1 is to be determined from the next order equation, which is

$$E^2(\nu E^2 - \partial_t)\psi_1 = \frac{1}{r^2}\left(\frac{\partial(\psi_0^r, E^2\psi_0^r)}{\partial(r,\mu)} + 2\cdot E^2\psi_0^r\cdot L\psi_0^r\right) \tag{2.66}$$

where ψ_0^r denotes the real part of the complex valued solution that has been found in subsection 2.3.3. Since ψ_0 is harmonic, the terms on the right hand side involve terms of the order $\sin^2\omega t$ and $\cos^2\omega t$, which may be decomposed into steady terms of frequency 0 and such of frequency 2ω. Thus ψ_1 is given by the real part of

$$\psi_1(r,\theta,t) = \psi_{10}(r,\theta) + \psi_{12}(r,\theta)\cdot\exp 2i\omega t. \tag{2.67}$$

The correction to the flow past a sphere in oscillatory motion is composed of a steady flow and a response of the fluid of frequency 2ω.

To rewrite the terms on the left hand side of equation (2.66), note that because of the differential equations for $f_0(r)$ and $g_0(r)$, (2.38) and (2.39),

$$E^2\psi_0(r,\theta,t) = \frac{i\omega}{\nu}f_0(r)\cdot\exp i\omega t\cdot\sin^2\theta. \tag{2.68}$$

Then the right hand side of equation (2.66) is equal to

$$\frac{2\omega}{\nu}\frac{\sin^2\theta\cos\theta}{r^2}\left[\mathrm{Re}\left(e^{i\omega t}F_0(r)\right)\cdot\mathrm{Im}\left(e^{i\omega t}\left(\frac{2}{r} - \partial_r\right)f_0(r)\right)\right] \tag{2.69}$$

where $\mathrm{Re}(x)$ and $\mathrm{Im}(x)$ denote the real and imaginary part of x. The term in square brackets can be decomposed in terms of the frequencies, such that it equals

$$\left[\frac{i}{2}F_0(r)\left(\frac{2}{r} - \partial_r\right)\overline{f_0(r)} - \frac{i}{2}F_0(r)\left(\frac{2}{r} - \partial_r\right)f_0(r)\cdot e^{2i\omega t}\right] \tag{2.70}$$

where $\overline{f_0(r)}$ is the complex conjugate of $f_0(r)$. The angular part separates for

$$\psi_{10}(r,\theta) = F_{10}(r)\cdot\sin^2\theta\cos\theta \tag{2.71}$$

$$\psi_{12}(r,\theta) = F_{12}(r)\cdot\sin^2\theta\cos\theta. \tag{2.72}$$

The angular dependence is giving rise to ordinary differential equations for F_{10} and F_{12}

$$\left(\partial_r^2-\frac{6}{r^2}\right)\left(\partial_r^2-\frac{6}{r^2}\right)F_{10}(r)=\frac{i\omega}{\nu^2r^2}\left[F_0(r)\left(\frac{2}{r}-\partial_r\right)\bar{f}_0(r)\right] \tag{2.73}$$

and

$$\left(\partial_r^2-\frac{6}{r^2}-\frac{2i\omega}{\nu}\right)\left(\partial_r^2-\frac{6}{r^2}\right)F_{12}(r)=-\frac{i\omega}{\nu^2r^2}\left[F_0(r)\left(\frac{2}{r}-\partial_r\right)f_0(r)\right] \tag{2.74}$$

which have to be solved in order to find the solution for $\mathbf{u}_1$. The details of this solution are given in appendix A.

A cross section of the stream function shows two vortices above the sphere and two vortices below the sphere, cf. figure 2.7. This corresponds to two counter rotating ring vortices. The x-axis is a symmetry axis, as before, but in addition, there is an antisymmetrical axis along $\theta=\pi/2$. The simple angular dependence of ψ_1 can only give rise to a small angular correction to the unsteady Stokes solution, which restricts the oscillation amplitudes to values which are small compared to the length of the structures of the flow, i.e. $D\ll k^{-1}$. This highlights the restriction of the unsteady Stokes equation from section 2.2 and relates it to the scaling arguments in subsection 2.1.2.

From the homogeneous solutions of equation (2.73) it is found that the steady streaming decays as $1/r^2$, lower than the potential streaming of the unsteady Stokes solution, which decays as $1/r^3$. The magnitude of the steady streaming relative to the time-dependent Stokes flow depends on the Reynolds number, such that for small Re it overtakes the potential flow at distances which are orders of magnitude larger than the sphere radius.

2.5.2 Velocity field of the correction

The equations for the solution of the flow are Whitehead's equations [69]. He tried to find an improved solution for the steady Stokes flow and found that the iterated solution is not regular at large distances, which is known as Whitehead's paradox. In contrast to his solution, the flow here is regular. The difference for the integration of the full time-dependent Stokes flow instead of the steady flow is that the advective term of the former is cut-off exponentially whereas the latter is algebraic. Therefore for the former

the integral is finite, whereas it diverges for the latter. Details of the equations are given in Appendix A.

Considering the perturbation flow, figure 2.7 shows $\psi_1(r, \theta, t)$, more precisely the real and imaginary part of the spatial parts. The flow displays the same symmetry as the nonlinear term. The real and imaginary part indicate that vortices are shedded in directions $\theta = \pi/4$ and $\theta = 3\pi/4$ with frequency 2ω: a time series of snapshots would show the real and imaginary part of $\psi_1(r, \theta, t)$ in an alternating sequence. Thus, the vortices there would appear to be spreading. These travelling vortices add to the vortices of the time-dependent Stokes flow and therefore the total flow looks like the time-dependent flow, but with the positions of the vortices slightly corrected. At this point, the advective term displays its meaning: the vortices are not exactly located at $\theta = \pi/2$, as suggested by the time-dependent Stokes flow, but are displaced slightly to the left and to the right. If this displacement is small compared to the structures of the flow, then the advective term will be small as well. Figure 2.7 shows that the flow is largest inside a finite range of width k^{-1} around the sphere. If this range is large compared to the displacement of the sphere, which is of order D, the advective terms will be small.

At the front and rear of the sphere, the correction term seems to be large. This is related to the pushing and pulling of the fluid at the rear and front: Since vortices are spread at the rear periodically, there will be regions of positive and negative flow in x-direction, which produces high velocity gradients in this region. At the upper and lower surface of the sphere, gradients of the velocity are perpendicular to the flow and advective terms are small. The largest value of the correction of time-dependent Stokes flow is found close to the sphere in axis of motion.

In figure 2.8 at each position the rms fluctuations of the correction and the time-dependent Stokes flow are compared to each other. At about $\theta = \pi/4$ and $3\pi/4$, the relative magnitude is lowest. The vortices related to $\psi_1(r, \theta, t)$ are found in this direction. Since at their centers the flow is at rest, cf. figure 2.7, the relative correction in this direction is small.

In panel (a), two dark spots to the left and the right of the sphere appear. This shows again the velocity gradients at the leading and trailing edge of the sphere. Panels (b) and (c) show large relative amplitudes at a finite range around the sphere. In panel (c), the boundary of this range seems to be well separated from the rest. This is because the particular solution for the perturbation involves terms, which are exponential with an argument κr (details in appendix A). Therefore, at distances large compared to k^{-1}

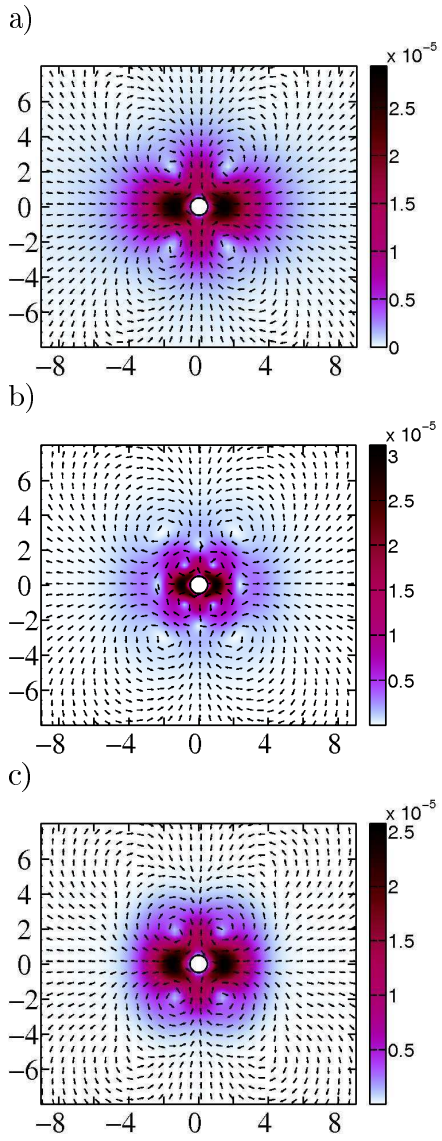

Figure 2.7: Correction of unsteady Stokes flow. The color shows the absolute value of the fluid velocity. (a) real part of the steady term. (b) real part of the 2ω-term. (c) imaginary part of the 2ω-term. Radius $R = 0.5$, $\omega = 20$ and $\nu = 10$. Amplitude of oscillation $D = 0.005$. Reynolds number $Re \approx 7 \cdot 10^{-3}$.

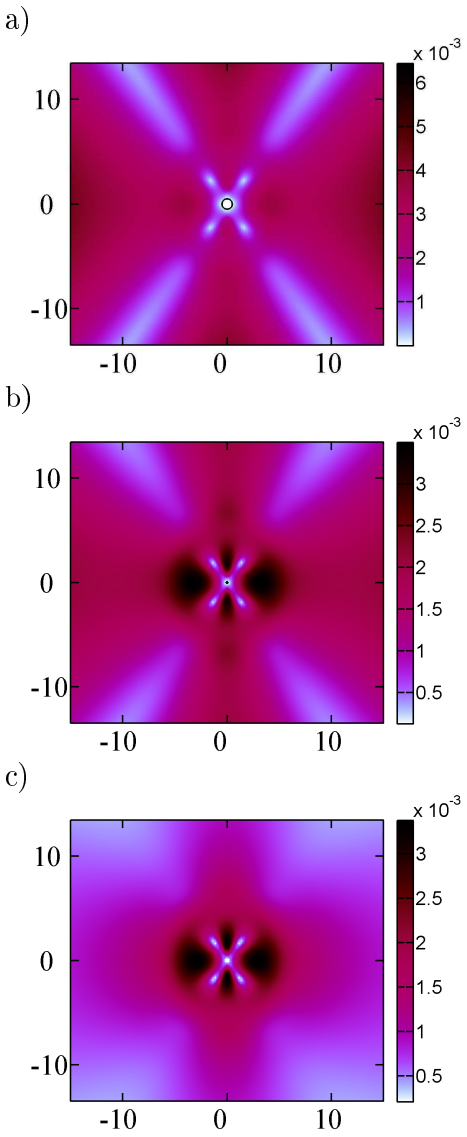

Figure 2.8: Comparison of the rms velocity fluctuations of the correction to the unsteady Stokes mean speed of the flow. (a) $R = 0.5$, (b) $R = 0.1$ and (c) $R = 0.01$ and $\omega = 20$, $\nu = 10$, $D = 0.005$. Note that the zero is suppressed in each case.

these terms must be small and the perturbation necessarily drops down.

Asymptotically as $r \to \infty$, the relative value seems to decrease for panels (b) and (c), while for (a) it seems to increase. Since the correction decays more weakly than the time-dependent Stokes flow, for all three of them the amplitudes diverge at large distances. This happens however in these cases at distances which are orders of magnitudes larger than the range of the figure and is thus not visible here.

In this section, the validity of the time-dependent solution has been checked with an expansion similar to that which has been used by Whitehead. In contrast to his solution, the first-order expansion of the time-dependent Stokes flow is regular at large distances. The correction to the steady Stokes flow is composed of a steady streaming and a streaming of frequency 2ω. The flow is composed of two counter rotating ring vortices and symmetrical about the x-axis and $\theta = \pi/2$. It has further been confirmed that unsteady Stokes is valid, if $D \ll \sqrt{\nu/\omega}$, i.e. the oscillation amplitude is much smaller than the viscous diffusion length. The comparison of the perturbative solutions to the time-dependent Stokes flow has shown, that the largest correction is found at leading and trailing edge of the sphere.

2.6 Equations of motion for the sphere

For the sphere to move oscillatory, an external force $\mathbf{F}^{(\text{ext})}$ has to be applied to satisfy the equation of motion. In addition to $\mathbf{F}^{(\text{ext})}$, the flow causes a backreaction onto the sphere, such that

$$m_S \dot{\mathbf{V}} = \mathbf{F}^{(\text{ext})} + \mathbf{F}^{(\text{fluid})} \tag{2.75}$$

with m_S being the mass of the sphere and $\mathbf{F}^{(\text{fluid})}$ the force from the flow.

The famous result in the case of steady flow around a sphere moving at constant velocity $\mathbf{V}$ is

$$\mathbf{F}^{(\text{fluid})} = -6\pi\mu R \cdot \mathbf{V} \tag{2.76}$$

where $\mu = \rho\nu$ is the dynamic viscosity of the fluid. The viscous drag $\mathbf{F}^{(\text{fluid})}$ is a friction force and counterbalances $\mathbf{F}^{(\text{ext})}$.

For the uniaxially oscillating sphere, one gets [65] for the component of the force in the direction of the motion

$$F^{(\text{fluid})} = -\left[\frac{m_F}{2} \cdot i\omega + 6\pi\mu R \cdot \left(1 + \sqrt{i}kR\right)\right] U e^{i\omega t}. \tag{2.77}$$

The mass of the fluid that is displaced by the sphere is denoted $m_F = 4\pi\rho R^3/3$. The first term on the right hand side is a consequence of the potential doublet streaming and

represents the force due to the instantaneous displacement of fluid by the sphere. This so-called added mass term is obtained also by considering only potential flow around the sphere [30, 66]. Why does the added-mass term not appear in the steady expression for the force? The added mass term represents the instantaneous acceleration of fluid due to a change of the sphere velocity. If the sphere moves steadily, there is still potential flow, but no instantaneous acceleration is related to it and the corresponding term therefore equal to zero. The force for steady flow has its only contribution from viscous gradients.

The modification of the viscous drag represents the impact of the vorticity that has been produced at earlier times and is acting back onto the sphere with a time-shift (note the complex valued prefactor).

Next, the velocity response of a sphere to an oscillatory force is studied. For a unidirectional force $\mathbf{F} = F_0 \exp(i\omega t)\mathbf{e}_x$, the velocity amplitude U of the sphere in x-direction is given by the equation

$$\left(m_S + \frac{1}{2}m_F\right) i\omega U = F_0 - 6\pi\mu R\left(1 + \sqrt{i}kR\right) U, \tag{2.78}$$

i.e.

$$U = \frac{F_0/6\pi\mu R}{1 + \sqrt{i}kR + \frac{2}{9}\left(\frac{\rho_S}{\rho} + \frac{1}{2}\right) \cdot ik^2R^2}. \tag{2.79}$$

The nominator $U_0 = F_0/6\pi\mu R$ is obtained as a response amplitude in the case $\nu \to \infty$, which is $k = 0$. This value corresponds to the balance of steady viscous drag and driving force.

The absolute value of U and the phase shift ϕ between force and velocity are shown in figure 2.9. Negative phase shift means that the velocity of the sphere lags behind the force. For small k (small in the sense that $kR \ll 1$, where R is kept fixed), the square-root behaviour dominates. The response amplitude is

$$U = U_0 \cdot \left(1 - \frac{kR}{\sqrt{2}}\right) \tag{2.80}$$

and the phase shift $\phi = -kR/\sqrt{2}$. Hence, the smaller k or equivalently the larger the structures of the flow, the smaller is the phase shift between the amplitude and the force. For $k = 0$, which for fixed ν is $\omega = 0$, steady viscous drag and driving force balance. This is the limit of a steadily moving sphere.

It is remarkable that the velocity response and the phase vary with the kinematic viscosity as $\sqrt{1/\nu}$. Even if the viscosity is large, the difference to the steady Stokes case might be considerable.

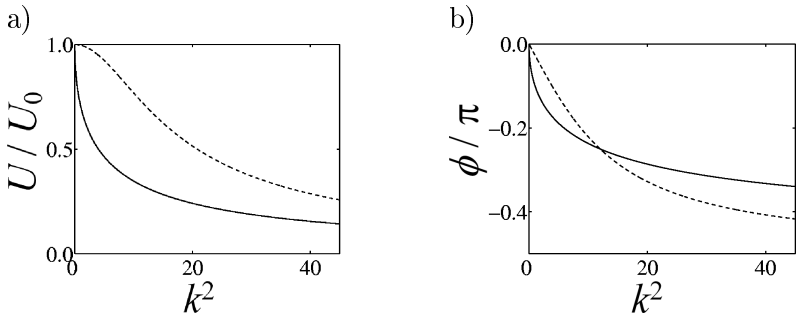

Figure 2.9: Velocity response amplitude U in terms of U_0 (a) and phase ϕ in terms of π (b) as predicted from the time-dependent Stokes equation plotted against $k^2 = \omega/\nu$ for $\rho_S = \rho$ and $R = 0.5$. Dashed lines show predictions of steady Stokes.

For comparison, the result for the response without the history and the added mass term term, i.e.

$$U = \frac{F_0/6\pi\mu R}{1 + \frac{2}{9}\frac{\rho_S}{\rho} ik^2 R^2} \tag{2.81}$$

is shown in figure 2.9 by dashed lines. It is clearly visible in all plots that the response predicted by steady Stokes is in contrast to the time-dependent prediction. In particular for small kR, the response is not linear in k. The difference between the two comes from the fact that for finite k the time-dependent force differs from the steady force.

Experiments have been performed by Abbad and Souhar [1, 2] to investigate the response of a particle to an oscillatory force at small Reynolds numbers. A fluid tank is adjusted on a vertically oscillating table. Therefore it is possible to impose a pseudo forces on the sphere which causes the sphere to oscillate in the tank. In addition, the sphere settles due to gravity. Gravitational motion and oscillation are treated separately. Steady motion coincides with the expression for the steady force. The oscillation is found in remarkable agreement with the time-dependent Stokes force. This shows that the motion may be interpreted as a linear composition of steady and oscillatory motion, which represents the linear character of the unsteady Stokes equation. The results for the oscillation are shown in figure 2.10. $\delta = \sqrt{2\nu/\omega}/R$ is the penetration depth of the vorticity, normalized to R. For the parameter range of the figure, ω was varied from about 4Hz (for $\delta = 2.5$) to 20Hz (for $\delta = 1$). Note that the oscillation amplitude D was fixed to approximately 5mm. Therefore as ω is increased (i.e. k is increased and δ is lowered), the amplitude is increased as well and vice versa.

In this section, the equations of motion for the harmonically forced sphere have been

(a)

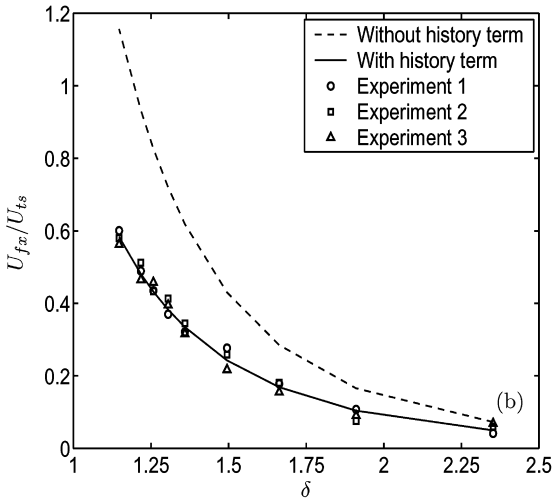

(b)

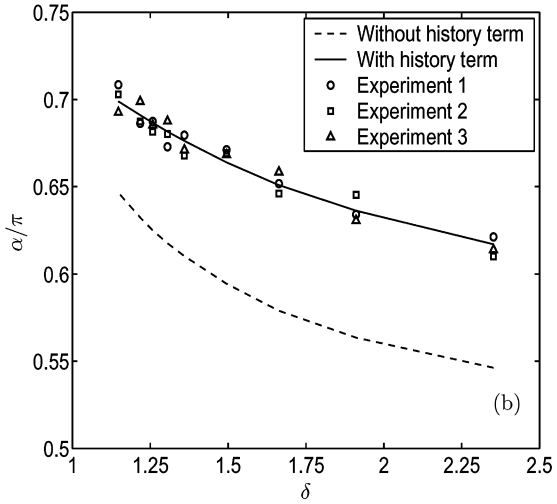

Figures 7a and 8a from [1] (with the friendly permission of the author).

Figure 2.10: Velocity response amplitude U_{fx} (a) and phase shift α (b) for the velocity response of a sphere to an oscillating force. The experiments were done with a teflon sphere of radius 2.5mm in glycerin with a kinematic viscosity of $69 \cdot 10^{-6} m^2/s$. $\rho = 1.257\text{g/cm}^3$ and $\rho_S/\rho = 1.75$. U_{ts} is the free fall velocity of the sphere.

formulated. Experimental measurements have shown that excellent agreement is found with the prediction from time-dependent Stokes flow, whereas the results are in striking contrast to the steady Stokes prediction. Note that these results are restricted to small Reynolds numbers. If the Reynolds number is finite, corrections of the force of the order of the Reynolds number become important [33, 37, 51].

2.7 Conclusions

It has been shown that the exclusion of the advective term in the Navier-Stokes equation, as eventually suggested by scaling arguments, does not a priori allow the exclusion of the partial time-derivative term. In contrary, taking into account time-dependence in the Stokes equation has a considerable effect on the flow: For a sphere in oscillatory motion, the flow is steady only inside a finite range $r < \sqrt{\nu/\omega}$ (with ν the kinematic viscosity and ω the oscillation frequency), where vorticity is in its diffusion equlibrium. Since vorticity is exponentially damped, it is hardly diffused beyond this range, such that the unsteady flow differs remarkably from the steady Stokes flow.

For the calculation of flow properties, it is important to question, whether for the distances in case vorticity diffusion is in steady state or not. For properties also involving the flow at large distances, the full time-dependent flow has to be taken into account, as has been exemplified here for the flux that is transported by the sphere: It is divergent for steady flow and equals the negative flux of the sphere for the time-dependent flow.

The validity range of the time-dependent Stokes equation has been found to be limited to small oscillation amplitudes D, such that the sphere is always inside the range of the viscous length $\sqrt{\nu/\omega}$. For oscillation amplitudes larger than that, advective terms get large and the neglection of the nonlinear term is no longer valid. Then, the steady and unsteady Stokes equation are both not valid.

Chapter 3

Flow past a sphere in arbitary motion

Stokes [65] gave an expression for the flow past a sphere, which moves at constant velocity $\mathbf{V}$ in a viscous fluid. This gives rise to an expression for the drag $\mathbf{F}$, that is exerted on the sphere, $\mathbf{F} = 6\pi R\mu\mathbf{V}$ with μ the dynamic viscosity of the fluid and R the radius of the sphere. Due to their simplicity, these expressions for flow and drag are often used also for a sphere in unsteady motion. Two implicit assumptions are made thereby: First, the sphere and the drag depend instantaneously on each other, $\mathbf{F}(t) \propto \mathbf{V}(t)$. Secondly, the flow $\mathbf{u}(t)$ and the velocity of the sphere depend instantaneously on each other and if r denotes the distance to the sphere, the flow decays as $1/r$, i.e. $\mathbf{u}(t) \propto \mathbf{V}(t)/r$.

The solution of the time-depedent Stokes equation for the flow past a sphere, whose center of mass is moving in one direction with arbitrary velocity, is known since Boussinesq [10, 11]. He obtained expressions for the flow and for the force, which the fluid exerts on the sphere. Basset [4], apparantly unaware of these works, obtained the same expression. He solved the flow for the sphere starting from rest and moving at constant velocity. By integrating this solution over the derivative of the sphere velocity, i.e. by adding up the solution for an infinitesimal change of the sphere velocity at each point of time, he found the solution for the flow past a sphere in uniaxial motion. The expression for the force, which is exerted by the viscous fluid on the sphere, is accounted to Basset [4, 5], Boussinesq [10, 11, 12] and Oseen [53] and sometimes called the BBO-equation. The calculation is based on the solution of the time-dependent Stokes equation and therefore in contrast to the expression from steady Stokes flow; force and flow involve not only the instantaneous velocity of the sphere at time t, but also contributions from the sphere velocity at former times $t' < t$. Computation of the flow and the equation of motion for an unsteadily moving sphere from the time-dependent Stokes equation gives results, which differ from the results that one obtains from the steady Stokes approach.

Experiments [1, 2, 31, 43] confirm these differences.

If in addition to the flow, which is caused by the sphere, there is an external flow field (e.g. a sphere that moves in turbulent flow), Maxey and Riley [35] computed an expression for the force, which is exerted on the sphere in this case. Their calculation assumes that the sphere follows the fluid so closely, that the induced perturbation of the flow by the sphere may be described by the unsteady Stokes equation.

In addition to time-dependence, the steady expressions miss out finite Reynolds number contributions to the force. When the Oseen equations (2.63) are used to take into account the advective term in the Navier-Stokes equation, corrections of order Reynolds number are found for the viscous drag on a steadily moving sphere at low Reynolds numbers (e.g. [52, 57]). The Oseen equations were also applied to obtain a correction to the BBO-equation at low Reynolds numbers by Lovalenti and Brady [33, 34]. Several attempts have been made to find easier, semi-empirical expressions for these equations. Reviews of these works have been given by Michaelides [41, 42].

Here, in order to show the deviation of time-dependent Stokes flow from steady Stokes flow, based on time-dependent Stokes flow, i.e. with the advective terms in the Navier-Stokes equation neglected, the equations for the flow and the viscous drag are reexamined. The equations for the flow are given in section 3.1. Then, the transition to steady Stokes flow is shown in section 3.2 for a sphere, which is at rest for time $t < 0$ and moves at constant velocity for $t \geq 0$. Section 3.3 recaptures the equation of motion for the sphere. The solution for a sedimenting sphere is reviewed in section 3.4.

3.1 Time-dependent Stokes flow

3.1.1 Unidirectionally moving sphere

General equations for the flow around a sphere which moves unidirectionally at arbitrary velocity are obtained by expanding the motion of the sphere into Fourier components, calculating the flow for each frequency, and finally integrating over all frequencies to recover the motion of the sphere. The velocity of a sphere $V(t)$ may be expanded into Fourier components $\hat{V}(\omega)$ such that

$$V(t) = \int_{-\infty}^{+\infty} \hat{V}(\omega) e^{i\omega t} d\omega. \tag{3.1}$$

The inverse expression for $\hat{V}(\omega)$ is then given by

$$\hat{V}(\omega) = \frac{1}{2\pi} \int_{-\infty}^{+\infty} V(t) e^{-i\omega t} dt. \tag{3.2}$$

For a single Fourier component the flow has been solved already in chapter 2. For the sphere moving at velocity $\hat{V}(\omega)(\exp i\omega t)$ in x-direction, we found that the Fourier amplitude $\hat{\psi}(r,\theta,\omega)$ of the stream function satisfies

$$\left(\frac{i\omega}{\nu} - E^2\right) E^2\hat{\psi}(r,\theta,\omega) = 0 \tag{3.3}$$

with E^2 defined as

$$E^2\hat{\psi} = \partial_r^2\hat{\psi} + \frac{\sin\theta}{r^2}\partial_\theta\left(\frac{1}{\sin\theta}\partial_\theta\hat{\psi}\right). \tag{3.4}$$

The solution is $\hat{\psi}(r,\theta,\omega) = \hat{V}(\omega)\hat{F}(r,\omega)\sin^2\theta$ and $\hat{F}(r,\omega) = \hat{f}(r,\omega)+\hat{g}_d(r,\omega)+\hat{g}_f(r,\omega)$. The single contributions to $\hat{F}(r,\omega)$ are

$$\hat{f}(r,\omega) = -\frac{3}{2}\frac{R}{r}\cdot\frac{1+\kappa r}{\kappa^2}e^{-\kappa(r-R)} \tag{3.5}$$

$$\hat{g}_d(r,\omega) = \frac{3}{2}\frac{R}{r}\cdot\frac{1+\kappa R+\kappa^2R^2/3}{\kappa^2} \tag{3.6}$$

$$\hat{g}_f(r,\omega) = -\frac{r^2}{2} \tag{3.7}$$

in terms of $\kappa = \sqrt{i\omega/\nu}$. For $\omega < 0$, the phase of κ is chosen as $-\pi/4$, whereas it is $\pi/4$ for $\omega > 0$, cf. equation (2.40). This ensures that the solution is regular for $r \to \infty$, since then $\hat{f}(r,\omega)$ in equation (3.5) is damped instead of growing exponentially.

The flow for a sphere moving at arbitrary velocity $V(t)$ is found by inverse Fourier transformation of $\hat{F}(r,\omega)$. In the inverse Fourier integral

$$F(r,t) = \int_{-\infty}^{+\infty}\hat{V}(\omega)\hat{F}(r,\omega)e^{i\omega t}d\omega, \tag{3.8}$$

substitute $\hat{V}(\omega)$ by the corresponding expression in terms of $V(t)$, given by equation (3.2). Then the integral equals

$$F(r,t) = \frac{1}{2\pi}\int_{-\infty}^{+\infty}dt'\left\{\int_{-\infty}^{+\infty}d\omega e^{i\omega(t-t')}\hat{F}(r,\omega)\right\}V(t'). \tag{3.9}$$

The harmonic stream function involves a singularity at $\omega = 0$ and the path for the Fourier integral has to be layed around that singularity. The argument $t-t'$ is positive, since the flow at a time t does not involve the velocity of the sphere at times t' later than t. The integral has to be layed such around the singularity that the integral vanishes for negative values of $t-t'$. The upper bound of the outer integral changes from $t' = \infty$ to $t' = t$.

Carrying out the transformation, one finds

$$\psi(r,\theta,t) = \sin^2\theta\cdot\int_{-\infty}^{t}dt'V(t')F(r,t-t') \tag{3.10}$$

and $F(r,\tau)$ in terms of

$$F(r,\tau) = f(r,\tau) + g^d(r,\tau) + g^f(r,\tau) \tag{3.11}$$

$$f(r,\tau) = -\frac{3R}{2}\left[\sqrt{\frac{\nu}{\pi\tau}}e^{-\frac{(r-R)^2}{4\nu\tau}} + \frac{\nu}{r}\mathrm{erfc}\left(\frac{r-R}{\sqrt{4\nu\tau}}\right)\right]\Theta(\tau) \tag{3.12}$$

$$g^d(r,\tau) = \frac{3R}{2}\left(\frac{\nu}{r} + \frac{R}{r}\sqrt{\frac{\nu}{\pi\tau}}\right)\Theta(\tau) + \frac{R^3}{2r}\delta(\tau) \tag{3.13}$$

$$g^f(r,\tau) = -\frac{r^2}{2}\delta(\tau). \tag{3.14}$$

$\delta(t)$ is the Dirac delta function and $\Theta(t)$ the Heaviside step function. For the definition of the complementary error function $\mathrm{erfc}(x)$, see equation (2.2).

Note that the potential doublet $g^d(r,\tau)$ decays as $1/r^3$, independent of the sphere motion. This is a result of the differential equation for potential flow (2.33), which does not involve a time-derivative term and describes a instantaneous reaction of the fluid to volume displacement.

$F(r,t)$ is the radial part of the stream function for a sphere moved at a velocity $V(t) = \delta(t)$. Basset's expression [4] for the time-dependent Stokes flow past a sphere is an integration of infinitesimal changes of the velocity; it involves $V'(t')$ instead of $V(t')$ and is obtained by a partial integration from the Greens function given above.

Apart from Bassets expression, the expressions for time-dependent Stokes flow past a sphere in arbitrary motion, (3.10) to (3.14), are found in literature. Ockendon [49] obtained an expression for the time-dependent flow at large distances from the sphere. Similar expressions for the solution of the time-dependent Stokes equation in the laboratory reference frame were found for instance by Asmolov [3] and Shu et al. [62]. All these expressions coincide with the expressions above when adapted to the notation that is used here.

3.1.2 Three-dimensional motion of the sphere

Consider a sphere moving at arbitrary velocity $\mathbf{V}(t)$. The contribution of the x-component of the velocity $V_x(t)$ to the flow may be obtained as follows: $H_x(r,t)$ denotes the integral of equation (3.10) with $V(t')$ substituted by $V_x(t')$, i.e.

$$H_x(r,t) = \int_{-\infty}^{t} dt' V_x(t') F(r, t-t'). \tag{3.15}$$

Then, transforming the radial and azimuthal component of the flow to cartesian coordinates (cf. figure 2.2) and substituting θ and ϕ by the corresponding expressions in terms

of x, y and z, one finds the flow given by

$$\begin{pmatrix} u_x \\ u_y \\ u_z \end{pmatrix} = \frac{2}{r^4}\begin{pmatrix} x^2 \\ yx \\ zx \end{pmatrix} H_x(r,t) - \frac{1}{r^4}\begin{pmatrix} x^2-r^2 \\ yx \\ zx \end{pmatrix} r\partial_r H_x(r,t) \tag{3.16}$$

with $r = \sqrt{x^2+y^2+z^2}$ being the distance to the center of the sphere. If the other components $H_y(r,t)$ and $H_z(r,t)$ are defined analogously, in component wise notation the flow $u_i(\mathbf{x},t)$ becomes

$$u_i(\mathbf{x},t) = \frac{1}{r^2}\left[\delta_{ij} r\partial_r H_j(r,t) + \frac{x_i x_j}{r^2}\left(2H_j(r,t) - r\partial_r H_j(r,t)\right)\right] \tag{3.17}$$

$$\begin{aligned} H_j(r,t) = {} & \left(\frac{R^3}{2r} - \frac{r^2}{2}\right) V_j(t) + \frac{3R}{2}\int_0^\infty d\tau V_j(t-\tau)\cdot \\ & \left[\sqrt{\frac{\nu}{\pi\tau}}\left(\frac{R}{r} - e^{-\frac{(r-R)^2}{4\nu\tau}}\right) + \frac{\nu}{r}\mathrm{erf}\left(\frac{r-R}{\sqrt{4\nu\tau}}\right)\right] \end{aligned} \tag{3.18}$$

with the Einstein sum convention for the sum over j and δ_{ij} denoting the Kronecker delta. Note that the integration variable in the definition of $H_j(r,t)$ has changed from t' to $\tau = t - t'$. Equations (3.17) and (3.18) give the complete solution for the time-dependent flow past a sphere, which moves with arbitrary velocity in all three directions.

3.2 Steady Stokes limit

Consider a sphere at rest for times $t < 0$ and moving with constant velocity V_0 for times $t \geq 0$, as investigated by Basset [4]. Here, the transient from zero fluid velocity to steady Stokes flow is investigated.

First, to obtain the stream function for constant sphere velocity from equation (3.10), equations (3.12) to (3.14) have to be integrated over time. Then an integration yields

$$\begin{aligned} V_0\int_0^t f(r,\tau)d\tau = {} & -\frac{3RV_0}{2r}\left[\nu t + \frac{R^2-r^2}{2}\right]\mathrm{erfc}\left(\frac{r-R}{\sqrt{4\nu t}}\right) \\ & -\frac{3RV_0}{2r}(r+R)\sqrt{\frac{\nu t}{\pi}}\exp\left(-\frac{(r-R)^2}{4\nu t}\right) \end{aligned} \tag{3.19}$$

$$V_0\int_0^t g^d(r,\tau)d\tau = \frac{3V_0R}{2r}\left(\nu t + 2R\sqrt{\frac{\nu t}{\pi}}\right) + \frac{R^3}{2r}V_0 \tag{3.20}$$

$$V_0\int_0^t g_f(r,\tau)d\tau = -\frac{r^2}{2}V_0. \tag{3.21}$$

These expressions are equal to the ones that have been found by Basset [4]. If t becomes large, the argument in the exponential and the complementary error function gets small

and the corresponding Taylor expansions may be used, for the latter

$$\operatorname{erfc}(x) = 1 - \frac{2}{\sqrt{\pi}}x + O(x^3). \tag{3.22}$$

Then with r fixed, in the limit $t \to \infty$ one finds

$$V_0 \int_0^t F(r,\tau) = -V_0 \frac{r^2}{2} + \frac{R^2}{4}\left(\frac{3r}{R} - \frac{R}{r}\right), \tag{3.23}$$

which is the steady Stokes stream function, equation (2.28). Note that for any finite t and ν, no matter how large, the expansion is only valid, if the distance r is such that $(r-R)/\sqrt{4\nu t} \ll 1$. Therefore, if distances are large and the condition is not fullfilled, the expansion fails. Then the time-dependent flow has to be used.

Figure 3.1 shows a sphere that started to move to the right from rest with constant velocity. At the surface of the sphere, the fluid moves with the sphere, whereas the fluid is at rest at large distances. The flow shows vortices, which are perpendicular to the direction of motion, much similar to the flow past a sphere in oscillatory motion. Figure

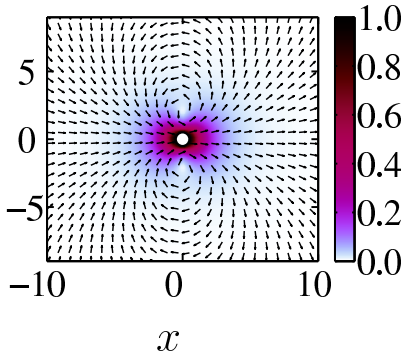

Figure 3.1: Flow after a time $t = 1$ past a sphere, which started from rest at $t = 0$ to move with constant velocity $V_0 = 1$. The sphere is moving in positive x-direction, which is to the right. The flow is shown in the laboratory reference frame and the snapshot is shown with the sphere in the center. The color shows the magnitued of the flow. Parameters: $R = 0.5$, $\nu = 1$.

3.2 shows the flow past the same sphere at later times. The flow is shown in laboratory reference frame, such that the flow is at rest at infinity[1]. As the sphere moves, the

[1]Note that the position of the x-axis is shifted in each panel with the sphere, such that the sphere is again seated in the origin.

vortices spread diffusively to larger distances. This is similar to the spreading of the vortices, when the sphere moves oscillatory, cf. figures 2.4 and 2.5, but there, vortices are generated periodically, whereas here the vortices are generated only once, when the sphere starts to move, and then are diffusing.

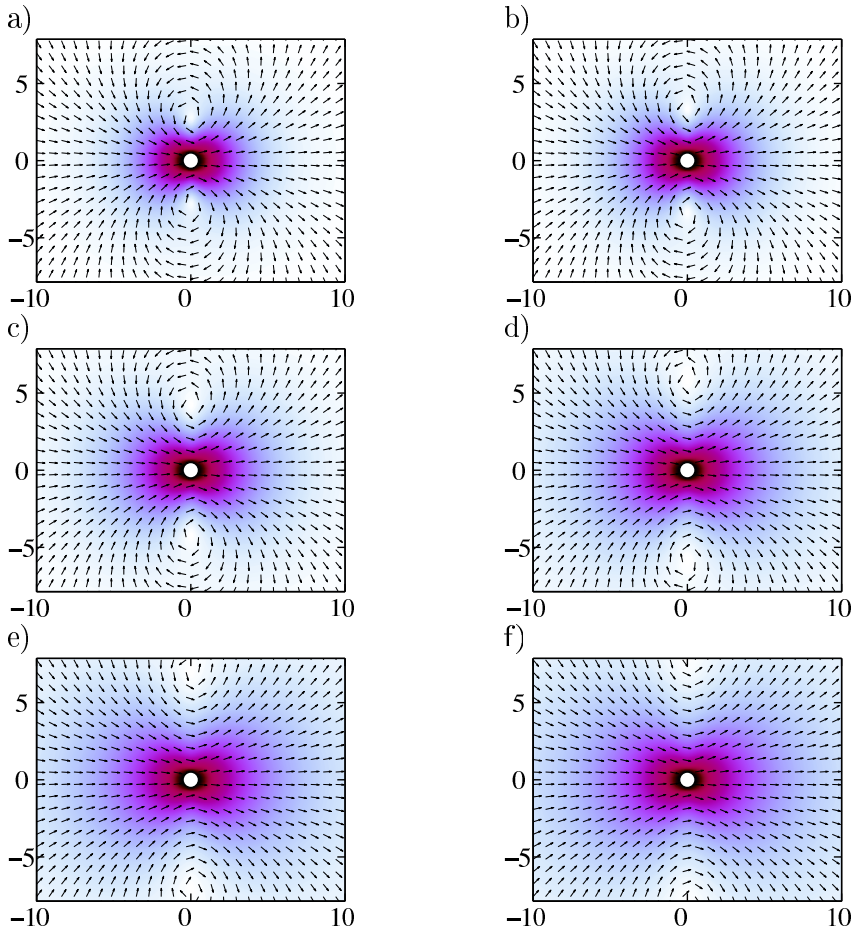

Figure 3.2: The flow for the sphere from figure 3.1 is shown at later times $t = 2$, 3, 5, 10, 15 and 20.

After a time t, the diffusion of the flow and the vortices spread to distances of order $\sqrt{\nu t}$. The flow is almost in steady state for $r < \sqrt{\nu t}$, whereas at larger distances there is sparse vorticity yet. Hence at a given time t, the flow obeys the steady Stokes equation for distances smaller than $\sqrt{\nu t}$. In the limit $\nu \to \infty$, this distance gets large, approaching infinity. However, for each finite ν and t, the validity of the steady Stokes equation is limited to distances $r < \sqrt{\nu t}$.

Another view is the following: at a distance r, there is little vorticity for times $t < r^2/\nu$, whereas at times larger than that, vorticity approaches its local equilibrium value. Hence, for fixed distance r, the flow nearly obeys the steady Stokes equation after times of order r^2/ν. As $\nu \to \infty$, the time for the validity of the steady Stokes solution approaches zero. But for any finite ν and distance r, the flow needs a time r^2/ν for the diffusion and the steady Stokes limit is not valid for times shorter than that.

At large times, the advective term becomes dominant: The neglection of the advective term is satisfied, if the displacement of the sphere is smaller than the extension of the flow, i.e. the scale of vorticity diffusion. Advective terms become important if the sphere advances faster than the diffusion front. In chapter 2, the displacement of the sphere is the oscillation amplitude, whereas the diffusion length is $k^{-1} = \sqrt{\nu/\omega}$. Thus the condition there for the advective term to be small is obtained as $kD \ll 1$. Here, the sphere displacement is given by Vt, whereas the diffusion length is $\sqrt{\nu t}$. Both equal at a time $t = \nu/V^2$. For smaller times, the flow obeys the time-dependent Stokes equations, whereas at larger times, advective terms are nonnegligible and the flow differs from time-dependent Stokes flow.

3.3 Equation of motion for the sphere

For a steadily moving sphere, forced by a constant force F_i and moving at velocity V_i in a viscous liquid, the force balance of F_i and the viscous drag due to the flow is given by

$$0 = F_i - 6\pi\mu R V_i. \tag{3.24}$$

The expression for the viscous drag has been given by Stokes [65]. This equation is obtained under the assumption, that vorticity has had enough time to spread to its equilibrium value and the flow obeys the steady Stokes equation. For steady Stokes flow, the equation of motion for a sphere in a viscous fluid, forced by an external force $F_i(t)$, is given by

$$m_S \frac{d}{dt} V_i(t) = F_i(t) - 6\pi\mu R V_i(t) \tag{3.25}$$

with m_S the mass of the sphere. The assumption for this equation is similar to that for equation (3.24): for distances of the order of the sphere radius vorticity diffuses instantaneously to its equilibrium value and the viscous drag instantaneously adjusts to the motion of the sphere.

The time-dependent equation of motion may be obtained from the inverse Fourier transformation of the expression for a single Fourier component, equation (2.78). In the

textbook by Landau and Lifshitz [30] the steps are relegated to the exercises: exercises §24.5 and §24.7 lead to equation (3.26). As given by Boussinesq, Basset and Oseen, the equation of motion is

$$\begin{aligned} m_S \frac{\mathrm{d}}{\mathrm{d}t} V_i(t) &= F_i(t) - \frac{1}{2} m_F \frac{\mathrm{d}}{\mathrm{d}t} V_i(t) \\ &\quad -6\pi R\mu \left[V_i(t) + \frac{R}{\sqrt{\pi\nu}} \int_{t_0}^{t} \frac{\mathrm{d}V_i(\tau)/\mathrm{d}\tau}{\sqrt{t-\tau}} \mathrm{d}\tau \right]. \end{aligned} \tag{3.26}$$

m_F is the mass of a fluid parcel, whose volume is equal to that of the sphere, i.e. the ratio m_S/m_F is given as the ratio of the two densities. Maxey and Riley [35] gave an expression for the motion of a sphere, forced by an external force $F_i(t)$ to move in an external flow. They assume that the sphere follows so closely the flow that the perturbation of the flow, which is induced by the sphere, may be described by the time-dependent Stokes equation. Thus, if the turbulent flow is set to zero, one recovers the equation of motion given above.

In equation (3.26) the uniform Stokes force, the third term on the right hand side, and the added mass term, the second term, are familiar from the oscillatory moving sphere. The last term finally is the Basset integral term. It has the following meaning: part of the flow produced by the sphere obeys a diffusion equation, namely that of vorticity diffusion. At a given distance, the flow does not follow the sphere instantaneously, as explained in section 3.2. Therefore, not only the momentary velocity of the sphere, but also all flow created formerly at $\tau \leq t$ has to be taken into account. The drag from that flow, the Basset integral term in equation (3.26), is obtained by an integral over the velocity at former times.

In contrast, in the equation of motion as obtained from the steady Stokes equation, the flow at earlier times does not have an effect on the motion of the sphere, since the flow adjusts instantaneously to the motion of the sphere.

3.4 Gravitational startup

Consider a sphere at rest for times $t < 0$ to be subject to a constant and unidirectional force F at times $t \geq 0$. The sphere starts to accelerate at $t = 0$ until it assumes an equilibrium velocity $V_0 = F/(6\pi\mu R)$. In terms of V_0 and the Stokes time $\tau_S = 2R^2\rho_S/(9\nu\rho)$, the equation of motion, obtained from the steady Stokes drag, equation (3.25), is given by

$$\tau_S \cdot V'(t) + V(t) = V_0 \tag{3.27}$$

and the solution is

$$V(t) = V_0 \cdot \left(1 - e^{-t/\tau_S}\right), \tag{3.28}$$

i.e. the velocity of the sphere approaches its equilibrium value after a time of the order of the Stokes time τ_S. Taking the effects of the fluid into account via the steady Stokes drag, the sphere is found to accelerate until driving force and steady Stokes drag balance.

The equation of motion for the unsteady Stokes solution is given in terms of $\tilde{\tau}_S = \tau_S(1 + \rho/2\rho_S)$ by

$$\tilde{\tau}_S \cdot V'(t) + V(t) + \sqrt{\frac{\tau_R}{\pi}} \int_0^t \frac{V'(s)}{\sqrt{t-s}} ds = V_0. \tag{3.29}$$

with $\tau_R = R^2/\nu$ being the time that vorticity needs to diffuse to a distance comparable to the radius of the sphere R. The equilbrium assumed by the sphere after the transient process is the same for the steady drag equation (3.27) and the BBO-equation (3.29) and equals $V_0 = F/6\pi\mu R$, since the Basset integral term involves the derivative of the velocity with an integral kernel $1/\sqrt{t-\tau}$ diverging for $\tau \to t$ slow enough to be integrable.

This integrodifferential equation has been solved for the unsteady start-up problem by Villat [67]. Abel's theorem implies that

$$F(t) = \int_0^t ds \frac{V'(s)}{\sqrt{t-s}} \quad \Longleftrightarrow \quad \int_0^t d\tau \frac{F(\tau)}{\sqrt{t-\tau}} = \pi(V(t) - V(0)). \tag{3.30}$$

This allows to rewrite the equation as a second order ordinary differential equation [8, 40, 66],

$$\tilde{\tau}_S^2 \ddot{V} + (2\tilde{\tau}_S - \tau_R)\dot{V} + V = V_0 \cdot \left(1 - \sqrt{\frac{\tau_R}{\pi t}}\right). \tag{3.31}$$

The transformation may also be obtained by fractional calculus methods [15, 16]. Equation (3.31) is the differential equation that will be solved to obtain the solution for the start-up problem. It also allows an asymptotic analysis: Assuming the sphere close to its equilibrium velocity, $V(t) = V_0 - \delta V(t)$ where $\delta V(t)$ is small compared to V_0, $\delta V(t)$ may be expanded into a series $t^{-1/2}$, $t^{-3/2}$, ... and $V(t)$ found to be

$$V(t) = V_0 \cdot \left(1 - \frac{R}{\sqrt{\pi\nu t}}\right) + O(t^{-3/2}). \tag{3.32}$$

Remarkably, the Stokes time τ_S does not contribute to this asymptotic solution and in fact, if $\tilde{\tau}_S$ is set to zero in equation (3.29) from the beginning, the same asymptotic limit is found. This shows that unsteady transient behaviour is happening as a balance of driving force, Basset history and Stokes force, i.e. the transient behaviour is determined by the slowly diffusing flow, with an algebraic $1/\sqrt{t}$-decay!

This is in contrast to the result that is obtained, when history forces are excluded, (3.28). Taking the flow into account as steady flow leads to an exponential transient, where the time-dependent Stokes solution decays as $1/\sqrt{t}$, much slower than exponential!

The full solution of equation (3.31) is found as follows: the characteristic equation $p^2 + 2bp + 1/\tilde{\tau}_S^2 = 0$ (where $b = (2\tilde{\tau}_S - \tau_R)/2\tilde{\tau}_S{}^2$) has solutions $p, q = -b \pm \sqrt{b^2 - 1/\tilde{\tau}_S^2}$ such that $p + q = -2b$ and $pq = 1/\tilde{\tau}_S$. This gives rise to homogenous solutions

$$V_1^{(h)}(t) = e^{pt} \qquad \text{and} \qquad V_2^{(h)}(t) = e^{qt}. \tag{3.33}$$

By the method of variation of coefficients, the solution is then obtained as

$$V(t) = V_0 \cdot \left[1 + \frac{\sqrt{\tau_R}}{\tilde{\tau}_S^2} \cdot \frac{1}{p-q} \cdot \left(\frac{e^{pt}\mathrm{erfc}\sqrt{\mathrm{pt}}}{\sqrt{p}} - \frac{e^{qt}\mathrm{erfc}\sqrt{\mathrm{qt}}}{\sqrt{q}}\right)\right]. \tag{3.34}$$

A partial integration of $\mathrm{erfc}(\xi)$ leads to an expansion for large arguments (see for instance [66]), which is given by

$$\begin{aligned} \mathrm{erfc}(\xi) &= \frac{2}{\sqrt{\pi}} \int_\xi^\infty e^{-\zeta^2} d\zeta \\ &= \frac{2}{\sqrt{\pi}} \left[\frac{e^{-\xi^2}}{2\xi} - \int_\xi^\infty \frac{e^{-\zeta^2}}{2\zeta^2} d\zeta\right] \end{aligned} \tag{3.35}$$

Note that in (3.34) not only the complementary error function $\mathrm{erfc}(\sqrt{pt})$, but also the exponential term $\exp(pt)$ enters, such that the product is algebraic again. This leads then to the large time transient expansion, which has been obtained directly from the differential equation above, see (3.32).

The properties of the sedimenting velocity are not obvious, since the argument in the error function may assume complex values with real positive part. Therefore oscillations can not a priori be excluded. For falling spheres Belmonte et al. [8] prooved that the sedimenting sphere in a viscous fluid indeed monotoneously approaches the steady state.

Figure 3.3 shows the start-up process for a sphere moving under the action of a constant force for variing density. Clearly, in figure 3.3(a) the exponential function of equation (3.27) strongly dampens the transient. The damping coefficient depends on the density of the sphere. Figure 3.3(b) shows the same data in a double logarithmic plot. The unsteady transients are shown to live for a much longer time, decaying algebraically. After times large compared to τ_S, they approach a unit transient, given by equation (3.32), which does not depend on the density of the sphere. This shows again that for a given force the density of the sphere does not have an influence on the asymptotic transient behaviour.

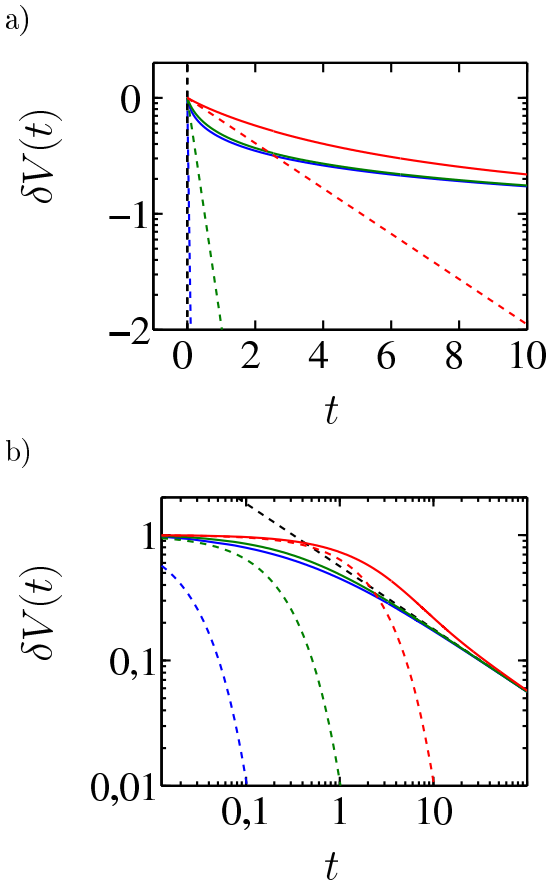

Figure 3.3: $\delta V(t) = V_0 - V(t)$ from the startup process of the sedimenting sphere for sphere density $\rho_S = .1$ (blue), 1 (green) and 10 (red). The value of the force is chosen such that $V_0 = 1$. Dashed lines show the steady Stokes solutions, given by equation 3.27. (b) shows unsteady solutions, obtained numerically with a backward differencing method [36] from equation (3.29). Parameters are $R = 1$, $\nu = 1$.

There are several ranges of the transient: At first, the Stokes time is dominant, if it is large; in figure 3.3(b), the red curve does not decay before times $t \approx \tau_S$. Next, the long transient behaviour is determined by the Basset history term and proportional to R, see equation (3.32). The Basset term is living for a long time. If it is small, the steady Stokes equilibrium finally is obtained. The flow expansion in terms of small R in section 3.5 from finite sphere radius to the Stokeslet flow corresponds for the motion of the particle to the assumption that the transient is damped sufficiently, not due to an observation at large times but due to sufficiently small sphere radii.

Mordant and Pinton [43] have studied the sinking velocity of a settling sphere at Reynolds numbers from 40 up to 7000. The sphere followed the algebraic prediction from the time-dependent Stokes equation for small times when velocity and Reynolds number were small. The sphere deviated from the unsteady Stokes behaviour for high Reynolds numbers. Then advective terms become dominant and the transient is again damped stronger than $1/\sqrt{t}$ [1, 24, 43].

3.5 Unsteady Stokeslet

In section 2.3, the solution of the time-dependent Stokes equation has been found for the flow past a sphere, whose center of mass is in oscillatory motion. The force which is acting from the fluid onto that sphere has been calculated in section 2.6. The equations have been used in sections 3.1 and 3.3 to obtain the flow past a sphere, if the center of mass is in arbitrary motion, and the force which is acting from the fluid on that sphere. Approximations of these equations are obtained, if at distances of the order of the sphere radius R the fluid responds instantaneously to the motion of the sphere, i.e. if at these distances the flow obeys the steady Stokes equation, and if the flow becomes time-dependent only at distances which are large compared to R. The approximations are given here both for the oscillatory motion and for the arbitrary motion of the sphere's center of mass. The equations which are given here generalize the steady Stokeslet, i.e. the steady Stokes response of the fluid to a point-like force, to the unsteady Stokeslet, which is the unsteady Stokes response of the fluid to a time-dependent point-like force [56].

3.5.1 Oscillatory motion of the center of mass

For the center of mass of the sphere moving at a velocity $U\exp(i\omega t)$, if the viscous length $k^{-1}=\sqrt{\nu/\omega}$ is much larger than R, i.e. if $kR \ll 1$, the stream function, given by equations (2.37) and (2.47) to (2.50) may be expanded in terms of kR and one obtains

$$\psi(r,\theta,t) = e^{i\omega t}\sin^2\theta\left[\frac{3U}{2r}\left(\frac{1}{ik^2}-\frac{1+\sqrt{i}kr}{ik^2}e^{-\sqrt{ik}r}\right)-\frac{Ur^2}{2}\right]+O(kR). \tag{3.36}$$

This is the approximation for the stream function, which describes the flow in the reference frame of the sphere. Note that part of the potential flow, in particular the term related to the mass displacement of the sphere, the last term in equation (3.13), vanishes in the Stokeslet limit.

In consistence with the equations for the flow, the force has to be expanded as well and one obtains for the component in motion direction

$$F(t) = 6\pi\mu RUe^{i\omega t}. \tag{3.37}$$

The flow responds instantaneously close to the sphere. Therefore, also the force responds instantaneously. Equation (3.37) is obtained in the limit of zero Stokes time, i.e. zero mass of the sphere. Thus, in addition to $R\to 0$ the Stokeslet approximation requires the ratio of sphere and fluid density to be finite.

Analogous to the considerations of subsection 3.1.2, the flow is transformed to cartesian coordinates and to the laboratory reference frame. As a next step, from the flow past a sphere, whose center of mass oscillates in one direction, the flow past a sphere, whose center of mass oscillates in all three directions is obtained as a superposition of the three components. Then, for the velocity of the sphere given by $\mathbf{V}(t)=\mathbf{U}\exp(i\omega t)$, we obtain for the flow in the laboratory reference frame

$$u_i(\mathbf{x},t) = \frac{3R}{2r}\left[\hat{A}(\kappa r)\delta_{ij}+\hat{B}(\kappa r)\frac{\delta x_i(t)\delta x_j(t)}{r^2}\right]V_i e^{i\omega t} \tag{3.38}$$

$$\hat{A}(\kappa r) = e^{-\kappa r}\frac{1+\kappa r+\kappa^2 r^2}{\kappa^2 r^2}-\frac{1}{\kappa^2 r^2} \tag{3.39}$$

$$\hat{B}(\kappa r) = -e^{-\kappa r}\frac{3+3\kappa r+\kappa^2 r^2}{\kappa^2 r^2}+\frac{3}{\kappa^2 r^2} \tag{3.40}$$

with $\kappa=\sqrt{i\omega/\nu}$, $\delta\mathbf{x}(t)=\mathbf{x}-\mathbf{X}(t)$ and $r=|\delta\mathbf{x}(t)|$, where $\mathbf{X}(t)$ is the instantaneous position of the sphere.

3.5.2 Arbitrary motion of the center of mass

If the center of mass of the sphere is moving at velocity $\mathbf{V}(t)$, from section 3.1 the approximated solution for the flow is found as

$$u_i(\mathbf{x},t) = \frac{3R}{2r}\int_0^\infty d\tau V_j(t-\tau) \left[\frac{\delta_{ij}}{r^2}(\xi\varphi'(\xi)-\varphi(\xi)) + \frac{\delta x_i(t)\delta x_j(t)}{r^4}(3\varphi(\xi)-\xi\varphi'(\xi))\right] \tag{3.41}$$

(note that the integration over t' has been replaced by an integration over $\tau = t - t'$) where

$$\xi = \frac{r}{\sqrt{4\nu\tau}} \tag{3.42}$$

$$\varphi(\xi) = \mathrm{erf}(\xi) - \frac{2}{\sqrt{\pi}}\xi e^{-\xi^2}, \tag{3.43}$$

$$\varphi'(\xi) = \frac{4}{\sqrt{\pi}}\xi^2 e^{-\xi^2}. \tag{3.44}$$

The error function $\mathrm{erf}(\xi)$ is defined as

$$\mathrm{erf}(\xi) = \frac{2}{\sqrt{\pi}}\int_0^\xi e^{-\zeta^2}d\zeta \tag{3.45}$$

and is related to the complementary error function $\mathrm{erfc}(\xi)$, cf. (2.2), via

$$\mathrm{erf}(\xi) + \mathrm{erfc}(\xi) = \frac{2}{\sqrt{\pi}}\int_0^\infty e^{-\zeta^2}d\zeta = 1. \tag{3.46}$$

The relation for the velocity of the sphere and the force, that pulls the sphere, is

$$\mathbf{F}(t) = 6\pi\mu R\mathbf{V}(t), \tag{3.47}$$

cf. equation (3.37). This gives rise to a different interpretation of the flow: an external force pulls the sphere through the fluid. The fluid reacts instantaneously close to the sphere, such that the viscous drag from the fluid balances the external force. In the limit $R \to 0$, the force can be interpreted as a point-like source of the flow. For the time-dependent Stokes equation in the laboratory reference frame with the force as a source term, one finds [55, 56]

$$\partial_t\mathbf{v} = -\nabla p + \nu\nabla^2\mathbf{v} + \frac{\mathbf{F}(t)}{\rho}\delta(\mathbf{x}-\mathbf{X}(t)). \tag{3.48}$$

However, due to one major difference, the equations above are not a solution of this equation: The time-dependent Stokes equation has been solved in the sphere reference

frame and then transformed to the laboratory reference frame, cf. section 2.2. Since the time-dependent Stokes equation is not Galilei invariant, when transformed to the laboratory reference frame, an additional advective term appears, which makes sure that the flow is advected with the particle. Then, the corresponding equations is

$$(\partial_t + (\mathbf{V}(t) \cdot \nabla))\mathbf{v} = -\nabla p + \nu \nabla^2 \mathbf{v} + \frac{\mathbf{F}(t)}{\rho} \delta(\mathbf{x} - \mathbf{X}(t)). \tag{3.49}$$

For a particle with vanishing radius, which is draged through a viscous fluid, this equation describes the flow with the force as a source of the flow.

3.6 Conclusions

The flow produced by a sphere, which is initially at rest and then moves at constant velocity, develops as a diffusion front due to diffusion of vorticity. At a prescribed distance from the sphere, the flow is potential flow before vorticity is diffused to that distance. Potential flow is the mass transport of the fluid due to the instantaneous displacement of the sphere. Vorticity is diffused to distances r at a time r^2/ν after the start of the sphere, and is in a stationary state for times greater than that. The steady Stokes equation describes the stationary state of the flow and is thus valid at a prescribed distance r from the particle for times larger than r^2/ν.

On the other hand, for a given time t, vorticity has diffused to distances $\sqrt{\nu t}$. At distances larger than that, the flow is still potential flow, since no vorticity diffused to these distances yet, whereas for smaller distances, vorticity is approximately in a stationary state and the steady Stokes equation applies.

The validity of the steady Stokes equation is limited for a given distance r to times larger than r^2/ν and for a given time t to distances smaller than $\sqrt{\nu t}$. This generalizes the results from chapter 2. For the sphere in oscillatory motion, vorticity is limited to distances below $\sqrt{\nu/\omega}$ and for the start-up it is limited to distances below $\sqrt{\nu t}$. Only below these distances, the steady Stokes equation gives a valid description of the flow.

The motion of a sphere, which is initially at rest and then forced by a constant force, involves several time scales. At the beginning, the sphere is at rest and accelerated until the drag from the viscous fluid and the driving force balance. The time scale for this beginning process, which is the Stokes time, is the same for the steady Stokes consideration and the BBO-description. For the steady Stokes consideration, on a time scale of the order of the Stokes time, the velocity of the sphere assumes its equilibrium value rather quickly, exponentially fast.

This is different for the BBO-consideration: Viscous drag and driving force balance, but force and flow are time-dependent and the viscous drag is restricted by diffusion of vorticity and approaches the asymptotic value rather slowly. At a time t, vorticity has diffused to a distance $\sqrt{\nu t}$. Since gradients of the flow are involved in the drag, the inverse distance $1/\sqrt{\nu t}$ enters the flow. The transient is found to decay as $U_0 R/\sqrt{\pi \nu t}$ with U_0 the equilibrium velocity and R the sphere radius. Thus the velocity of the sphere approaches its equilibrium value algebraically as $1/\sqrt{t}$, much slower than for the steady consideration!

When the sphere radius R is such, that the flow is approximately steady at distances from the sphere of order R, the flow can be approximated and expanded in terms of R. Then, the force can be interpreted as a point-like momentum source of the flow.

Chapter 4

Fluctuations in particle suspensions

Caflisch and Luke [14] describe a problem occuring in the sedimentation of particles. The steady Stokes flow past a sphere decays as 1/distance. In an independent particle approximation, the velocity field of the fluid in the middle of a suspension is a superposition of all particle fields. The number of particles in a shell of radius r and width dr increases like $r^2 dr$ and since the variance of the velocity fluctuations is proportional to the velocity of the fluid squared, i.e. proportional to $1/r^2$, each shell contributes equally to the fluctuations and at each point the fluctuations diverge with the volume.

Simulations confirm this divergence [17, 25, 27, 28]. Unfortunately, this is in contrast to experimental investigations. Nicolai and Guazzelli [48] vary the size of the fluid vessel and find that the fluctuations do not depend on the vessel size. Other experiments [21, 60, 61] show moreover that the fluctuations scale linearly with the interparticle distance. These results have been found with the particle concentration such that the interparticle separation does not exceed the width of the vessel.

The discrepancy of experimental and theoretical results has led to studies on the impact of the wall [13] on the fluctuations. Experimentally, the fluctuations become independent of the interparticle distance only if the interparticle separation exceeds the width of the vessel, i.e. at low values of the particle concentration [9].

Renormalization group methods have been used to investigate particle concentration fluctuations and their influence on the fluid velocity fluctuations [32]. The theoretical results agree qualitatively with experimental measurements.

However, all theoretical studies rely on the description of the flow by the steady Stokes equation. Here, we show that the fluctations are regularized for a homogeneous distribution of particles when the time-dependent Stokes equation is used for the description of the flow.

For steady Stokes flow, a particle of velocity $V(t)$ produces a velocity field which decays as $V(t)/r$, independent of the particle's frequency. Therefore, particles oscillating at high frequencies have the same long-range flow as particles oscillating at low frequencies. However, we have seen in chapter 2 that the fluid responds instantaneously to the motion of each particle only up to a finite distance from the particle. For viscosity ν and frequency ω, the field is cut-off at a distance of order $\sqrt{\nu/\omega}$. This distance decreases with increasing ω. The flow decays as $1/r^3$ at distances large compared to that. For particles which oscillate at high frequencies, the flow obeys the steady Stokes equation only very close to the particle. For larger distances, the calculations from chapter 2 show that the flow drops off more rapidly. Therefore, the reasoning of Caflisch and Luke [14] has to be reconsidered taking into account time-dependence of the Stokes equation.

Before treating the case of suspended particles, an analogous diffusional problem will be investigated in section 4.1 to highlight the differences between the calculation of the fluctuations with and without time-dependence. Then, in section 4.2, for a suspension of point-like particles the velocity fluctuations will be investigated for time-dependent Stokes flow.

4.1 Diffusion with random sources

The fluid velocity produced by a particle has been found in chapters 2 and 3 to respond instantaneously to the motion of the particle only at finite distances from the particle. There, the flow is described by the steady Stokes equation. Steady and unsteady Stokes flow has two contributions: One is potential flow, which results from the instantaneous displacement of fluid by the sphere, and the other one is vorticity driven flow. When advective terms are neglected, the vorticity field obeys a diffusion equation. Close to the particle, the vorticity field adapts instantaneously to the motion of the particle and is in an instantaneous equilibrium state. However, this equilibrium is limited to finite distances from the particle. At larger distances vorticity is not in an equilbrium state and time-dependence becomes important. Then, for an appropriate description of the flow, the more general time-dependent Stokes equation has to be used.

The drop-off of the flow at large distances due to time-dependence of vorticity diffusion suggests to investigate the fluctuations of a concentration field, which obeys a diffusion equation. The impact of the drop-off of the field on the fluctuations will become more transparent for the diffusional concentration field than for the unsteady Stokes flow.

Suppose a localized source, which is set, to emit a substance continuously in time. Suppose further that the substance spreads diffusively, such that the concentration field of the substance obeys a diffusion equation. Close to the source, the concentration field responds instantaneously to the source and decays as 1/distance. This is much similar to the steady Stokes response of a fluid to the motion of a particle in the fluid. Further away, the diffusively spreading concentration field does not respond instantaneously and decays more rapidly.

The fluctuations of the concentration field at a prescribed point are given by the square of the local concentration difference to the local time mean value. Close to a particle, the contribution of that particle to the fluctuations is as $1/r^2$ with distance r. If one calculates the concentration fluctuations for a homogenous distribution of sources and sinks and does not take into account, that at large distances the drop-off of the concentration field is more rapid than $1/r$, one obtains that the fluctuations diverge, similar to the divergence described by Caflisch and Luke [14] for sedimentation of particles. The regularization of the fluctuations by the cut-off of the concentration field at large distances is investigated in this section.

4.1.1 Greens functions for the diffusion equation

Consider the concentration field $c(\mathbf{r}, t)$ for a substance that spreads diffusively with a diffusion constant D from a source of strength $q(t)$ localized at $\mathbf{r}_0$. The field obeys the diffusion equation

$$\partial_t c = D\left[\nabla^2 c + q(t)\delta(\mathbf{r} - \mathbf{r}_0)\right]. \tag{4.1}$$

The scaling of the source with the diffusion constant helps in the limit $D \to \infty$, such that the source and the diffusion term scale alike. Dividing the equation by D, the time-derivative term on the left hand side becomes proportional to $1/D$ and hence subdominant compared to the terms on the right hand side. One might, therefore, expect that for large D the concentration follows the steady equation. We have seen in the previous chapters that vorticity diffusion does not reach to large distances and as a consequence the flow differs from steady Stokes flow. To test this for the concentration field, we use the well-known complete time-dependent solution of (4.1).

First, for constant source $q(t) = q_0$, the steady solution of equation (4.1) is given by

$$c(r) = \frac{q_0}{4\pi r}, \tag{4.2}$$

which shows the same slow $1/r$-decay as the steadily moving sphere. Then, for the case

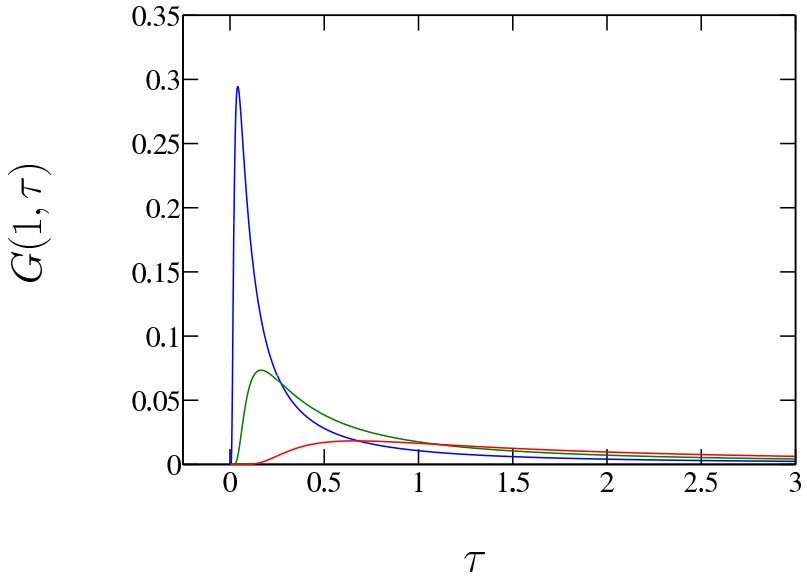

Figure 4.1: $G(r,\tau)$ from equation (4.4) at $r = 1$ plotted as a function of τ for $D = 4.0$ (blue), 1.0 (green) and 0.25 (red).

of an arbitrary source, the time-dependent solution for the concentration field is given by

$$c(r,t) = \int_{-\infty}^{t} G(r, t-t')q(t')dt' \tag{4.3}$$

with the kernel

$$G(r,\tau) = \begin{cases} \frac{D}{(4\pi D\tau)^{3/2}} e^{-\frac{r^2}{4D\tau}} & \text{for} \quad \tau > 0 \\ 0 & \text{for} \quad \tau < 0 \end{cases} \tag{4.4}$$

Figure 4.1 shows the kernel, given by equation (4.4) as a function of time for various diffusion constants D and fixed r. As $\tau \to \infty$, the kernel approaches zero because of the prefactor $1/\sqrt{\tau^3 D}$. Thus, for large times τ, large values for D dampen the kernel. This becomes visible in figure 4.1: As $\tau \to \infty$, the function values for the red curve ($D = 0.25$) are higher than for the green curve ($D = 1.0$) and for the blue curve ($D = 4.0$).

As $\tau \to 0$, the argument in the exponential function in equation (4.4) becomes $-\infty$ and the exponential function dampens the kernel down to zero. Until the argument becomes of order one, a time of order $r^2/(4D)$ elapses. At $\tau_M = r^2/(6D)$, the kernel assumes its maximum value, which is

$$G(r,\tau_M) = e^{-3/2} \left(\frac{3}{2\pi}\right)^{3/2} \frac{D}{r^3}. \tag{4.5}$$

Therefore, as D is increased to infinity, the maximum value of the kernel is increased to infinity, whereas the time for the kernel to approach its maximum value is decreased to zero. The kernel becomes narrower and steeper.

The areas under the curves are constant: substituting τ by $\xi = r/\sqrt{4D\tau}$, the integral becomes

$$\int_0^\infty G(r,\tau)d\tau = \frac{1}{2\pi^{3/2}r}\int_0^\infty e^{-\xi^2}d\xi = \frac{1}{4\pi r}. \tag{4.6}$$

The time integral over the kernel is independent of D! As $D \to \infty$, the kernel approaches a δ-function. The remarkable features are that even though the kernel approaches a delta-function with the singularity at $\tau = 0$, the value for the kernel is equal to zero at $\tau = 0$ and the kernel is not symmetrical about its maximum!

The decay of the kernel as $\tau \to \infty$ indicates that the significant contribution of $q(t)$ to the kernel is from a finite range of τ. An effective time-width of the kernel can be estimated as follows: The height of the kernel is given by equation (4.5). The effective width of the kernel $\Delta\tau$ times the height $G(r,\tau_M)$ is equal the area of the kernel, which is $1/(4\pi r)$, cf. equation (4.6). Then the width $\Delta\tau$ is

$$\Delta\tau = e^{3/2}\sqrt{\frac{\pi}{54}}\frac{r^2}{D} \approx 1.08\frac{r^2}{D}. \tag{4.7}$$

Thus if the source $q(t)$ is smooth on a time scale r^2/D, then the values of $q(t)$, which contribute to the concentration field, are roughly constant over the time range which is relevant for the kernel and up to distances r the concentration field adjusts instantaneously to the source.

In the limit $D \to \infty$, the concentration field responds instantaneously, if $q(t)$ is smooth on evanescent time scales. One then obtains

$$c(r,t) = \frac{q(t)}{4\pi r}. \tag{4.8}$$

This suggests that in the limit $D \to \infty$, the concentration field adjusts instantaneously at any distance. However, for any finite D, no matter how large, the instantaneous range of the concentration field is limitted to finite distances. The limits $D \to \infty$ and $r \to \infty$ do not commute!

For any distance r, the concentration field only responds instantaneously, if the source is smooth on time scales r^2/D. If on the other hand $q(t)$ is smooth on time scales T, then the concentration field responds instantaneously only up to distances $\sqrt{DT}$, whereas it differs from the instantaneous field for distances larger than that.

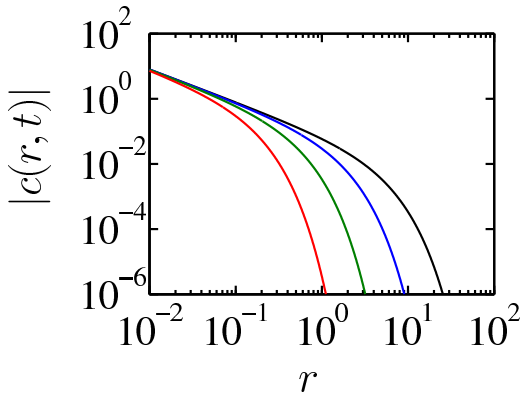

Figure 4.2: Oscillation amplitudes for the concentration fields which are measured at distances r (obtained from equation 4.9), plotted as a function of r. Frequencies $\omega = 0.1$ (black), 1 (blue), 10 (green) and 100 (red). Diffusion constant $D = 1$.

This becomes explicit for the time-dependent concentration field for a source $q(t) = q_0 \exp i\omega t$ (such that the source is actually a source and a sink, alternating in time). This is

$$c(r,t) = \frac{q_0}{4\pi r} e^{-\sqrt{i}kr + i\omega t} \tag{4.9}$$

where $k = \sqrt{\omega/D}$ is the damping rate of the exponential function and also the inverse wave length of the oscillation of the concentration field at a fixed distance from the source. Here, k plays the same role as the damping rate $k = \sqrt{\nu/\omega}$ of the vorticity driven flow past a sphere in oscillatory motion, cf. subsection 2.3.3. The square root $\sqrt{i}$ is selected such that the exponential function vanishes in the limit $r \to \infty$, cf. equation (2.40).

For the concentration field given by equation (4.9), the concentration, which is measured as a function of time at a prescribed distance from the source, is oscillating. Figure 4.2 shows the oscillation amplitude of the local concentration as a function of the distance, where it is measured, for various oscillation frequencies. Clearly, the extension of the instantaneous concentration field depends on the frequency. For a prescribed frequency, the source is smooth on a time scale $T = \omega^{-1}$. Referring to the discussion above, the concentration field is assumed instantaneously for distances from the source up to $\sqrt{DT} = \sqrt{D/\omega}$. For larger distances, the source is not smooth on time scales r^2/D. As a consequence then, the time scale of the oscillation is smaller than the time scale of the integral in equation (4.3). Therefore, if the integral over the source is performed

to obtain the concentration field, part of the integral cancels out. The field does not decay as the instantaneous field, but from equation (4.9) decays exponentially, much more radid. If the distance is prescribed, the concentration field is the instantaneous one for frequencies $\omega < D/r^2$. For larger frequencies, the rapid oscillation dampens the concentration field.

If the source is inactive for $t < 0$ and then starts to supply material at a strength q_0, the time-dependent solution is

$$c(r,t) = \frac{q_0}{4\pi r}\mathrm{erfc}\left(\frac{r}{\sqrt{4Dt}}\right) \tag{4.10}$$

where the complementary error function is defined as

$$\mathrm{erfc}(\xi) = \frac{2}{\sqrt{\pi}}\int_{\xi}^{\infty} e^{-\zeta^2} d\zeta. \tag{4.11}$$

For $\xi \to 0$, erfc(ξ) is erfc(0) = 1. For $\xi > 1$, erfc(ξ) becomes exponentially small, cf. the introdution of chapter 2. For $\xi \to \infty$, erfc(ξ) becomes equal to 0.

Figure 4.3 shows equation 4.10 as a function of the radius for various times. For fixed time t, if $r \ll \sqrt{4Dt}$, the argument of the complementary error function in equation (4.10) is small and since erfc(0) $\to$ 1, in figure 4.3 all three curves meet the stationary solution $q_0/(4\pi r)$. Hence, for each time, there is a finite range where the concentration field is nearly stationary. Similarly, for fixed distance and $t \gg 4D/r^2$, one finds again that $r/\sqrt{4Dt} \ll 1$ and $c(r,t)$ becomes stationary, i.e. at each distance from the source, if one waits for a sufficiently long time, the concentration field approaches a steady value. Thus, the concentration field is a diffusional front emerging from the source: It is in a stationary state for $r < \sqrt{4Dt}$ and exponentially small for distances $r > \sqrt{4Dt}$. As time is increased, cf. figure 4.3, the front spreads to larger distances, but for any finite D and t, the cut-off for the stationary state is at a finite distance from the source. For distances larger than $\sqrt{4Dt}$, the concentration field is not in a stationary state.

It has been shown, that the concentration field, which is produced by a source that is smooth on time scales T, responds instantaneously only up to distances $\sqrt{D/T}$. As the distance is increased beyond this range, the concentration field decays much stronger than the instantaneous concentration field. In the following part, the fluctuations of the concentration field are calculated, taken into account this cut-off.

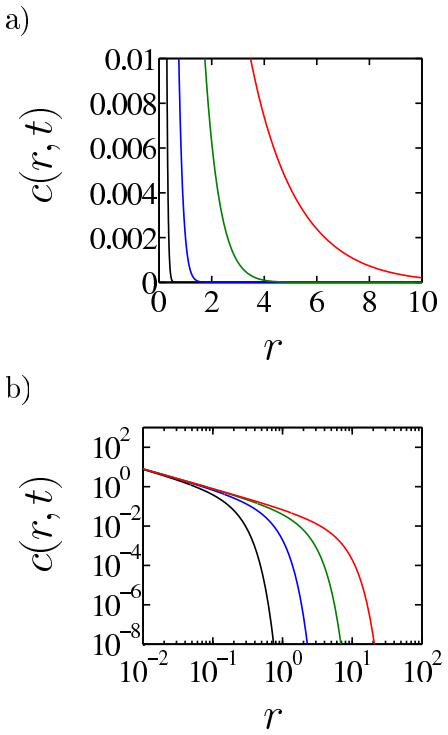

Figure 4.3: Concentration field for a source, which starts emitting at a time $t = 0$ plotted as a function of r, obtained from equation (4.10). The curves show the concentration field at times $t = 0.01$ (black), 0.1 (blue), 1 (green) and 10 (red). $q_0 = 1$ and $D = 1$. (a) and (b) show the same curves plotted on linear and double logarithmic scales.

4.1.2 Fluctuations

The concentration field, which is generated by many sources $\alpha = 1, ..., N$ of strength $q^{(\alpha)}(t)$ at positions $\mathbf{r}_\alpha$, is given by

$$c(\mathbf{r},t) = \sum_\alpha \int_{-\infty}^{t} G(|\mathbf{r}-\mathbf{r}_\alpha|, t-t')q^{(\alpha)}(t')dt'. \tag{4.12}$$

If the sources are constant and active for a time t, each contributes a field that drops off like $1/r$ for distances below $r_t = \sqrt{Dt}$. Since they drop off exponentially for larger distances, r_t is the greatest distance to which they can contribute. For a uniform distribution of sources, the number of particles for a shell of radius r and width dr is given by $4\pi r^2 dr$. If all particles up to a distance r_t are taken into account, one finds, that the overall concentration field is proportional to $\int 4\pi r dr \propto r_t^2$. Since $r_t = \sqrt{Dt}$, the increase of the concentration field with time is as t. If, instead, the sources are positive and negative, such that there are sources and sinks, the average concentration field may be kept at a constant mean value $\overline{c(r)} = \langle c(r,t)\rangle_t$, positive or negative. The average $\langle ...\rangle_t$ is a time mean and defined as

$$\langle c(r,t)\rangle_t = \lim_{T\to\infty} \frac{1}{T}\int_0^T c(r,t)dt. \tag{4.13}$$

The next question is about the fluctuations of the concentration field. They are given by the time mean square of the deviation of the concentration field from the local mean concentration, $\langle [c(r,t) - \overline{c(r)}]^2\rangle_t$. If the mean value of the concentration is zero, the fluctuations are given by

$$\langle c(r,t)^2\rangle_t = \sum_{\alpha,\beta} \int_{-\infty}^{t} dt' \int_{-\infty}^{t} dt''$$
$$G(|\mathbf{r}-\mathbf{r}_\alpha|, t-t')G(|\mathbf{r}-\mathbf{r}_\beta|, t-t'')\langle q^{(\alpha)}(t')q^{(\beta)}(t'')\rangle_t. \tag{4.14}$$

For independent particles

$$\langle q^{(\alpha)}(t')q^{(\beta)}(t'')\rangle_t = \delta_{\alpha\beta}\langle q^{(\alpha)}(t')q^{(\alpha)}(t'')\rangle_t. \tag{4.15}$$

If, in the independent particle approximation, $c(r,t)$ is approximated by the instantaneous response in the limit $D\to\infty$, such that $G(|\mathbf{r}-\mathbf{r}_i|,\tau)$ is substituted by $\delta(\tau)/(4\pi r)$, then

$$\langle c(r,t)^2\rangle_t = \sum_\alpha \frac{\langle q^{(\alpha)}(t')q^{(\alpha)}(t'')\rangle_t}{(4\pi|\mathbf{r}-\mathbf{r}_\alpha|)^2}. \tag{4.16}$$

the fluctuations decay as $1/r^2$ from each source. If the fluctuations are then integrated over the volume, assuming that the sources are homogeneously distributed, each shell of radius r and width dr contributes equally, such that the integral over all shells diverges.

For the instantaneous response, for every particle all frequencies contribute an instantaneously responding concentration field, such that the concentration at any distance displays the same time-dependence as the source and decays as 1/distance. Caflisch and Luke [14] described the divergence for the fluctuations of steady Stokes flow for sedimenting particles and the problem is exactly analogous to the diffusion problem above. The substitution of $G(r,\tau)$ by the steady limit is not valid at all distances, such that distant shells contribute less. It will be shown now that fluctuations are finite when the concentration field $c(r,t)$ is treated time-dependent.

Fluctuations in terms of the Greens function

The concentration field of a single source $q(t)$ is given by

$$c(r,t) = \int_{-\infty}^{0} \frac{D}{(4\pi D(t-t'))^{3/2}} e^{-\frac{r^2}{4D(t-t')}} q(t')dt'. \tag{4.17}$$

Consider $q(t)$ to be composed of a finite number of harmonically oscillating sources with Fourier amplitudes $\hat{q}_n$ and equally spaced frequencies, $\omega_n = n\omega_{\min}$. Then

$$q(t) = \sum_{n=-N}^{N} \hat{q}_n e^{i\omega t}. \tag{4.18}$$

The largest frequency in the system is $\omega_N = \omega_{\max} = N\omega_{\min}$ and the smallest frequency is $\omega_1 = \omega_{\min}$. Figure 4.4 shows an example. For each n, a value between 0 and ∞ is assigned to $|\hat{q}_n|$, with a Gaussian probability. The phase of $\hat{q}_n$ is arbitrary between $-\pi$ and π. Panel (a) shows the absolute values of $\hat{q}_n$. The histogram in panel (b) shows the distribution of the absolute values. Note that the source is normalized such that $\langle q(t)^2 \rangle_t = 1$.

In figure 4.5, the concentration field of that source is shown at various distances from the source. Panel (a) shows the source itself. From subsection 4.1.1, if $q(t)$ is smooth on a length scale T, the concentration field is the instantaneous one for distances smaller than $\sqrt{DT}$. The source is smooth on a time scale $1/\omega_{\max}$, prescribed by the highest frequency in the system. Thus, the cut-off distance for the concentration field in this case is at $r \approx 0.3$. In panel (b), at a distance $r = 0.1$, the normalized concentration field $4\pi r c(r,t)$ is equal to the source strength itself. Clearly, in the other panels, the

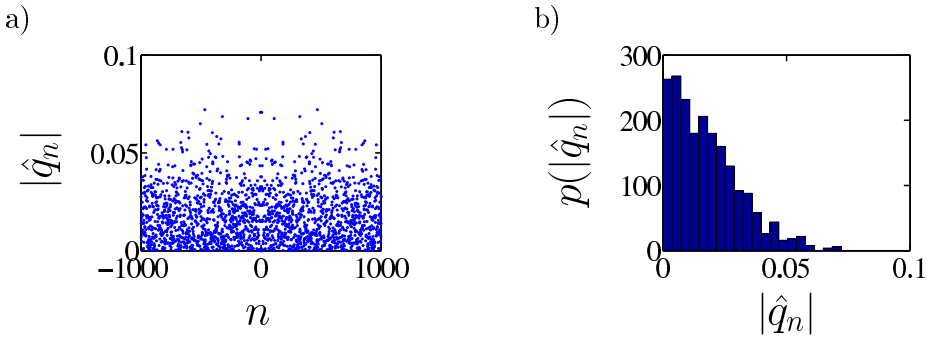

Figure 4.4: Randomly assigned Fourier amplitudes for frequencies $\omega_n = n\omega_{\min}$, $n = -N$, ..., N. The probabilities for the Fourier amplitudes are Gaussian. (a) shows $|\hat{q}_n|$, (b) shows the distribution for $|\hat{q}_n|$. The phase of $\hat{q}_n$ is random between $-\pi$ and π and $\langle q^2(t)\rangle_t = 1$.

distances are above the cut-off distance 0.3 and the concentration fields differ from the instantaneous one.

The amplitude of the normalized concentration field drops from (c) to (d) approximately from a value 0.5 to a value 0.2. From (d) to (e), the concentration field drops from 0.2 to 0.1. The ratios of the amplitudes of $4\pi rc(r,t)$ correspond respectively to the inverse ratios of the distances, such that

$$c(r,t) \propto \frac{1}{r^2}. \tag{4.19}$$

From (e) to (f) the concentration field amplitude drops by a factor of 20, more rapid. Furthermore, in panels (c) to (e) the shape of the concentration field is similar, but smoothed out with the distance. The concentration field is deformed and smooth on a length scale of order of the periodicity for the signal in panel (f).

The drop off as $1/r^2$ becomes transparent in a simplified picture. The kernel of the integral in equation (4.17) is of finite width, which is of order $t_i = r^2/D$, cf. subsection 4.1.1. Furthermore, at times $\tau = 0$ there is no contribution to the integral yet, whereas it rises quickly to be at a maximum at time $\tau = r^2/(6D) = t_i/6$. For an estimation, the kernel is roughly approximated by a constant kernel of the same area, but finite width t_i, i.e.

$$G^{(C)}(r,\tau) = \begin{cases} 0 & \text{for} \quad \tau < t_i/6 \\ \frac{1}{4\pi r t_i} & \text{for} \quad t_i/6 < \tau < 7t_i/6 \\ 0 & \text{for} \quad 7t_i/6 < \tau \end{cases} \tag{4.20}$$

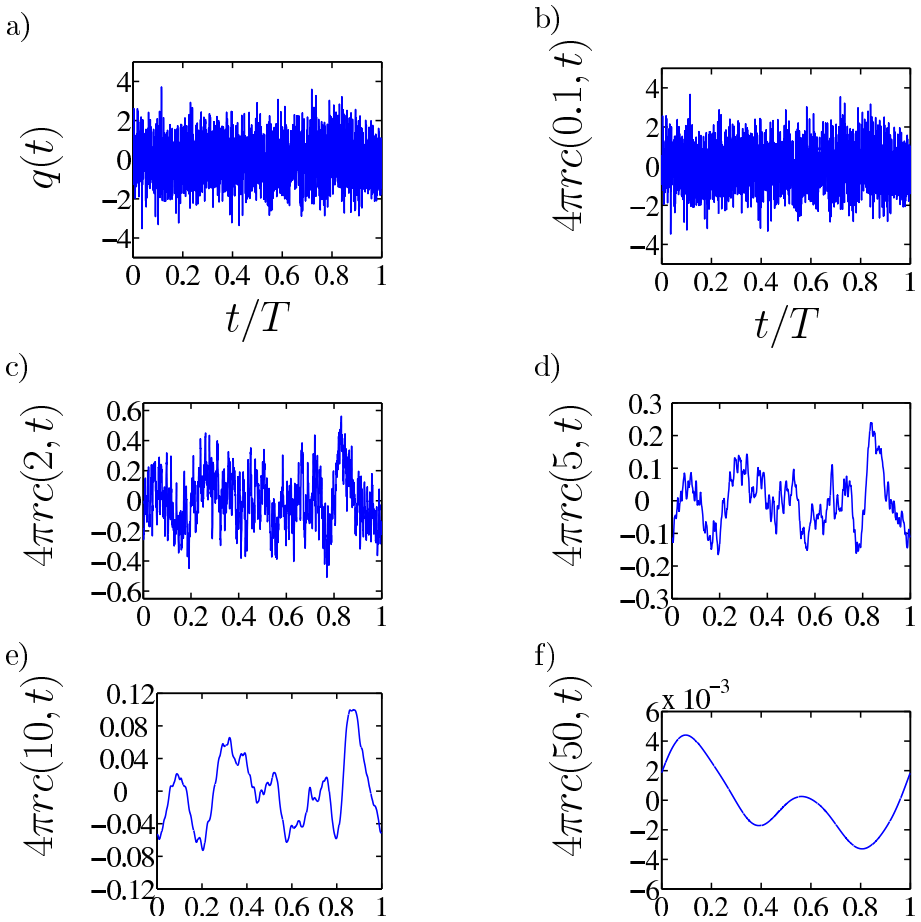

Figure 4.5: (a): source from figure 4.4 as a function of time, plottet over t/T, where $T = 2\pi/\omega_{\min}$ is the periodicity of the source. (b) to (f): concentration field as a function of time at distances r, where $r = 0.1$ (b), 2 (c), 5 (d), 10 (e) and 50 (f). (b) to (f): concentration field at distances r where $r = 0.1$, 2, 5, 10 and 50. Parameters are $D = 0.1$, $\omega_{\min} = 0.001$, $N = 1000$.

Moreover, due to the construction of the Fourier coefficients in figure 4.4, there is no distinguished frequency dependence. All frequencies contribute equally. Thus, there is no correlation on time scales larger than $1/\omega_{\max}$. Constant amplitudes of the Fourier coefficients means random fluctuation of the source [29]. The source changes its value ramdomly at intervals Δt, which are given in terms of the the largest frequency in the system, i.e. $\Delta t \propto 1/\omega_{\max}$. The kernel width contains $n = \omega_{\max} r^2/D$ steps and the sum over the randomly changing source is of order $\sqrt{n}$. The integral hence is given by $\sqrt{n}\Delta t/t_i$ and since $t_i = n\Delta t$, one obtains for the concentration field at a distance $r > \sqrt{D/\omega_{\max}}$

$$c(r,t) \approx \int_0^\infty G^{(C)}(r,\tau) q(t-\tau) d\tau \propto \frac{1}{\pi r \sqrt{n}} = \frac{1}{4\pi r^2} \sqrt{\frac{D}{\omega_{\max}}}, \tag{4.21}$$

i.e. the concentration field decays as $1/r^2$. The result is recovered that has been obtained from the amplitudes in figure 4.5.

At distances larger than $\sqrt{D/\omega_{\min}}$, which is larger than 10 in figure 4.5, the source is periodic. Therefore, due to the harmonic solution of the diffusion equation of subsection 4.1.1, the concentration field decays exponentially. This finally explains the rapid decay in figure 4.5 from panel (e) to panel (f).

The black curve ($D = 0.1$) in figure 4.6(a) shows the fluctuations of the concentration field, calculated for the example above. The fluctuations are given as the square of the concentration field. The three ranges from the consideration above become explicit graphically: From the figure, at small distances the fluctuations decay as

$$\langle c(r,t)^2 \rangle_t = \frac{\langle q(t)^2 \rangle_t}{(4\pi r)^2}. \tag{4.22}$$

Graphically, at a distance $r \approx 0.3$ there is a cut-off. The crossover is from the simple analysis above also at $\sqrt{D/\omega_{\max}} \approx 0.3$, which fits to the graphically determined value. From this distance on, the concentration field deviates from the instantaneous response and decays more rapid. The investigation of the concentration field in terms of the simplified kernel has shown that the fluctuations decay as

$$\langle c(r,t)^2 \rangle_t \propto \frac{D}{4\pi^2 \omega_{\max} r^4}. \tag{4.23}$$

The $1/r^4$-dependence of the fluctuations is recovered from figure 4.6. A further cut-off is found graphically at $r \approx 20$. There, the signal from the source becomes periodic and the concentration field cut-off exponentially. From the analysis, the the exponential range starts at $r \approx \sqrt{D/\omega_{\min}} = 10$,

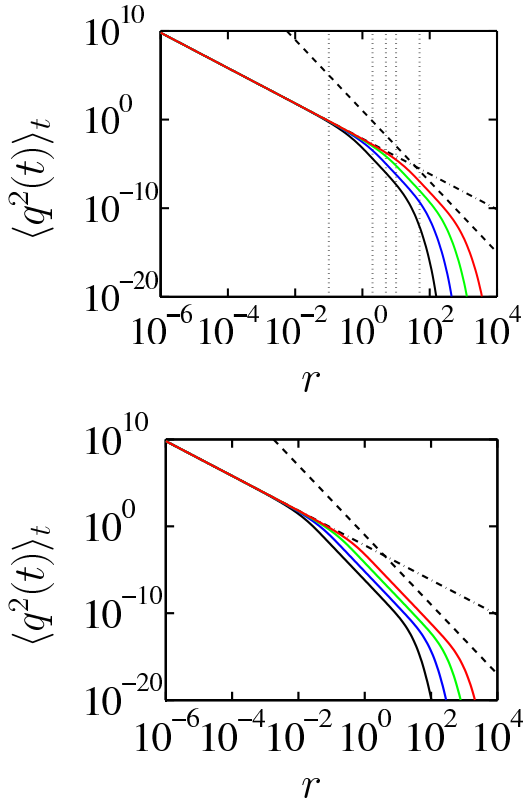

Figure 4.6: (a): Fluctuations for the random source from figure 4.4 as a function of the distance for $D = 0.1$ (black), $D = 1$ (blue), $D = 10$ (green) and $D = 100$ (red) The dot-dashed line shows the fluctuations as obtained from an instantaneously responding concentration field. The dashed line shows a $1/r^4$-decay. The vertical dotted lines indicate the distances which correspond to figures 4.10(b) to 4.10(f) (there $D = 0.1$). (b): Same as (a) for $\omega_{\min}$, as before, but $N = 10^6$.

The beginning of the cut-off for the instantaneous field depends on the highest frequency $\omega_{\max}$, whereas the beginning of the exponential decay of the fluctutations dependes on the lowest frequency $\omega_{\min}$. Thus, as the number of Fourier components is increased, as in figure 4.6(b) to 10^6, the range where the source may be treated as randomly fluctuating gets wider, i.e. it starts at $\sqrt{10^{-3}D}$ end ends at $\sqrt{10^3 D}$. Thus for 6 decades of frequencies, one obtains the $1/r^4$-range of the fluctuations to be extended graphically over 3 decades for the distance.

An integral of the expression for the fluctuations obtained from the instantaneous concentration field for a homogeneous distribution of particles is found to diverge, since the fluctuations decay as slow as $1/r^2$. Instead, if the source is smooth on a time scale T, the cut-off of the instantaneous concentration field at a distance $\sqrt{DT}$ leads to a stronger decay of the fluctuations, as D/r^4 for a randomly fluctuating source. This regularizes the fluctuations at large distances.

Fluctuations in Fourier space

It is also of some value to analyse the fluctuations in frequency space. As in the last part, we assume that the ω_n are equidistantly spaced, $\omega_n = n\omega_{\min}$ with a lowest frequency $\omega_{\min}$ and a highest frequency $\omega_N = \omega_{\max}$. Then, the local concentration is given by

$$c(r,t) = \sum_{n=-N}^{N} e^{i\omega_n t}\hat{G}_n(r)\hat{q}_n \tag{4.24}$$

$$\hat{G}_n(r) = \frac{e^{-\kappa_n r}}{4\pi r} \tag{4.25}$$

with $\kappa_n = \sqrt{i\omega_n/D}$. The function $\hat{G}_n(r)$ is the harmonic solution of the diffusion equation, see equation (4.9).

The temporal correlation function $\langle q(t)q(t+\delta t)\rangle_t$ becomes in terms of the Fourier coefficients $\hat{q}_n$

$$\langle q(t)q(t+\delta t)\rangle_t = \sum_{n=-N}^{N} |\hat{q}_n|^2 e^{i\omega_n \delta t} \tag{4.26}$$

and the fluctuations become

$$\langle c^2(r,t)\rangle_t = \sum_{n=-N}^{N} \left|\hat{G}_n(r)\right|^2 |\hat{q}_n|^2 . \tag{4.27}$$

Suppose that the amplitudes in Fourier space all have the same value $|\hat{q}_n|^2$ and the correlation function $\langle q(t)^2\rangle_t = Q$. Then from equation 4.26, the amplitude is

$$|\hat{q}_n| = \sqrt{\frac{Q}{2N}}. \tag{4.28}$$

The three ranges, that have been identified above, may be identified as follows: first, as before the smallest time scale is given by $1/\omega_{\max}$ and therefore for distances $r < \sqrt{D/\omega_{\max}}$, the exponential function in equation (4.25) becomes approximately one. Then, the fluctuations are given by

$$\langle c(r,t)^2 \rangle_t = \frac{Q}{(4\pi r)^2}. \tag{4.29}$$

This is the equation for the fluctuations up to distances, where the concentration field is instantaneous, which we had before in equation 4.22

Next, if the distance r from the source is larger than $\sqrt{D/\omega_{\max}}$, but smaller than $\sqrt{D/\omega_{\min}}$, then high frequencies are cut-off exponentially, whereas low frequencies still contribute the instantaneously responding field. All frequencies above D/r^2 are cut off. Below D/r^2, a number of roughly $D/(r^2\omega_{\max})$ out of N frequencies contribute. Then the fluctuations are

$$\langle c^2(r,t) \rangle_t = \frac{Q^2 D}{16\pi^2 \omega_{\max} r^4}. \tag{4.30}$$

Thus, what has been found as a result of a randomly emitting source in terms of the Greens function may be alternatively interpreted as a cut-off in frequency space.

For distances larger than $\sqrt{D/\omega_{\min}}$, only the lowest frequency contributes, but it is exponentially suppressed.

The investigations of the fluctuations in terms of the Greens function and in Fourier space of course both lead to the same results. Whereas in terms of the Greens function, the emphasis is on a finite extension of the kernel in time, in Fourier space the suppression of frequencies at large distances is pronounced.

If Γ denotes the number of sources per volume and the fluctuation of each source is equal to Q^2, then all sources up to a distance $r_c = \sqrt{D/\omega_{\max}}$ contribute as $1/r^2$ to the fluctuations, whereas all particles further away contribute as $1/r^4$ (if the low-frequency cut-off is not taken into account). Then for a homogeneous distribution of sources one finds that the fluctutions at each point

$$\langle c^2(\mathbf{x},t) \rangle_t = Q^2\Gamma \left[\int_0^{r_c} \frac{4\pi r^2}{(4\pi r)^2} dr + \int_{r_c}^{\infty} \frac{4\pi r^2 D}{16\pi^2 \omega_{\max} r^4} dr \right] \tag{4.31}$$

are finite, namely

$$\langle c^2(\mathbf{x},t) \rangle_t = \frac{Q^2\Gamma}{2\pi} \sqrt{\frac{D}{\omega_{\max}}}. \tag{4.32}$$

Note that both integrals contribute equally to this value of the fluctuations!

The results show that there is a high frequency regularization of the concentration fluctuations due to the time dependence in the equations. Estimates based on the instantaneous time-independent fields miss out this averaging and give divergent results.

4.2 Particle suspensions

In section 4.1, the concentration field obeys a diffusion equation and thus does not respond instantaneously at any distance. Thus the concentration field is cut-off at a finite distance from the source. This has been shown to regularize the fluctuations of the concentration field.

The flow past a particle is steady Stokes flow, if vorticity responds instantaneously to the motion of the particle. Since vorticity also obeys a diffusion equation, at a certain distance from the particle the fluid does not respond instantaneously and deviates significantly from steady Stokes flow. Then the time-dependent Stokes equation has to be used, as has been shown in chapters 2 and 3. For a suspension of particles, it will be shown here that the cut-off of the steady Stokes flow regularizes the velocity fluctuations.

An expression for the fluctuations will be derived for a suspension of homogeneously distributed, independently moving particles. The expression will be compared to experimental findings.

4.2.1 Greens functions for unsteady Stokes flow

Consider the flow of a particle, located at position $\mathbf{X}(t)$ and moving at a velocity $\mathbf{V}(t) = d\mathbf{X}/dt$ in the limit of low Reynolds numbers, such that the time-dependent Stokes equation applies. Here, we calculate the flow in the reference frame of the particle. Then the time-dependent Stokes equation

$$\partial_t \mathbf{u} = -\nabla p + \nu \nabla^2 \mathbf{u} \tag{4.33}$$

has to be solved with boundary conditions at infinity and at the surface of the sphere. The transformation of the time-dependent Stokes equation from the reference frame of the sphere to the laboratory reference frame produces an advective term, cf. section 2.2. Then the flow in the laboratory reference obeys

$$(\partial_t + \mathbf{V}(t) \cdot \nabla)\mathbf{u} = -\nabla p + \nu \nabla^2 \mathbf{u}. \tag{4.34}$$

Close to the sphere surface, the flow past the sphere is steady Stokes flow, i.e. responds instantaneously to the motion of the sphere. Diffusion of vorticity limits the reach of the steady Stokes equation to finite distances. If the reach is much larger than the sphere radius R, an approximate solution for the flow is obtained, see section 3.5. In this limit, the viscous drag responds instantaneously to the external force $\mathbf{F}(t)$, which forces the

sphere to move. In terms of the force per unit viscosity $\mathbf{q}(t) = \mathbf{F}(t)/\mu$

$$\mathbf{q}(t) = 6\pi R\mathbf{V}(t). \tag{4.35}$$

Scaling the force with $1/\mu$ helps in the limit $\mu \to \infty$, since then for a prescribed velocity of the particle $\mathbf{q}(t)$ is still finite, whereas $\mathbf{F}(t)$ diverges. The force may be interpreted as a source of momentum (cf. section 3.5) and with this interpretation one obtains for the time-dependent Stokes equation in this limit

$$(\partial_t + \mathbf{V}(t)\cdot\nabla)\mathbf{u} = -\nabla p + \nu\left[\nabla^2\mathbf{u} + \mathbf{q}(t)\delta(\mathbf{x}-\mathbf{X}(t))\right]. \tag{4.36}$$

This equation is analogous to the diffusion equation (4.1): For the time-dependent Stokes equation, the force corresponds to the source term in the diffusion equation. As a response to the source the flow corresponds to the concentration field in section 4.1.

Similar than for the concentration field, the limit $\nu \to \infty$ suggests that the time-derivative and the advective term on the left hand side become subdominant. The assuption then is that the flow is described by the steady Stokes equation. It has been shown in the preceeding chapters for various cases that this assumption fails at large distances.

If the particle is forced steadily for an infinite amount of time, i.e. $\mathbf{q}(t) = \mathbf{q}_0$ is constant, the steady solution for the flow is given by

$$u_i(\mathbf{x}) = G^{(s)}_{ij}(\delta\mathbf{x}(t))q_{0,j} \tag{4.37}$$

($\delta\mathbf{x}(t) = \mathbf{x} - \mathbf{X}(t)$) in terms of the Oseen tensor [56]

$$G^{(s)}_{ij}(\mathbf{y}) = \frac{1}{8\pi r}\left[\delta_{ij} + \frac{y_i y_j}{r^2}\right] \tag{4.38}$$

(where $r = |\mathbf{y}|$). The Einstein sum convention is used for the sum over the index j and $q_{0,j}$ denotes the j-th component of $\mathbf{q}_0$. The decay of the flow is as 1/distance, as the decay of the steady concentration field (4.2).

In section 3.5 the solution to equation (4.36) for an arbitrary time-dependent force is given by

$$u_i(\mathbf{x},t) = \int_0^\infty d\tau G_{ij}(\delta\mathbf{x}(t),\tau)q_j(t-\tau). \tag{4.39}$$

where

$$G_{ij}(\mathbf{y},\tau) = \frac{\nu}{4\pi r^3}\left[(\xi\varphi'(\xi) - \varphi(\xi))\delta_{ij} + (3\varphi(\xi) - \xi\varphi'(\xi))\frac{y_i y_j}{r^2}\right] \tag{4.40}$$

and

$$\xi = \frac{r}{\sqrt{4\nu\tau}} \tag{4.41}$$

$$\varphi(\xi) = \mathrm{erf}(\xi) - \frac{2}{\sqrt{\pi}}\xi e^{-\xi^2} \tag{4.42}$$

$$\varphi'(\xi) = \frac{4}{\sqrt{\pi}}\xi^2 e^{-\xi^2}. \tag{4.43}$$

Since the flow is solved in the particle reference frame, the flow only depends on the instantaneous distance from the particle $\delta\mathbf{x}(t) = \mathbf{x} - \mathbf{X}(t)$. The history of the particle is taken solely into account by the integration of the force over time. The solution (4.39) of the time-dependent Stokes equation, which describes the flow past a single particle, is the analogon to the solution of the diffusion equation for the concentration field, equation (4.3).

Figure 4.7 shows the Greens function, given by equation (4.40) as a function of time for various viscosities ν and fixed distance r: For an impulsive force at $t = 0$, $\mathbf{q}(t) = \mathbf{e}_x\delta(t)$, panel (b) and (c) show the flow at the points $\mathbf{e}_x$ and $\mathbf{e}_y$, (cf. panel (a)), respectively given by

$$u_x(\mathbf{e}_x, t) = \frac{\nu}{4\pi r^3} 2\varphi(\xi) \qquad \text{and} \qquad u_x(\mathbf{e}_y, t) = \frac{\nu}{4\pi r^3}(\xi\varphi'(\xi) - \varphi). \tag{4.44}$$

The negative sign in panel (c) at $\tau = 0$ comes from the ring vortex that is shedded at the center of the force $\mathbf{y} = 0$ and passes through the observation point. This ring vortex is visible also for the start of a sphere, section 3.2.

Remarkably and in contrast to the kernel function from subsection 4.1.1, at $\tau = 0$ there is a signal from the flow. The displacement causes an instantaneous response of the fluid! The response at $\tau = 0$ is due to potential flow: The contributions to $\varphi(\xi) = f(\xi) + g^d(\xi)$, deduced from equations (3.12) and (3.13), are given by

$$f(\xi) = -\left[\frac{2}{\sqrt{\pi}}\xi e^{-\xi^2} + \mathrm{erfc}(\xi)\right] \tag{4.45}$$

$$g^d(\xi) = 1. \tag{4.46}$$

Note that the complementary error function $\mathrm{erfc}(\xi)$ and the constant value of the potential flow stream function add up to the error function $\mathrm{erf}(\xi)$ for $\varphi(\xi)$ in equation (4.42). Thus, the vorticity driven part $f(\xi)$ of the stream function does not cause an instantaneous response ($\tau = 0$, i.e. $\xi = r/\sqrt{4\nu\tau} \to \infty$ and $f(\xi) = 0$). A finite contribution at $\tau = 0$ from $g^d(\tau)$ is remaining. The flow past the particle in the absence of the vorticity

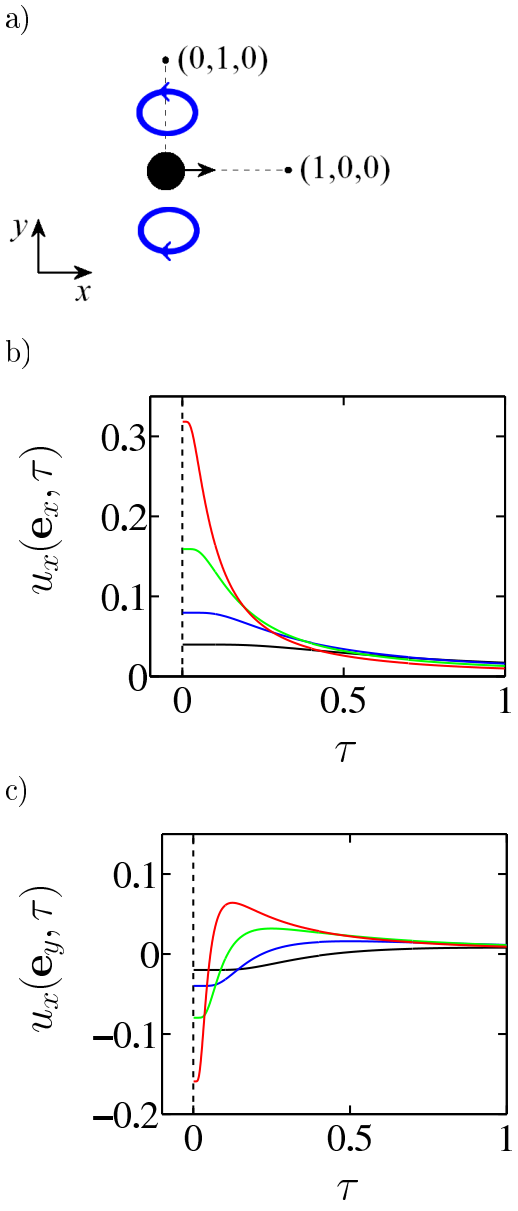

Figure 4.7: The sphere moves at velocity $V(t) = \delta(t)$, indicated in panel (a). (b) and (c) show the observed flow at $\mathbf{e}_x$ and $\mathbf{e}_y$ for different values of the viscosity: $\nu = 0.25$ (black), 0.5 (blue), 1.0 (green) and 2.0 (red).

driven flow, i.e. the potential flow contribution, is

$$G_{ij}^{d}(\mathbf{y},\tau) = \frac{\nu}{4\pi r^3}\left[-\delta_{ij} + 3\frac{y_i y_j}{r^2}\right]. \tag{4.47}$$

The superscript d indicates the origin of the tensor, the potential doublet. The flow due the potential doublet is decaying as $1/r^3$, as for the oscillating sphere in section 2.3.

As the distance r diverges, ξ diverges as well. The value for ξ diverges in two limits: In the limit of vanishing time and prescribed distance and in the limit of diverging distance for fixed time. This is related to the spreading of vorticity as a diffusion front: For large values of ξ, $f(\xi)$ is suppressed exponentially and rises suddenly as ξ gets of order one. Therefore, for a fixed time τ, the diffusion front is at $\sqrt{4\nu\tau}$ and for distances $r < \sqrt{4\nu\tau}$, the value which is assumed by $f(\xi)$ is $f(0) = 1$. For $r > \sqrt{4\nu\tau}$, $f(\xi)$ is exponentially small. On the other hand, if the distance r is prescribed, vorticity needs a time $r^2/(4\nu)$ to spread diffusively to distances of order r. There is little vorticity at times $t < r^2/(4\nu)$, whereas at times $t > r^2/(4\nu)$ asymptotically $\xi \to 0$ and $f(\xi) \to 1$.

The difference to the concentration field in subsection 4.1.1 is the composition of time-dependent Stokes flow of vorticity driven flow and potential flow. Whereas the first spreads as a diffusion front and at large distances decays exponentially with distance, the latter responds instantaneous to the motion of the particle and decays more weakly as $1/r^3$.

For large values of ν, there is a strong response at small times, which decays quickly, whereas for smaller values of ν the response is weaker and smoothed out in time. The areas under the curves are constant: The integration of $G_{ij}(\mathbf{y},\tau)$ from $\tau = 0$ to ∞ is conveniently done in terms of $\xi = r/\sqrt{4\nu\tau}$. With $d\tau = -d\xi \cdot r^2/(2\nu\xi^3)$,

$$\int_0^\infty \frac{d\xi}{\xi^3}\varphi(\xi) = 1 \qquad \text{and} \qquad \int_0^\infty \frac{d\xi}{\xi^3}\xi\varphi'(\xi) = 2 \tag{4.48}$$

such that the integral of both arguments of the Greens function tensor $(3\varphi - \xi\varphi')/\xi^3$ and $(\xi\varphi' - \varphi)/\xi^3$ is equal to one. Then, the Oseen tensor is obtained,

$$\int_0^\infty G_{ij}(\mathbf{y},\tau)d\tau = G_{ij}^{(s)}(\mathbf{y}). \tag{4.49}$$

For $\nu \to \infty$ the signal of the fluid gets narrower and steeper, as the signal from the kernel in subsection 4.1.1. Therefore, the time-dependence of the flow approaches a δ-function in the limit $\nu \to \infty$, similar to the diffusion kernel. In the limit $\nu \to \infty$ the fluid responds instantaneously to the force, which drives the particle and the flow obeys the steady Stokes equation.

As deduced from figure 4.7, the kernel is extended over a finite width of τ. For small viscosities, the extension is over a large width, whereas for large viscosities, the kernel becomes narrow. The width of the kernel is estimated here.

For the two terms which appear in the kernel, which are $\xi\varphi'(\xi) - \varphi(\xi)$ and $3\varphi(\xi) - \xi\varphi'(\xi)$ from equation (4.40), the maximum values are found at $\xi = 1$ and $\xi = 0$, respectively. For each of the terms, the integral over time equals $r^2/(2\nu)$. The maximum values are given respectively by

$$(\xi\varphi'(\xi) - \varphi(\xi))|_{\xi=1} = \frac{6}{\sqrt{\pi}}e^{-1} - \mathrm{erf}(1) \approx 0.4 \tag{4.50}$$

$$(3\varphi(\xi) - \xi\varphi'(\xi))|_{\xi=0} = 3. \tag{4.51}$$

These values, both of order 1, are independent of r and ν. If the width of the kernel is estimated as in subsection 4.1.1, one obtains for both terms a width of order $\Delta\tau = r^2/\nu$, as before for the concentration field kernel. To be more precisely, the width is given approximately as $1.2r^2/\nu$ and $0.2r^2/\nu$, respectively, but for the purpose of this analysis, the scaling as r^2/ν is more relevant than the exact prefactors, as long as these are of order one.

The arguments from subsection 4.1.1 apply. The finite width of the kernel implies a cut-off of the instantaneous velocity field. For a prescribed distance r, the fluid responds instantaneously to the force, if the force is smooth on a time-scale r^2/ν. For the force being not smooth on such a time scale, the contribution of $q(t)$ to equation (4.39) is not constant and the flow deviates from steady Stokes flow. On the other hand, if the source is smooth on a time-scale T, the fluid responds instantaneously up to distances $\sqrt{\nu T}$. Further out, the flow deviates from steady Stokes flow.

For the problem of the sphere starting at $t = 0$ with constant velocity V, the solution has been given in chapter 3. In terms of the Stokeslet approximation, the time-integration of the Greens tensor is most conveniently done in terms of ξ. Then for $\xi_t = |\delta\mathbf{x}|/\sqrt{4\nu t}$, the integration yields for the startup problem, where the particle is forced with constant force $q_j(t) = q_{0,j}$ from $t = 0$ on,

$$u_i(t) = \int_0^t G_{ij}(\delta\mathbf{x}, \tau) q_{0,j} d\tau \tag{4.52}$$

$$= \frac{1}{8\pi r}\left[\tilde{A}(\xi_t)\delta_{ij} + \tilde{B}(\xi_t)\frac{y_i y_j}{r^2}\right] q_{0,j} \tag{4.53}$$

$$\tilde{A}(\xi_t) = \frac{e^{-\xi_t^2}}{\sqrt{\pi}\xi_t} + 1 - \left(1 + \frac{1}{2\xi_t^2}\right)\mathrm{erf}(\xi_t) \tag{4.54}$$

$$\tilde{B}(\xi_t) = 1 - \frac{3e^{-\xi_t^2}}{\sqrt{\pi}\xi_t} - \left(1 - \frac{3}{2\xi_t^2}\right)\mathrm{erf}(\xi_t). \tag{4.55}$$

Figure 4.8 shows the flow produced by a localized sphere, which is initially at rest and then starts to move in x-direction with unit velocity. The flow at $\mathbf{e}_x$ shown in figure 4.8(a), which is the functions plotted in figure 4.7(b) integrated over time, shows a monotoneous rise of the flow for small times. Instead, the flow at $\mathbf{e}_y$, i.e. the functions in figure 4.7(c) integrated over time, still displays a change from negative to positive values due to the vortex which passes the observation point. Due to the finite value of the Greens tensor at $\tau = 0$ (cf. to figure 4.7), i.e. due to potential flow, both at $\mathbf{e}_x$ and $\mathbf{e}_y$ the flow rises as t for small times smaller than $r^2/(4\nu)$. From the integration of $G^d_{ij}(\mathbf{y}, \tau)$ from equation (4.47) over time or by expansion of $\tilde{A}(\kappa r)$ and $\tilde{B}(\kappa r)$ from above, one obtains for the potential flow at small times, in the absence of the vorticity driven flow $u_i = G^d_{ij}(\delta\mathbf{x}(t), t)q_{0,j}$ and

$$G^d_{ij}(\mathbf{y}, t) = \frac{\nu t}{4\pi r^3}\left[-\delta_{ij} + 3\frac{y_i y_j}{r^2}\right]. \tag{4.56}$$

The difference to the start-up concentration field (4.10) of subsection 4.1.1, where the whole concentration field is exponentially supressed until at a distance r a time of order $r^2/(4\nu)$ elapsed, is the potential flow contribution, which is not related to a diffusion equation and behaves differently.

At a time of order $r^2/(4\nu)$, vorticity driven flow spreads diffusively past the observation point and the flow rises to its stationary state. Figures (a) and (b) show that this happens on a time scale which varies as $1/\nu$. The integral of $G_{ij}(\mathbf{y}, \tau)$ over τ is the Oseen tensor, cf. equation (4.49). In figure 4.8 at the points $\mathbf{e}_x$ and $\mathbf{e}_y$, the flow assumes the values

$$u^{(s)}_x(\mathbf{e}_x) = \frac{1}{4\pi} \approx 0.080 \qquad \text{and} \qquad u^{(s)}_x(\mathbf{e}_y) = \frac{1}{8\pi} \approx 0.040. \tag{4.57}$$

Figure (c) shows the difference of the fluid velocity to the stationary value at the point $\mathbf{e}_x$. The stationary flow is approached as $1/\sqrt{t}$, remarkably slow! This clearly represents the diffusive spreading of the time-dependent flow.

For the oscillating sphere, as we have seen in chapter 2, the extension of the instantaneously responding flow depends on the frequency. Consider the sphere forced oscillatory, i.e. $q_j(t) = \hat{q}_j \exp(i\omega t)$. Then the flow is given by

$$u_i(\mathbf{x}, t) = \hat{G}_{ij}(\delta\mathbf{x}, \omega)\hat{q}_j e^{i\omega t} \tag{4.58}$$

with $\kappa = \sqrt{i\omega/\nu}$ and

$$\hat{G}_{ij}(\mathbf{y}, \omega) \;=\; \frac{1}{4\pi r}\left[\hat{A}(\kappa r)\delta_{ij} + \hat{B}(\kappa r)\frac{y_i y_j}{r^2}\right] \tag{4.59}$$

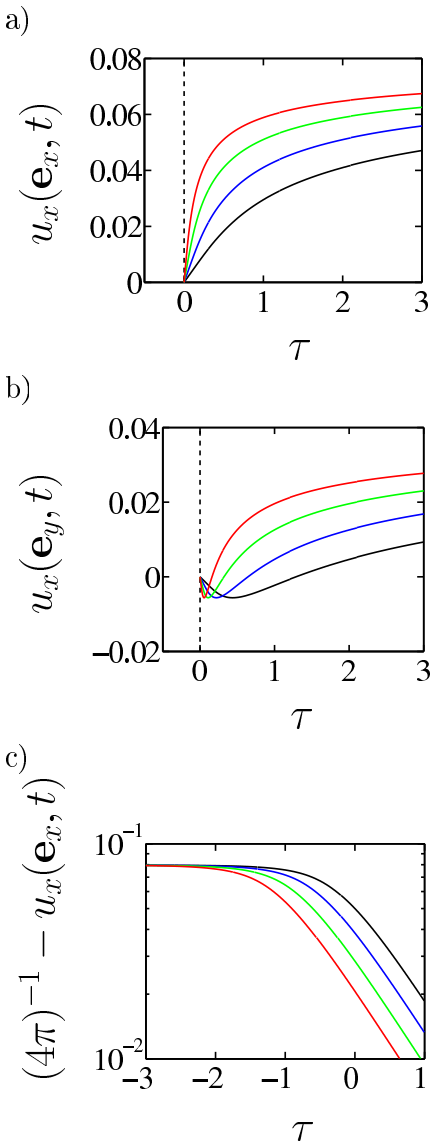

Figure 4.8: Flow produced by a sphere, which is at rest for $t < 0$ and moves at unit velocity for $t \geq 0$, given by equation (4.53). (a) shows the x-component at position $\mathbf{x} = \mathbf{e}_x$, plotted as a function of time. (b) shows the x-component at position $\mathbf{x} = \mathbf{e}_y$. (c) shows $(4\pi)^{-1} - u_x(\mathbf{e}_x)$, the deviation of the flow in figure (a) from the asymptotic value. Viscosities $\nu = 0.25$ (black), 0.5 (blue), 1 (green) and 2 (red).

$$\hat{A}(\kappa r) = \frac{1+\kappa r+\kappa^2 r^2}{\kappa^2 r^2} e^{-\kappa r} - \frac{1}{\kappa^2 r^2} \tag{4.60}$$

$$\hat{B}(\kappa r) = -\frac{3+3\kappa r+\kappa^2 r^2}{\kappa^2 r^2} e^{-\kappa r} + \frac{3}{\kappa^2 r^2} \tag{4.61}$$

($r = |\mathbf{y}|$). For a prescribed frequency ω, the force is smooth on a time scale $1/\omega$, such that, with the arguments above, up to distances $\sqrt{\nu/\omega}$ the fluid responds instantaneously to the momentum source. This is similar to the oscillatory source of subsection 4.1.1. From equations (4.60) and (4.61), the flow may be expanded in terms of κr and one obtains the Oseen tensor. Thus the results from chapter 2 are recovered: Up to distances $\sqrt{\nu/\omega}$, the flow is steady Stokes flow. Further away than $\sqrt{\nu/\omega}$ from the particle, vorticity is suppressed exponentially and the remaining flow is potential flow, decaying as $1/r^3$.

For a prescribed distance r, the fluid responds instantaneously to the force for frequencies up to ν/r^2, whereas vorticity driven flow is exponentially small and the flow deviates from steady Stokes flow for larger frequencies.

Vorticity spreads diffusively and the arguments from subsection 4.1.1 apply here as well. If the force is smooth on a time scale T, diffusive spreading is limited to distances below $\sqrt{\nu T}$. Much similar to the results obtained for the concentration field in subsection 4.1.1, the flow differs from steady Stokes flow at larger distances, but then it is dominated by potential flow, which decays as $1/r^3$, more rapid than the instantaneous response. In the next subsection, the fluctuations of time-dependent Stokes flow for a suspension of particles will be calculated.

4.2.2 Fluctuations

Many particles at positions $\mathbf{x}^{(\alpha)}(t)$ (where α is the index that counts the particles), which are forced by $\mathbf{q}^{(\alpha)}(t)$, generate a flow, which is given by

$$u_i(\mathbf{x},t) = \sum_\alpha \int_0^\infty G_{ij}\left(\delta\mathbf{x}^{(\alpha)}(t), t'\right) q_j^{(\alpha)}(t-t')dt' \tag{4.62}$$

with $\delta\mathbf{x}^{(\alpha)}(t) = \mathbf{x} - \mathbf{x}^{(\alpha)}(t)$ and $G_{ij}(\mathbf{y},\tau)$ defined in equation (4.40).

For a sediment, gravity drives the particles and hydrodynamic interaction gives rise to fluctuations of the particle velocities. The details of this process are far from clear. Comprehensive investigation has to be done to understand this process. The regularization of the velocity fluctuations can be understood seperately for a suspension of particles with zero mean velocity for each particle. Then, if the particles are homogeneously distributed and move randomly in all directions, the time mean of the flow at a

fixed position vanishes. The fluctuation of the fluid velocity at a fixed position is given as the absolute value of the flow squared,

$$\langle u_i(\mathbf{x},t)u_i(\mathbf{x},t)\rangle_t = \sum_{\alpha,\beta}\int_0^\infty dt' \int_0^\infty dt'' \left\langle G_{ij}(\delta\mathbf{x}^{(\alpha)}(t),t')G_{ik}(\delta\mathbf{x}^{(\beta)}(t),t'')q_j^{(\alpha)}(t-t')q_k^{(\beta)}(t-t'')\right\rangle_t \tag{4.63}$$

with the time mean $\langle ...\rangle_t$ as defined in equation (4.13). The Einstein sum convention is again used for the sum over i, j and k.

The components of the tensor $G_{ij}(\delta\mathbf{x}^{(\alpha)}(t),\tau)$ are nonlinear functions of the position (relative to each particle) $\delta\mathbf{x}^{(\alpha)}(t) = \mathbf{x} - \mathbf{x}^{(\alpha)}(t)$: In equation (4.40), $G_{ij}(\mathbf{y},\tau)$ depends on $r = |\mathbf{y}|$ directly and via $\varphi(\xi)$.

For the determination of the velocity fluctuations, we approximate the instantaneous position of the particle in the kernel by the mean position of the particle, i.e. $\delta\mathbf{x}^{(\alpha)}(t)$ is substituted by $\overline{\delta\mathbf{x}^{(\alpha)}} = \langle\delta\mathbf{x}^{(\alpha)}(t)\rangle_t$. To obtain the restrictions of this analysis, the kernel is expanded into a Taylor series, i.e.

$$\begin{aligned} G_{ij}(\delta\mathbf{x}^{(\alpha)}(t),\tau) &= G_{ij}(\overline{\delta\mathbf{x}^{(\alpha)}},\tau) \\ &+ \frac{d}{d\mathbf{y}}G_{ij}(\mathbf{y},\tau)\Big|_{\mathbf{y}=\overline{\delta\mathbf{x}^{(\alpha)}}} \cdot \left(\delta\mathbf{x}^{(\alpha)}(t) - \overline{\delta\mathbf{x}^{(\alpha)}}\right). \end{aligned} \tag{4.64}$$

To estimate the size of the derivative term, consider the harmonic solution $\hat{G}_{ij}(\mathbf{y})$, equation (4.59). It involves r explicitely and products kr where $k = \sqrt{\omega/\nu}$. Thus the gradient term involves inverse lengths $1/r$ and k. The difference of the particle from its mean position is of the order of the oscillation amplitude D. Then, for the gradient of the tensor to be small compared to the first term on the right hand side of equation (4.64),

$$\frac{D}{r} \ll 1, \tag{4.65}$$

and

$$\sqrt{\frac{\omega}{\nu}}D \ll 1. \tag{4.66}$$

The first condition states that the expansion is valid only at distances from the particle larger than D. The latter condition has been obtained in chapter 2 as a condition for the validity of the time-dependent Stokes equation. The amplitude of the oscillation D has to be small compared to $\sqrt{\nu/\omega}$, the cut-off distance of the steady Stokes solution.

In the following part, we assume that these two conditions are satisfied and approximate the position of the particle in the kernel by its mean position. Then the velocity

fluctuations for a suspension of particles are approximately given by

$$\langle u_i(\mathbf{x},t)u_i(\mathbf{x},t)\rangle_t = \sum_{\alpha,\beta}\int_0^\infty dt' \int_0^\infty dt'' \\ G_{ij}(\overline{\delta\mathbf{x}^{(\alpha)}},t')G_{ik}(\overline{\delta\mathbf{x}^{(\beta)}},t'')\langle q_j^{(\alpha)}(t-t')q_k^{(\beta)}(t-t'')\rangle_t. \tag{4.67}$$

Velocity fluctuations of the fluid are investigated in the following part for a randomly moving particle.

Fluctuations in terms of the Greens function

The flow of a single particle at $\mathbf{X}(t)$ is given by

$$u_i(\mathbf{x},t) = \int_0^\infty G_{ij}(\delta\mathbf{x}(t),\tau)q_j(t-\tau)d\tau \tag{4.68}$$

($\delta\mathbf{x}(t) = \mathbf{x} - \mathbf{X}(t)$) with the integral kernel given by equation (4.40). Similar as for the source in subsection 4.1.2, the force which acts on the particle is supposed to be composed of oscillatory forces,

$$q_j(t) = \sum_{n=-N}^{N} \hat{q}_{j,n}e^{i\omega_n t}. \tag{4.69}$$

The frequencies are assumed equally spaced, with a minimum value for the frequency $\omega_{\min}$ and a maximum value for the frequency $\omega_{\max}$, such that $\omega_n = n\omega_{\min}$, $n = -N$, ..., N, as before. Figure 4.9 shows an example. The components of the force are random. For each frequency and each component the Fourier amplitude is chosen between 0 and ∞ with a Gaussian probability and a random phase. Subsequently, the amplitudes of each component are normalized, $\langle q_j(t)^2\rangle_t = 1$. Panel (a) shows the absolute values for the Fourier amplitudes $\hat{q}_{x,n}$. Similar distributions are obtained for $\hat{q}_{y,n}$ and $\hat{q}_{z,n}$. The distribution of the values is shown for the three components in panels (b) to (d).

Figure 4.10 shows the flow produced by that paticle. The paramters are chosen as in subsection 4.1.2 to compare the fluctuations of the concentration field to the fluctuations of the fluid velocity. The x-component of the force is shown in panel (a) and $4\pi r u_x(r\mathbf{e}_x,t)$ is shown at various distances r from the particle in panels (b) to (f). At distances, which are smaller than the distance given by the largest frequency, $\sqrt{\nu/(N\omega_0)}$ (approximimately 0.3 for the example of figure 4.10), the time window of the kernel in equation (4.68) is small and $G_{ij}(\mathbf{y},\tau)$ may be replaced by the Oseen tensor. The flow field responds instantaneously to the force, i.e. the force and the normalized

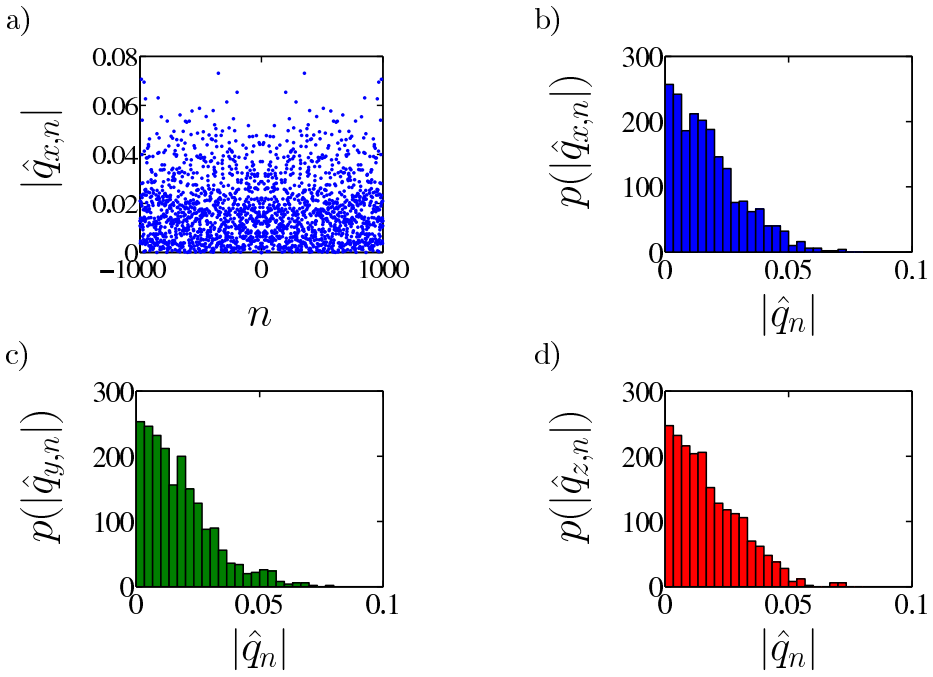

Figure 4.9: Randomly assigned Fourier amplitudes for frequencies $\omega_n = n\omega_{\min}$, $n = -N, ..., N$. The probabilities for the Fourier amplitudes are Gaussian. (a) $|\hat{q}_{n,x}|$. (b) distribution for $|\hat{q}_{n,x}|$, (c) distribution for $|\hat{q}_{n,y}|$, (d) distribution for $|\hat{q}_{n,z}|$. For each amplitude $\hat{q}_{n,j}$, the phase is random between $-\pi$ and π and each force component is normalized such that $\langle q_j^2(t)\rangle_t = 1$.

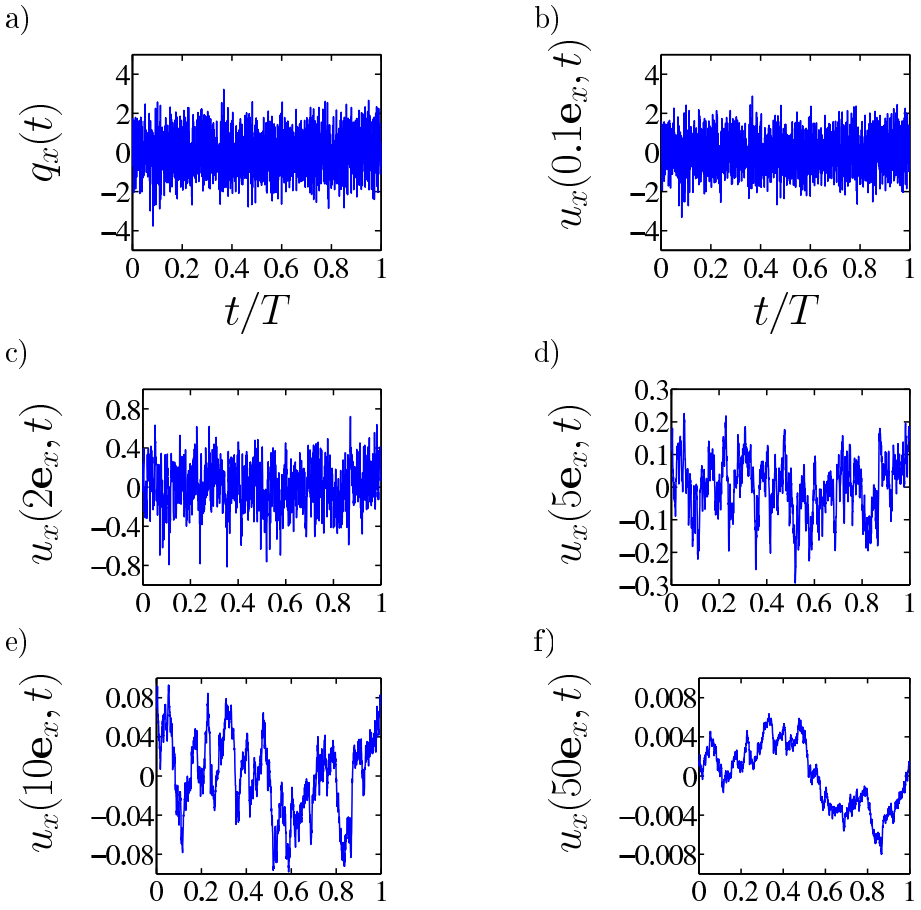

Figure 4.10: (a): x-component of the force from figure 4.9 as a function of time, plotted over t/T, where $T = 2\pi/\omega_{\min}$ is the period of the force. (b) to (f): x-component of the flow as observed at distances r along the x-axis, where $r = 0.1$ (b), 2 (c), 5 (d), 10 (e) and 50 (f). Parameters are $\nu = 0.1$, $\omega_{\min} = 0.001$, $N = 1000$.

flow coincide for distance $r = 0.1$, which is panel (b). Thus, the signal from the particle is instantaneously transmitted to $0.1\mathbf{e}_x$, i.e.

$$u_x(r\mathbf{e}_x, t) = \frac{q_x(t)}{4\pi r}. \tag{4.70}$$

Note that $q_y(t)$ and $q_z(t)$ are different from zero, but do not contribute to u_x along the x-axis.

As the distance is increased, from panel (c) to panel (d) the flow drops roughly from 0.5 to 0.2. Then from panel (d) to panel (e) the flow drop from 0.2 to 0.1. The ratios 0.5/0.2 and 0.2/0.1 corresponds to the inverse ratio of the distances, 5/2 and 10/5. Thus, as has been obtained already for the concentration field of subsection 4.1.2, at distances from the particle larger than $\sqrt{\nu/\omega_{\max}}$, the flow drops as $1/r^2$. A reasoning similar to that of subsection 4.1.2 applies: Since the Fourier amplitudes are distributed homogeneously in frequency space, the force may be treated as randomly fluctuating, changing its value after a time $\Delta t = 1/\omega_{\max}$. The integral of the randomly fluctuating force over a time width r^2/ν is of order $r/\sqrt{\omega_{\max}\nu}$. Taking into account the prefactor $\nu/(4\pi r^3)$ of equation (4.40), for the magnitude of the flow, one obtains

$$u_x(r\mathbf{e}_x, t) \propto \frac{\sqrt{\nu/\omega_{\max}}}{4\pi r^2}. \tag{4.71}$$

This is the same scaling as for the concentration field.

Further away from the particle, at distances larger than $\sqrt{\nu/\omega_{\min}}$, the vorticity driven contribution to the flow is suppressed exponentially. This corresponds in the example above for $r > 10$. The remaining potential flow decays as $1/r^3$, as was shown in subsection 4.2.1. From panel (e) to panel (f), the drop of the magnitude of $4\pi r u_x(r\mathbf{e}_x, t)$ is indeed by a factor of more than 10, considerably larger than the ratio of the magnitudes, which is 5.

As in subsection 4.1.2, depending on the distance, the flow responds instantaneously to the force and the magnitude of the flow drops as $1/r$ for distances up to $\sqrt{\nu/\omega_{\max}}$. For larger distances, up to $\sqrt{\nu/\omega_{\min}}$, the flow drops as $1/r^2$. The time width of the kernel is large in this range, such that the force can be treated as randomly fluctuating. For distances larger than $r > \sqrt{\nu/\omega_{\min}}$, the time width of the kernel exceeds the period of the particle and the flow decays as $1/r^3$. Remarkably, in this range the flow is not smooth, as the concentration field above, but it clearly does not show the time-dependence that is prescribed by the force. The flow at large distances will be investigated further in the next part, when the fluctuations are calculated in frequency space.

The black line in figure 4.11(a) shows the fluctuations for the example from figure 4.9, for $\nu = 0.1$, 1, 10 and 100. The three ranges, which have been identified above, are represented there. The black line shows the velocity fluctuations for $\nu = 0.1$. The squares correspond to the fluctuations for the distances in panels (b) to (f) from figure 4.10. Graphically, up to a distance of about 0.1, the flow responds instantaneously and the velocity fluctuations decay as $1/r^2$. The transition to the ν/r^4 decay is from the analytical estimates at 0.3, which fits well with the graphically determined value 0.1. The next range, the ν/r^4-decay, is graphically up to distances of roughly 20. The analytical estimate for the transition to the $1/r^6$-decay is 10.

As ν is increased, the $1/r^2$ range is extended over a wider range. As $\nu \to \infty$, the fluid responds instantaneously to the motion of the particle up to infinite distances and the fluctuations decay as $1/r^2$ everywhere. This is the steady Stokes limit, which gives rise to the divergence of the velocity fluctuations that has been pointed out by Caflisch and Luke [14]. For any finite ν, the velocity fluctuations of a single particle are cut off at a finite distance, which regularizes the fluctuations for a homogeneous distribution.

The transitions of three ranges are at $\sqrt{\nu/\omega_{\max}}$ and at $\sqrt{\nu/\omega_{\min}}$. Hence, if the number of frequencies is increased, the ν/r^4-range gets extended. This is shown in panel(b) of figure 4.11, where $2 \cdot 10^6$ frequencies are used. The range is extended therefore over three orders of magnitude. Note that compared to figure 4.6, the transitions between the three ranges seem to be extended over a wider range. We have seen in the previous subsection, that the time width estimates for the two contributions to the Greens tensor differ by a factor of 6. Hence also the transition region is expected to be extended over at least that factor, which is half an order of magnitude.

The fluctuations of the concentration field of section 4.1 and of the time-dependent Stokes flow here are similar. The results differ at large distances, where the flow decays as $1/r^3$, whereas the concentration field decays exponentially. Next, the fluctuations will be investigated in frequency space.

Fluctuations in Fourier space

For the force as composed in equation (4.69), the flow is given by

$$u_i(\mathbf{x}, t) = \sum_n e^{i\omega_n t} \hat{G}_{n,ij}(\delta\mathbf{x}(t)) \hat{q}_{n,j} \tag{4.72}$$

where in terms of $\kappa_n = \sqrt{i\omega_n/\nu}$ (cf. equation (2.40))

$$\hat{G}_{n,ij}(\mathbf{y}, \omega) = \frac{1}{4\pi r} \left[\hat{A}(\kappa_n r)\delta_{ij} + \hat{B}(\kappa_n r)\frac{y_i y_j}{r^2} \right] \tag{4.73}$$

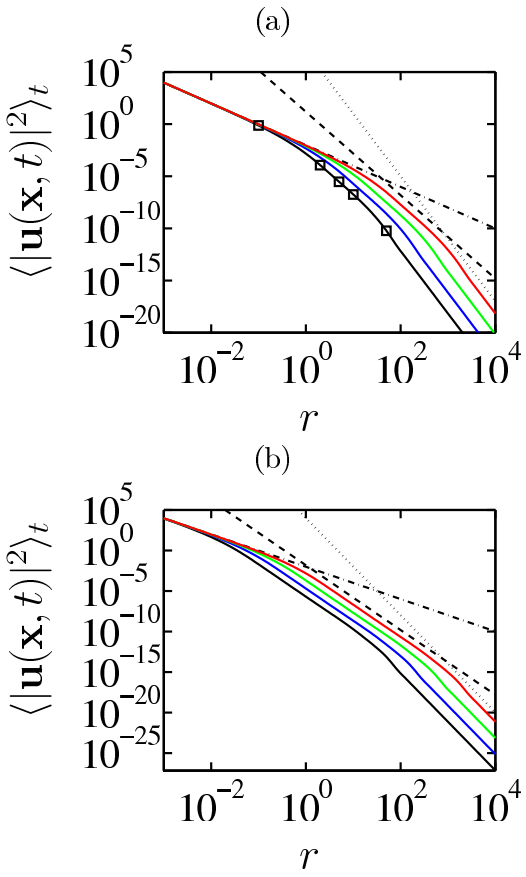

Figure 4.11: (a): Fluctuations for the randomly moving particle from figure 4.9 along the x-axis as a function of the distance for viscosities $\nu = 0.1$ (black), $\nu = 1$ (blue), $\nu = 10$ (green) and $\nu = 100$ (red) The dot-dashed line shows the fluctuations as obtained from steady Stokes flow. The dashed line shows a $1/r^4$-decay and the dotted line shows a $1/r^6$-decay. The squares indicate the points of the curve, which are obtained from figures 4.10(b) to 4.10(f) (there $\nu = 0.1$). (b): Same as (a) but $N = 10^6$.

$$\hat{A}(\kappa_n r) = \frac{1+\kappa_n r+\kappa_n^2 r^2}{\kappa_n^2 r^2} e^{-\kappa_n r} - \frac{1}{\kappa_n^2 r^2} \tag{4.74}$$

$$\hat{B}(\kappa_n r) = -\frac{3+3\kappa_n r+\kappa_n^2 r^2}{\kappa_n^2 r^2} e^{-\kappa_n r} + \frac{3}{\kappa_n^2 r^2}. \tag{4.75}$$

In terms of the Fourier coefficients $\hat{q}_{n,j}$ the time correlation function is

$$\langle q_j(t) q_k(t+\delta t)\rangle_t = \sum_n \hat{q}_{n,j}\hat{q}_{-n,k} e^{-i\omega_n \delta t}. \tag{4.76}$$

Then for the fluctuations one obtains

$$\langle |\mathbf{u}(\mathbf{x},t)|^2\rangle_t = \sum_n \hat{G}_{n,ij}(\overline{\delta\mathbf{x}})\hat{G}_{-n,ik}(\overline{\delta\mathbf{x}})\hat{q}_{n,j}\hat{q}_{-n,k}. \tag{4.77}$$

For simplicity, we assume that the components of the force are uncorrelated. Furthermore the force fluctuation is assumed to be the same in all three directions, such that

$$\langle q_j(t) q_k(t)\rangle_t = Q\delta_{jk}. \tag{4.78}$$

Then with equation (4.76), if $\hat{q}_{j,n}$ is constant for all n,

$$|\hat{q}_{j,n}| = \sqrt{\frac{Q}{2N}} \tag{4.79}$$

which corresponds to equation (4.28), the source amplitudes for the diffusion problem. With this assumption for the Fourier amplitudes, the fluctuations become

$$\langle |\mathbf{u}(\mathbf{x},t)|^2\rangle_t = \frac{Q}{2N}\sum_{n,i,j}\left|\hat{G}_{n,ij}(\overline{\delta\mathbf{x}})\right|^2. \tag{4.80}$$

From equation (4.73) one obtains

$$\langle |\mathbf{u}(\mathbf{x},t)|^2\rangle_t = \frac{Q}{2N}\frac{1}{(4\pi r)^2}\sum_n\left[2\left|\hat{A}_n(\kappa_n r)\right|^2 + \left|\hat{A}_n(\kappa_n r)+\hat{B}_n(\kappa_n r)\right|^2\right]. \tag{4.81}$$

This expression serves as a starting point for the discussion of the three limits, that have been found above.

In the limit $\kappa_N r \to 0$, i.e. if $r \ll \sqrt{\nu/\omega_{\max}}$, $\hat{G}_{n,ij}(\mathbf{y})$ becomes the Oseen tensor $\hat{G}^{(s)}_{n,ij}(\mathbf{y})$. Then $\hat{A}_n(\kappa_n r) = \hat{B}_n(\kappa_n r) = 1/2$ and one finds for the fluctuations

$$\langle |\mathbf{u}(\mathbf{x},t)|^2\rangle_t = \frac{3Q}{32\pi^2 r^2}. \tag{4.82}$$

This is the expression for the fluctuations if the flow is described by the steady Stokes equation, i.e. if the fluid is assumed to respond instantaneously to the force. The validity

of this expression is limited to distances $r \ll \sqrt{\nu/\omega_{\max}}$, which is consistent with the result that has been obtained above.

If $r > \sqrt{\nu/\omega_{\max}}$, but $r < \sqrt{\nu/\omega_{\min}}$, the contribution from vorticity to $\hat{G}_{n,ij}(\mathbf{y})$ is damped exponentially and the flow is potential flow for all frequencies $\omega_n > \nu/r^2$, whereas roughly the fluid responds instantaneously for all frequencies $\omega_n < \nu/r^2$. Taking only into account the low frequencies and the instantaneous response of the fluid and neglecting contributions from potential flow, one obtains for the fluctuations

$$\langle |\mathbf{u}(\mathbf{x},t)|^2 \rangle_t = \frac{3\nu Q}{32\pi^2 \omega_{\max} r^4}. \tag{4.83}$$

Contributions to fluctuations from potential flow are of order $\nu^2/(\omega_0^2 r^6)$ and small compared to the expression for the fluctuations above. To be more explicit, they are small for distances $r < \sqrt{\nu/\omega_{\min}}$, which is the outer bound of the range that is considered here.

Finally, for $r > \sqrt{\nu/\omega_{\min}}$, the vorticity driven contribution to the flow is damped exponentially for each frequency. Then from equations (4.74) and (4.75) one obtains

$$\hat{A}_n(\kappa_n r) = -\frac{1}{\kappa_n^2 r^2} \tag{4.84}$$

$$\hat{B}_n(\kappa_n r) = \frac{3}{\kappa_n^2 r^2} \tag{4.85}$$

and the fluctuations are

$$\langle |\mathbf{u}(\mathbf{x},t)|^2 \rangle_t = \frac{3\nu^2}{16\pi^2 r^6} \sum_{n=-N}^{N} \frac{Q}{N\omega_n^2}. \tag{4.86}$$

This shows that at large distances not all frequencies contribute equally to the velocity field. High frequencies contribute less than low frequencies and in figure 4.10 low frequencies are responsible for the global shape of the velocity field, whereas it is rough at small time scales due to high frequency contributions.

The sum

$$\sum_{n=1}^{\infty} \frac{1}{n^2} = \frac{\pi^2}{6} \tag{4.87}$$

allows to approximate equation (4.86), if the number of frequencies in the system is large. Then

$$\langle |\mathbf{u}(\mathbf{x},t)|^2 \rangle_t = \frac{\nu^2 Q}{16\omega_{\min}^2 N r^6} \cdot (1 + O(N^{-1})). \tag{4.88}$$

The decay is proportional to ν^2 and to $1/r^6$.

The fluctuations for the potential flow have been found with the radius of the sphere neglected. When this is taken into account, $\hat{A}_n = -R^2/(3r^2)$ and $\hat{B}_n = R^2/r^2$. Then from equation (4.81)

$$\langle |\mathbf{u}(\mathbf{x},t)|^2 \rangle_t = \frac{QR^4}{12\pi^2 r^6} \tag{4.89}$$

The Stokeslet flow fluctuations, equation (4.86), dominate the fluctuations as given in equation (4.89), if

$$R \ll \sqrt[4]{\frac{\nu^2}{\omega_0 \omega_N}}. \tag{4.90}$$

The expression for the velocity fluctuations obtained from the flow in frequency space and in real space coincide. Similar than for the concentration field of section 4.1, three ranges and an expression for each range have been found for the decay of the fluctuations. First, for distances lower than $\sqrt{\nu/\omega_{\max}}$, prescribed by the largest frequency of the force, the fluid responds instantaneously to the motion of the particles and one obtains that the fluctuations decay as $1/r^2$. For distances larger than that, but smaller than $\sqrt{\nu/\omega_{\min}}$ which is prescribed by the lowest frequency in the system, the fluctuations decay as ν/r^4. For distances larger than $\sqrt{\nu/\omega_{\min}}$, the decay is as ν^2/r^6.

4.2.3 Comparison to experimental findings

Correlations

Experiments [21, 60, 61] show for sedimentation of particles that the flow is organized in swirls. The size of the swirls depends on the interparticle distance. For a volume ratio ϕ of particle volume to fluid volume, the interparticle distance is of order $D_{ip} = R\phi^{-1/3}$, where R is the radius of a single (spherical) particle. The correlation length of the flow, the size of the swirls, is found experimentally to be about $10R\phi^{-1/3}$.

The linear dependence of the correlation length on the interparticle distance in experiments can be explained from the considerations of subsection 4.2.1: Each particle is subject to the flow of all other particles. Consider a particle moving oscillatory with a frequency ω. Then the flow decays weakly, as $1/r$, up to distances $\sqrt{\nu/\omega}$. It decays more rapidly at distances larger than that. Hydrodynamic interaction is strongest inside a range $r < \sqrt{\nu/\omega}$. When the interparticle distance exceeds $\sqrt{\nu/\omega}$, the particle does not drive other particles. As a consequence, the frequency is not maintained in the system[1].

[1] To be more explicit, few particles are driven strongly at small distances, whereas a large number of particles is driven weakly at large distances. Taking the number of driven particles into account, hydrodynamic interaction is most efficient at distances of order $\sqrt{\nu/\omega}$. Then, if the interparticle

Thus the interparticle distance D_{ip} prescribes a maximum value for the frequencies in the system, which is $\omega_{\max} \propto \nu/D_{ip}^2$. The maximum frequency determines the size of the structures in the flow. As a consequence, the correlation length of the flow is of the order of the interparticle distance.

Fluctuations

With the results for the velocity fluctuations from subsection 4.2.2, an expression is obtained for a homogeneous distribution of particles as follows: At a fixed point, the fluid responds instantaneously to the motion of all particles inside a sphere with a radius of order D_{ip}, since this is the cut-off distance of the steady Stokes flow, prescribed by the largest frequency in the system. In this range, the velocity fluctuations decay as $1/r^2$. The fluctuations due to the flow from particles at larger distances decay as $\nu/(\omega_{\max} r^4)$, as obtained in subsection 4.2.2. Let Γ denote the number of particles per unit volume. Then in terms of the fluctuation of the force $\langle|\mathbf{q}(t)|^2\rangle_t$ which drives each particle (4.35), the fluctuations are given as the sum of the integrals over both ranges (when the low-frequency cut-off at large distances is neglected), i.e.

$$\langle|\mathbf{u}(\mathbf{x},t)|^2\rangle_t = \langle|\mathbf{q}(t)|^2\rangle_t \Gamma \left[\int_0^{D_{ip}} \frac{4\pi r^2}{32\pi^2 r^2} dr + \int_{D_{ip}}^{\infty} \frac{4\pi r^2 \nu}{32\pi^2 \omega_{\max} r^4} dr\right]. \tag{4.91}$$

Since the maximum frequency in the system depends on the interparticle distance as $\omega_{\max} = \nu/D_{ip}^2$, one finds that the fluctuations at each point are given by

$$\langle|\mathbf{u}(\mathbf{x},t)|^2\rangle_t = \frac{\Gamma D_{ip}}{8\pi} \langle|\mathbf{q}(t)|^2\rangle_t. \tag{4.92}$$

The particle force (per unit viscosity) is $\mathbf{q}(t) = 6\pi R \mathbf{V}(t)$ (cf. equation (4.35)). The driving force of a sediment is gravity. Thus as an estimate, the deviation of the particle velocity from its mean value V_s is assumed to be of the same order as the sedimentation velocity

$$V_s = \frac{2R^2(\rho_S - \rho)g}{9\rho\nu} \tag{4.93}$$

with the acceleration due to gravity on earth g and the fluid and particle density ρ and ρ_S, respectively. With this estimate,

$$\langle|\mathbf{u}(\mathbf{x},t)|^2\rangle_t = 9\pi\Gamma R^2 D_{ip} V_s^2. \tag{4.94}$$

distance exceeds $\sqrt{\nu/\omega}$, hydrodynamic interaction is not efficient.

Note that the volume occupied by a single particle is equal to D_{ip}^3. Therefore

$$\Gamma \propto \frac{1}{D_{ip}^3}. \tag{4.95}$$

Furthermore note that the ratio ϕ of the volume occupied by all particles to the volume occupied by the fluid is (for low values of ϕ) given by

$$\phi \propto \frac{R^3}{D_{ip}^3}. \tag{4.96}$$

Then the velocity fluctuations are

$$\langle |\mathbf{u}(\mathbf{x},t)|^2 \rangle_t \propto V_s^2 \phi^{2/3}. \tag{4.97}$$

This is the dependence of the fluctuations on the volume ratio which has been measured experimentally [21, 60, 61]. Segrè et al. [61] obtain this scaling for the fluctuations by an estimate based on the assumption that the motion of a particle is a random walk with a mean free distance which is of the order of the correlation length. This corresponds to the estimate of the velocity fluctuations for a single particle from subsection 4.2.2.

Levine et al. [32] calculate the impact of particle concentration fluctuations on the velocity fluctuations. Based on steady Stokes flow, but based on a diffusion equation for the particle concentration, they also obtain this scaling of the velocity fluctuations. Simulations and theories which do not take into account diffusional processes do not find such a dependence [13, 17, 28]!

The correlation length of the flow and the velocity fluctuations have been estimated here for a suspension of particles. The dependence of the velocity fluctuations on the particle concentration is in agreement with experimental measurements. One assumption has been made here which remains to be verified: The difference of the particle velocity to the sedimentation velocity is of the order of the sedimentation velocity.

4.3 Conclusions

In the first part, the concentration field due to an emitting source has been investigated. The concentration field obeys a diffusion equation and responds instantaneously to the source close to the source. Then the fluctuations of the concentration field are finite. If the time-dependence is left out, then the fluctuations of the concentration field diverge.

For a suspension of independent particles, the fluctuations of the flow diverge with the volume of the fluid if the steady Stokes equation is used to describe the flow, as has

been pointed out by Caflisch and Luke [14]. Steady Stokes flow is obtained with the assumption that vorticity responds instantaneously to the motion of a particle. Vorticity obeys a diffusion equation and as a consequence, analogous to the diffusion equation for the concentration field, the flow does not respond instantaneously at large distances from the particle. It has been shown that for time-dependent Stokes flow the fluctuations are finite and do not diverge with the volume. The estimate for the fluctuations agrees with experimental findings.

Chapter 5

Conclusions

The situation which usually is called *steady Stokes flow* assumes that the velocity field around a sphere instantaneously assumes the velocity field around a sphere that has moved with the same instantaneous velocity steadily for an infinite amount of time. As was shown in section 2, this assumption poses restrictions on the rate of change of the particle velocity which become more stringent the further away one is from the sphere. The validity of steady Stokes flow is limited by diffusion of vorticity and the flow responds instantaneously to the motion of the sphere only up to a distance $\sqrt{\nu T}$, where T is the period of modulation. The flow differs significantly from steady Stokes flow at larger distances. This has been shown for a sphere in oscillatory motion with oscillation frequency ω, i.e. $T = \omega^{-1}$, and for a sphere which started from rest; then T is the time which has elapsed since the start of the sphere.

The differences between steady and unsteady Stokes flow show up quite strikingly in the amount of fluid displaced by the sphere: in the case of the steady flow, this is infinite, whereas in the case of the unsteady flow it is finite for all ω. This shows rather clearly the differences between the limits $t \to \infty$ and $r \to \infty$, which cannot be interchanged.

In order to see the effects of a time-dependent solution rather more clearly and not clouded by technicalities, we consider the situation of diffusional spreading from localized, sat fluctuating sources. For a homogeneous distribution of sources it has been shown that the fluctuations of the concentration field are finite if the full time-dependent equation is used for the concentration field. In contrast, if the concentration field is approximated by the quasisteady concentration field, the fluctuations diverge. The concentration field model suggests new experiments to check time-dependence effects.

Caflisch and Luke [14] point out that velocity fluctuations for a suspension of particles diverge. This is in agreement with numerical simulations which are based on steady

Stokes flow [28]. Here, we show that the fluctuations are finite if the flow around the particles is described by the time-dependent Stokes equation. Thus, the fluctuations in numerical simulations should change significantly, when time-dependence is taken into account. Then, comparison to experiments possibly uncovers the hitherto existing discrepancy between experiment and simulation.

The fluctuations are regularized essentially due to the cut-off of the steady Stokes flow velocity field. For an oscillating particle, if the frequency is so large that the flow is cut-off below the interparticle distance, the oscillation of the particle cannot be carried over to other particles and is suppressed in the system. Assuming that the interparticle distance sets an upper limit on the frequencies of the particle motion in the system, we have found that the difference of the particle velocity to its mean value scales linearly with the interparticle distance. This scaling is in agreement with experiments [60].

Experiments measure time correlations [48] and distance correlations [21, 60] of the velocity fluctuations. These measurements show that particle velocities are correlated at finite distances and times. In section 4.2, the motion of a particle has been prescribed such that the motion is smooth at small time scales and uncorrelated at large time scales. These features should also be reflected in the temporal and spatial correlation functions of the particle velocities. A theoretical investigation of these correlation functions for time-dependent Stokes flow would enable a comparison to the experimental measurements.

The ideas here for a suspension of particles may be transferred also to bacteria herds. A new starting point to understand the experiments by Wu and Libchaber [70] involves an extension of the expressions for the flow of self-propelled organisms, which are based on steady Stokes flow [54, 64, 68], to expressions which are based on time-dependent Stokes flow. Then, a numerical simulation of a flock of particles may yield results which agree with the experiment.

It is clearly shown that the time-dependence of Stokes flow is important for the dynamics of a particle suspension. This thesis initiates further investigations on particle suspensions and related problems, which take into account time-dependent Stokes flow.

Appendix A

Correction to unsteady Stokes

In the following part, the analytical details for the calculation of the perturbation from section 2.5 are shown. First, the nonlinear terms are rewritten as a series of terms $\kappa^n r^n \exp(-\kappa r)$. Subsequently, the particular and homogeneous solutions of equations (2.73) and (2.74) are found.

A.1 Nonlinear Terms

For the inhomogenity of equation (2.73), only the real part contributes. In contrast to $F_{12}(r)$, the homogenous solutions for $F_{10}(r)$ are real and in equation (2.73) purely imaginary terms on the right hand side may be omitted. Then, with $\kappa = \sqrt{i}k = \sqrt{i\omega/\nu}$, for the inhomogenity, the right hand side of equation (2.73), one finds

$$\begin{aligned} \frac{9}{4}\frac{U^2R^2}{\nu}\kappa^3 \cdot \Bigg[e^{-\sqrt{2}k(r-R)} \left(\frac{1}{\kappa^2 r^2} + \frac{1}{\kappa^3 r^3} \right) \\ - e^{-\kappa(r-R)} \Bigg((1 + \bar{\kappa}R + \bar{\kappa}^2 R^2/3) \cdot \left(\frac{1}{\kappa^3 r^3} + \frac{3}{\kappa^4 r^4} + \frac{3}{\kappa^5 r^5} \right) \\ + \frac{1}{3\kappa R} \left(1 + \frac{3}{\kappa r} + \frac{3}{\kappa^2 r^2} \right) \Bigg) \Bigg] \end{aligned} \tag{A.1}$$

(note that k only appears in the first exponential function, whereas otherwise κ appears instead) and the right hand side of equation (2.74) equals

$$\begin{aligned} -\frac{9}{4}\frac{U^2R^2}{\nu}\kappa^3 \cdot \Bigg[e^{-2\kappa(r-R)} \left(\frac{1}{\kappa^2 r^2} + \frac{4}{\kappa^3 r^3} + \frac{6}{\kappa^4 r^4} + \frac{3}{\kappa^5 r^5} \right) \\ - e^{-\kappa(r-R)} \Bigg((1 + \kappa R + \kappa^2 R^2/3) \cdot \left(\frac{1}{\kappa^3 r^3} + \frac{3}{\kappa^4 r^4} + \frac{3}{\kappa^5 r^5} \right) \\ - \frac{1}{3\kappa R} \left(1 + \frac{3}{\kappa r} + \frac{3}{\kappa^2 r^2} \right) \Bigg) \Bigg] . \end{aligned} \tag{A.2}$$

The $1/\kappa R$ terms stem from the product of the diffusion equation solution $f_0(r)$ with the free flow $g_0^f(r)$ and therefore are, including the prefactor, linear in the sphere radius, whereas the other terms involve squares of the diffusion flow $f_0(r)$ and doublet flow $g_0^d(r)$ and are of order R^2. Note moreover that the oscillation amplitude solely appears in terms of U in the prefactor. All restrictions involving U may be discussed from the prefactor.

A.2 Solution

In the following part, first the homogenous solutions of equations (2.73) and (2.74) are shown. Then particular solutions are found with the method of variation of constants. The full solution is found by a superposition of both such that the boundary conditions are fullfilled.

A.2.1 Homogenous solution

The homogenous solutions of equation (2.73) are given by

$$\Psi_{01}(r) = r^5 \tag{A.3}$$
$$\Psi_{02}(r) = r^3 \tag{A.4}$$
$$\Psi_{03}(r) = r^0 = 1 \tag{A.5}$$
$$\Psi_{04}(r) = r^{-2} \tag{A.6}$$

For the homogeneous solutions of equation (2.74) one obtains

$$\Psi_{21}(r) = e^{-\sqrt{2}\kappa(r-R)} \cdot \left(\frac{1}{2\kappa^2 r^2} + \frac{1}{\sqrt{2}\kappa r} + \frac{1}{3}\right) \tag{A.7}$$
$$\Psi_{22}(r) = e^{+\sqrt{2}\kappa(r-R)} \cdot \left(\frac{1}{2\kappa^2 r^2} - \frac{1}{\sqrt{2}\kappa r} + \frac{1}{3}\right) \tag{A.8}$$
$$\Psi_{23}(r) = r^3 \tag{A.9}$$
$$\Psi_{24}(r) = r^{-2}. \tag{A.10}$$

A.2.2 Particular solution

Equations (A.1) and (A.2) are composed of terms which involve $\kappa^n r^n \exp(-\gamma(r-R))$ for various n and $\gamma = \kappa$, $\sqrt{2}\kappa$ and 2κ. Hence if $\varphi_{10}^{(n,\gamma)}$ and $\varphi_{12}^{(n,\gamma)}$ satisfy the equations

$$\left(\partial_r^2 - \frac{6}{r^2}\right)\left(\partial_r^2 - \frac{6}{r^2}\right)\varphi_{10}^{(n,\gamma)}(r) = \kappa^n r^n e^{-\gamma(r-R)} \tag{A.11}$$

$$\left(\partial_r^2 - \frac{6}{r^2} - 2\kappa^2\right)\left(\partial_r^2 - \frac{6}{r^2}\right)\varphi_{12}^{(n,\gamma)}(r) \;=\; \kappa^n r^n e^{-\gamma(r-R)}, \tag{A.12}$$

the particular contribution to the solutions $F_{10}(r)$ and $F_{12}(r)$ in equations (2.73) and (2.74) are composed of terms $\varphi_{10}^{(n,\gamma)}(r)$ and $\varphi_{12}^{(n,\gamma)}(r)$.

The particular solutions are found by variation of constants as

$$\varphi_{10}^{(n,\gamma)}(r) = \sum_{i=1}^{4} A_{0i}^{(n,\gamma)}(r)\Psi_{0i}(r) \tag{A.13}$$

$$\varphi_{12}^{(n,\gamma)}(r) = \sum_{i=1}^{4} A_{2i}^{(n,\gamma)}(r)\Psi_{2i}(r). \tag{A.14}$$

where the $A_{ij}^{(n,\gamma)}(r)$ are

$$A_{01}^{(n,\gamma)}(r) \;=\; +\frac{\kappa^2}{70}\cdot B^{(n-2,\gamma)}(r) \tag{A.15}$$

$$A_{02}^{(n,\gamma)}(r) \;=\; -\frac{1}{30}\cdot B^{(n,\gamma)}(r) \tag{A.16}$$

$$A_{03}^{(n,\gamma)}(r) \;=\; +\frac{1}{30\kappa^3}\cdot B^{(n+3,\gamma)}(r) \tag{A.17}$$

$$A_{04}^{(n,\gamma)}(r) \;=\; -\frac{1}{70\kappa^5}\cdot B^{(n+5,\gamma)}(r) \tag{A.18}$$

$$\begin{aligned} A_{21}^{(n,\gamma)}(r) \;=\; & -\frac{9\sqrt{2}}{8}\frac{1}{\kappa^3}\left[\frac{1}{2}B^{(n-2,\gamma-\sqrt{2}\kappa)}(r)\right. \\ & \left. -\frac{1}{\sqrt{2}}B^{(n-1,\gamma-\sqrt{2}\kappa)}(r) + \frac{1}{3}B^{(n,\gamma-\sqrt{2}\kappa)}(r)\right] \end{aligned} \tag{A.19}$$

$$\begin{aligned} A_{22}^{(n,\gamma)}(r) \;=\; & +\frac{9\sqrt{2}}{8}\frac{1}{\kappa^3}\left[\frac{1}{2}B^{(n-2,\gamma+\sqrt{2}\kappa)}(r)\right. \\ & \left. +\frac{1}{\sqrt{2}}B^{(n-1,\gamma+\sqrt{2}\kappa)}(r) + \frac{1}{3}B^{(n,\gamma+\sqrt{2}\kappa)}(r)\right] \end{aligned} \tag{A.20}$$

$$A_{23}^{(n,\gamma)}(r) \;=\; -\frac{1}{10}\cdot B^{(n-2,\gamma)}(r) \tag{A.21}$$

$$A_{24}^{(n,\gamma)}(r) \;=\; \frac{1}{10\kappa^5}\cdot B^{(n+3,\gamma)}(r) \tag{A.22}$$

in terms of the integral functions

$$B^{(m,\gamma)}(r) = -\int_r^\infty e^{-\gamma(\tilde{r}-R)}\cdot\kappa^m\tilde{r}^m\cdot d\tilde{r}. \tag{A.23}$$

The particular solution of equations (2.73) and (2.74) is given by a sum of $\varphi_{10}^{(n,\gamma)}(r)$ and $\varphi_{12}^{(n,\gamma)}(r)$, one for each term in equations (A.1) and (A.2). Then, the homogenous solutions with decaying velocity fields, in particular $\Psi_{03}(r)$ and $\Psi_{04}(r)$ for $F_{10}(r)$ and $\Psi_{21}(r)$ and $\Psi_{24}(r)$ for $F_{12}(r)$, are added such that the boundary conditions

$$F_{10}(r)|_{r=R} = 0 \qquad \text{and} \qquad F_{10}'(r)|_{r=R} = 0 \tag{A.24}$$

$$F_{12}(r)|_{r=R} = 0 \qquad \text{and} \qquad F_{12}'(r)|_{r=R} = 0 \tag{A.25}$$

are fullfilled.

For the computation of the integral functions, the following recursive relations may be found: For $n > 0$

$$B^{(n,\gamma)}(r) = -\frac{\kappa^n r^n}{\gamma} e^{-\gamma(r-R)} + \frac{n\kappa}{\gamma} \cdot B^{(n-1,\gamma)}(r) \tag{A.26}$$

whereas for $n < -1$

$$B^{(n,\gamma)}(r) = \frac{k^n r^{n+1}}{n+1} e^{-\gamma(r-R)} + \frac{\gamma}{k(n+1)} B^{(n+1,\gamma)}(r). \tag{A.27}$$

The cases $n = 0$ and $n = -1$ are given by

$$B^{(0,\gamma)}(r) = -\frac{e^{-\gamma(r-R)}}{\gamma} \tag{A.28}$$

$$B^{(-1,\gamma)}(r) = -\frac{e^{\gamma R}}{\kappa} \mathrm{Ei}(\gamma r) \tag{A.29}$$

where

$$\mathrm{Ei}(x) = \int_1^\infty dt \frac{e^{-xt}}{t} \tag{A.30}$$

is the exponential integral.

The flow obtained here is regular. The particular solution is obtained in terms of the exponential integrals $B^{(n,\gamma)}(r)$, which are finite and thus contribute to a regular flow, see subsection 2.5.1. The homogeneous solutions are regular as well, such that the flow is regular. Whitehead [69] has solved the same equations in order to get an improved solution for steady Stokes flow. He found that the solution is diverging as it approaches infinity. This does not happen here, since the solution that is integrated is the full time-dependent Stokes solution, which does not decay as $1/r$ but drops down exponentially with the distance[1]. Solving the equations with the full time-dependent solution instead of the steady Stokes solution regularizes the first order correction.

[1]The potential flow solution decays as $1/r^3$ but the advective term, which is integrated for the particular solution, is cut off exponentially, since it does not involve the potential flow solution squared.

Bibliography

[1] Mustapha Abbad and Mohamed Souhar. Effects of the history force on an oscillating rigid sphere at low Reynolds number. *Exp. Fluids*, 36:775, 2004.

[2] Mustapha Abbad and Mohamed Souhar. Experimental investigation on the history force acting on oscillating fluid spheres at low Reynolds number. *Phys. Fluids*, 16:3808, 2004.

[3] Evgeny S. Asmolov. Flow past a sphere undergoing unsteady rectilinear motion and unsteady drag at small Reynolds number. *J. Fluid Mech.*, 446:95, 2001.

[4] A. B. Basset. On the motion of a sphere in a viscous liquid. *Phil. Trans. R. Soc. Lond. Ser. A*, 179:43, 1888.

[5] A. B. Basset. *Treatise on Hydrodynamics*, volume 2. Deighton Bell, London, 1888.

[6] G. K. Batchelor. *An introduction to fluid dynamics.* Cambridge Mathematical Library, 1967.

[7] G. K. Batchelor. Sedimentation in a dilute dispersion of spheres. *J. Fluid Mech.*, 52:245, 1972.

[8] Andrew Belmonte, Jon Jacobsen, and Anandhan Jayaraman. Monotone solutions of a nonautonomous differential equation for a sedimenting sphere. *Electron. J. Diff. Eq.*, 62:1, 2001.

[9] G. Bernard-Michel, A. Monavon, D. Lhuillier, D. Abdo, and H. Simon. Particle velocity fluctuations and correlation lengths in dilute sedimenting suspensions. *Phys. Fluids*, 14:2339, 2002.

[10] J. Boussinesq. *Application des potentiels à l'étude de l'équilibre et du mouvement des solides élastiques.* Gauthiers-Villars, Paris, 1885.

[11] J. Boussinesq. Sur la résistance qu'oppose un liquide indéfini en repos, sans pesanteur, au mouvement varié d'une sphère solide qu'il mouille sur toute sa surface, quand les vitesses restent bien continues et assez faibles pour que leurs carrés et produits soient négligeables. *Comptes Rendus Acad Sci Paris*, 100:935–937, 1885.

[12] J. Boussinesq. *Theorie Analytique de la Chaleur*, volume 2. L'École Polytechnique, Paris, 1903.

[13] Michael P. Brenner. Screening mechanisms in sedimentation. *Phys. Fluids*, 11:754, 1999.

[14] Russel E. Caflisch and Jonathan H. C. Luke. Variance in the sedimentation speed of a suspension. *Phys. Fluids*, 28:759, 1985.

[15] C. F. M. Coimbra and R. H. Rangel. General solution of the particle momentum equation in unsteady Stokes flows. *J. Fluid Mech.*, 370:53, 1998.

[16] Carlos F. M. Coimbra. Mechanics with variable-order differential operators. *Ann. Phys.*, 12:692–703, 2003.

[17] F. R. Cunha, G. C. Abade, A. J. Sousa, and E. J. Hinch. Modeling and direct simulation of velocity fluctuations and particle-velocity correlations in sedimentation. *J. Fluids Eng.*, 79:2574, 2002.

[18] R. H. Davis and A. Acrivos. Sedimentation of noncolloidal particles at low Reynolds numbers. *Annu. Rev. Fluid Mech.*, 17:91, 1985.

[19] Noriyoshi Dohara. The unsteady flow around an oscillating sphere in a viscous fluid. *J. Phys. Soc. Jpn.*, 51:4095, 1982.

[20] A. Fasano, M. Espedal, K. H. Karlsen, and A. Mikelić. Filtration in porous media and industrial application. In *Lecture Notes in Mathematics*. Springer, 1998. http://books.google.com/books search for book+Sedimentation+industrial.

[21] Élisabeth Guazzelli. Evolution of particle-velocity correlations in sedimentation. *Phys. Fluids*, 13:1537, 2001.

[22] Juan P. Hernandez-Ortiz, Christopher G. Stoltz, and Michael D. Graham. Transport and collective dynamics in suspensions of confined swimming particles. *Phys. Rev. Lett.*, 95:204501, 2005.

[23] W. O. Kermack, A. G. M'Kendrick, and E. Ponder. The stability of suspensions. III. The velocities of sedimentation and of cataphoresis of suspensions in a viscous liquid. *Proc. R. Soc. Edinburgh*, 49:170, 1929.

[24] Inchul Kim, Said Elghobashi, and William A. Sirignano. On the equation for spherical-particle motion: effect of Reynolds and acceleration numbers. *J. Fluid Mech.*, 367:221, 1998.

[25] Donald L. Koch. Hydrodynamic diffusion in a suspension of sedimenting point particles with periodic boundary conditions. *Phys. Fluids*, 6:2894, 1994.

[26] A. J. C. Ladd. Dynamic simulations of sedimenting spheres. *Phys. Fluids A*, 5:299, 1993.

[27] A. J. C. Ladd. Sedimentation of homogeneous suspensions of non-brownian spheres. *Phys. Fluids*, 9:491, 1997.

[28] A. J. C. Ladd. Effects of container walls on the velocity fluctuations of sedimenting spheres. *Phys. Rev. Lett.*, 88:048301, 2002.

[29] L. D. Landau and E. M. Lifschitz. Band V: Statistische Physik Teil 1. In *Lehrbuch der theoretischen Physik*. Akademie-Verlag Berlin, 1987.

[30] L. D. Landau and E. M. Lifschitz. Band VI: Hydrodynamik. In *Lehrbuch der theoretischen Physik*. Verlag Harri Deutsch, 1997.

[31] D. L'Espérance, C. F. M. Coimbra, J. D. Trollinger, and R. H. Rangel. Experimental verification of fractional history effects on the viscous dynamics of small spherical particles. *Exp. Fluids*, 38:112, 2005.

[32] Alex Levine, Sriram Ramaswamy, Erwin Frey, and Roijn Bruinsma. Screened and unscreened phases in sedimenting suspensions. *Phys. Rev. Lett.*, 81:5944, 1998.

[33] Phillip M. Lovalenti and John F. Brady. The force on a sphere in a uniform flow with small-amplitude oscillations at finite Reynolds number. *J. Fluid Mech.*, 256:607, 1993.

[34] Phillip M. Lovalenti and John F. Brady. The hydrodynamic force on a rigid particle undergoing arbitrary time-dependent motion at small Reynolds number. *J. Fluid Mech.*, 256:561, 1993.

[35] M. R. Maxey and J. J. Riley. Equation of motion for a small rigid sphere in a nonuniform flow. *Phys. Fluids*, 26:883, 1983.

[36] S. McKee and A. Stokes. Product integration methods for the nonlinear Basset equation. *SIAM J. Numer. Anal.*, 20:143, 1983.

[37] Renwei Mei. Flow due to an oscillating sphere and an expression for unsteady drag on the sphere at finite Reynolds number. *J. Fluid Mech.*, 270:133, 1994.

[38] Renwei Mei and Ronal J. Adrian. Flow past a sphere with an oscillation in the free-stream velocity and unsteady drag at finite reynolds number. *J. Fluid Mech.*, 237:323, 1992.

[39] Renwei Mei and Christopher J. Lawrence. The flow field due to a body in inpulsive motion. *J. Fluid Mech.*, 325:79, 1996.

[40] Efstathios E. Michaelides. A novel way of computing the Basset term in unsteady multiphase flow computations. *Phys. Fluids A*, 4:1579, 1992.

[41] Efstathios E. Michaelides. Review - The transient equation of motion for particles, bubbles, and droplets. *J. Fluids Eng.*, 119:233, 1997.

[42] Efstathios E. Michaelides. Hydrodynamic force and heat/mass transfer from particles, bubbles, and drops - the Freeman scholar lecture. *J. Fluids Eng.*, 125:209, 2003.

[43] N. Mordant and J.F. Pinton. Velocity measurement of a settling sphere. *Eur. Phys. J. B.*, 18:343–352, 2000.

[44] P. J. Mucha and M. P. Brenner. Diffusivities and front propagation in sedimentation. *Phys. Fluids*, 15:1305, 2003.

[45] Peter J. Mucha, Shang-You Tee, David A. Weitz, Boris I. Shraiman, and Michael P. Brenner. A model for velocity fluctuations in sedimentation. *J. Fluid Mech.*, 501:71, 2004.

[46] Masato Nakanishi, Teruhiko Kida, and Tomoya Nakajima. Asymptotic solutions for two-dimensional low Reynolds number flow around an impulsively started circular cylinder. *Journal of Fluid Mechanics*, 334:31–59, 1997.

[47] H. Nicolai, B. Herzhaft, E. J. Hinch, L. Oger, and E. Guazzelli. Particle velocity fluctuations and hydrodynamic self-diffusion of sedimenting non-brownian spheres. *Phys. Fluids*, 7:12, 1995.

[48] Hélène Nicolai and Elisabeth Guazzelli. Effect of the vessel size on the hydrodynamic diffusion of sedimenting spheres. *Phys. Fluids*, 7:3, 1995.

[49] J. R. Ockendon. The unsteady motion of a small sphere in a viscous liquid. *J. Fluid Mech.*, 34:229, 1968.

[50] F. Odar and W. S. Hamilton. Forces on a sphere accelerating in a viscous fluid. *J. Fluid Mech.*, 18:302, 1964.

[51] F. Odar and W. S. Hamilton. Verification of the proposed equation for calculation of the forces on a sphere accelerating in a viscous fluid. *J. Fluid Mech.*, 25:591, 1966.

[52] C. W. Oseen. Über die Stokes'sche Formel und über eine verwandte Aufgabe in der Hydrodynamik. *Ark. f. Mat. Astr. og Fys.*, 6:29, 1910.

[53] C. W. Oseen. *Neuere Methoden und Ergebnisse in der Hydrodynamik.* Leipzig, 1927.

[54] T. J. Pedley and J. O. Kessler. Hydrodynamic phenomena in suspensions of swimming microorganisms. *Annu. Rev. Fluid Mech.*, 24:313, 1992.

[55] C. Pozrikidis. A singularity method for unsteady linearized flow. *Phys. Fluids A*, 1:9, 1989.

[56] C. Pozrikidis. *Boundary Integral and Singularity Methods for Linearized Viscous Flow.* Cambridge University Press, 1992.

[57] Ian Proudman and J. R. A. Pearson. Expansions at small Reynolds numbers for the flow past a sphere and a circular cylinder. *J. Fluid Mech.*, 2:237, 1957.

[58] J. F. Richardson and Zaki W. N. Sedimentation and fluidization: I. *Trans. Inst. Chem. Eng.*, 32:35, 1954.

[59] N. Riley. On a sphere oscillating in a viscous fluid. *Quart. J. Mech. App. Math.*, 19:461, 1966.

[60] P. N. Segrè, E. Herbolzheimer, and P. M. Chaikin. Long-range correlations in sedimentation. *Phys. Rev. Lett.*, 79:2574, 1997.

[61] P. N. Segrè, F. Liu, P. Umbanhowar, and D. A. Weitz. An effective gravitational temperature for sedimentation. *Nature*, 409:594, 2001.

[62] Jian-Jun Shu and Allen T. Chwang. Generalized fundamental solutions for unsteady viscous flows. *Phys. Rev. E*, 63:051201, 2001.

[63] Arthur Shuster and Arthur E. Shipley. *Britain's Heritage of Science. London.* Constable & Co. Ltd., 1917.

[64] R. Aditi Simha and Sriram Ramaswamy. Hydrodynamic fluctuations and instabilities in ordered suspensions of self-propelled particles. *Phys. Rev. Lett.*, 89:058101, 2002.

[65] George Gabriel Stokes. On the effect of the internal friction of fluids on the motion of pendulums. *Trans. Camb. Phil. Soc.*, 9:8, 1851.

[66] F. Sy, W. Taunton, and E. N. Lightfoot. Transient creeping flow around spheres. *AIChE*, 16:386, 1970.

[67] H. Villat. *Lecons sur les Fluides Visqueux.* Gauthier-Villars, Paris, 1943.

[68] André W. Visser. Hydromechanical signals in the plankton. *Mar Ecol Prog Ser*, 222:1, 2001.

[69] A. N. Whitehead. Second approximations to viscous fluid motion. *Quart. J. Math.*, 23:143, 1889.

[70] Xiao-Lun Wu and Albert Libchaber. Particle diffusion in a quasi-two-dimensional bacterial bath. *Phys. Rev. Lett.*, 84:3017, 2000.

Zum Schluss möchte ich noch all jenen danken, die zum Gelingen dieser Arbeit beigetragen haben. Mein besonderer Dank gilt Bruno für die Aufnahme in seine Arbeitsgruppe und für wegweisende Ideen und die Betreuung dieser Arbeit. Herrn Großmann möchte ich herzlich für die ausführlichen und hilfreichen Tips und Bemerkungen zu meinem Manuskript danken. Des Weiteren sei der gesamten Arbeitsgruppe Komplexe und Biologische Systeme gedankt, insbesondere Florian für das Lesen eines großen Teils der Arbeit, auch noch kurzfristig zum Schluss, und Tobias für die Hilfe bei der Erstellung der Titelseite und ebenfalls für das Lesen der Arbeit. Bei Herrn Stark möchte ich mich für die Begutachtung dieser Arbeit bedanken. Ralf und Barbara danke ich dafür, dass sie mir ihren Drucker zur Verfügung gestellt haben. Boris danke ich für die gemeinsamen Unternehmungen und die langen und gewinnbringenden Diskussionen.

Schließlich möchte ich meiner lieben Lebensgefährtin Sarah-Anne danke sagen dafür, dass sie mir insbesondere in den schwierigen Phasen dieser Arbeit Mut gemacht hat und mir vor allem in der letzten Phase dieser Arbeit zur Seite gestanden ist.

Wissenschaftlicher Werdegang

10/1998 – 04/2004	Studium der Physik an der Universiät Ulm
09/2000	Vordiplom für Physik
09/2000 – 06/2001	Studium der Physik und Mathematik and der University of Leeds
06/2001	Bachelor of Science
02/2003 – 02/2004	Diplomarbeit bei Prof. Dr. S. Herminghaus (Universität Ulm). Titel: "Freie Flüssigkeitsoberflächen in elektrischen Feldern am Beispiel der Elektrobenetzung"
28.04.2004	Diplomprüfung und Abschluß des Studiums
seit 05/2004	Wissenschaftlicher Mitarbeiter in der Arbeitsgruppe Komplexe Systeme, Fachbereich Physik der Philipps-Universität Marburg